ASYMPTOTIC RAY METHOD IN SEISMOLOGY

A TUTORIAL

Johana Brokešová

Contents

Preface

The topic of this course is the asymptotic ray theory for propagation of high-frequency seismic body waves in elastic structures. The course notes have been created in the framework of the Marie Curie Research Training Network (RTN) SPICE (Seismic wave propagation and imaging in complex media: a European network) in the 6th Framework Program of the European Commission. The focus of the network is research and training in computational seismology with the aim to develop, verify and apply computational tools for wave propagation and imaging problems at all scales.

This manuscript has developed from material I have presented in the 2nd SPICE RTN Workshop held in Smolenice, Slovakia, September 4 - 9, 2005. It has also grown out of my experience teaching the regular course on the asymptotic ray theory at Charles University in Prague. The book is set up with the aim of introducing the basic elements of the ray theory and providing a brief self-consistent overview of the use of the ray method to model seismic wavefields both in isotropic and anisotropic media. The goal I was trying to reach is to provide the reader with basics of the theory behind the method and to explain, without discussing some practical details, the basic procedure for obtaining ray synthetic seismograms.

This book is intended as a text for a graduate or research level course. A certain basic knowledge of applied mathematics and linear algebra is needed to understand the calculus. Some knowledge of seismology and wave propagation is expected. I assume that the student taking a course that uses this book has had a course on continuum mechanics.

Many excellent books cover the subject comprehensively, especially recent books by Červený (2001) and Chapman (2004). Unlike these in-depth, state-of-art texts, the presented course notes aim to provide a concise guide to the method for students who are not familiar with it. The theory presented here is mainly after the Červený book, from which several figures are also taken. Some of the figures are taken from lecture notes by Pšenčík (1994).

The theory is presented for general 3D structures. Two and one-dimensional media are understood only as simplified, special cases (although, for the sake of simplicity, some figures are plotted in 2D). However, the book is complemented by a CD containing the numerical code ZRAYAMP, designed for ray computations in 1D models only. This is because of the general decision, accepted in the 1st SPICE RTN Workshop (Venice, Italy, 2004), to treat only 1D models in numerical exercises. This should allow students to more easily compare certain aspects of individual numerical techniques presented on the RTN workshops. The program ZRAYAMP allows for calculations in a spherically symmetrical structure. The program is not meant

only as a training tool to elucidate the use of the ray method on simple examples, but it may even be used to solve some simple problems belonging to global seismology. Several numerical examples, involving models, input data and results, are included in the CD and described in Chapter 8. The code is also supplemented by a user's guide and troubleshooting tips.

1 Introduction

In modern theoretical seismology, there is a need to compute seismic wavefields in increasingly more complex 2D and mainly 3D structures. The propagation of seismic waves in inhomogeneous, laterally varying 2D/3D layered/blocky structures is a very complicated process.

In such complex structures, analytical solutions are not known and many standard modeling techniques, developed for 1D models, are not applicable. Common approaches to calculate synthetic seismograms in such types of structures are:

1. Methods based on direct numerical solution of the elastodynamic equation (EDE), like finite-difference (FDM, see Moczo et al., 2004) or finite-element methods.

2. Approximate high-frequency methods using asymptotic solution of EDE. The most important representative of these techniques is the ray method (RM) which is based on the asymptotic ray theory. The solution is usually sought in the form of the so-called ray series or even only the leading term of such a series is taken into account (zero-order ray solution).

In these lecture notes, the focus is on the use of the **standard zero-order ray method** to calculate seismic wavefields (travel times, amplitudes, synthetic seismograms, etc.).

The RM is very general and flexible in the following sense: it is applicable both in isotropic and anisotropic models containing curved interfaces, separating layers or blocks situated arbitrarily in space. The model parameters inside layers/blocks may also vary both in vertical and lateral directions. The RM is applicable to arbitrary source-receiver configurations (it is also easy to implement finite-extent sources simulating arbitrarily oriented faults).

Let's start with a qualitative comparison of the RM and the FDM, the two representative techniques applicable to complex 2D/3D models. (For simple models, many other modeling techniques could be brought to comparison with RM, however, advantages of RM are more considerable when dealing with 2D/3D models.)

It is well known that the FDM is numerically expensive for large models and/or high frequencies. The size of the model is 'measured' in wavelength. In this context, by 'large model' we understand the model with an extent exceeding, let us say, several wavelengths. On the other hand, large models and high frequencies do not represent any problem for RM and the higher the frequency is, the more accurate the solution could, in principle, be.

It has been already mentioned that the RM is applicable to very general complex structures. This is true but under one condition: the models must

COMPARISON OF REPRESENTATIVE APPROACHES APPLICABLE IN 2D/3D MODELS

FINITE-DIFFERENCE method	vs.	**RAY method** (standard zero-order)
:-| expensive for large models and/or high frequencies		:-) effective for large models and/or high frequencies (accuracy increases with increasing frequency)
:-) applicable in models with arbitrary complex local structure		:-| applicable in smooth models with limited number of layers
:-) yields COMPLETE WAVEFIELD ("exact" solution)		:-| yields only (high-frequency) APPROXIMATION OF THE WAVEFIELD

Right column details under APPROXIMATION OF THE WAVEFIELD:

-no surface or interference waves
-no head waves *
-no inhomogeneous (evanescent) waves
-no waves in dissipative media
-no diffracted waves
-no near-field terms *
-only finite number of elementary body waves

:-) conceptually simple (separation of phases, energy flux trajectories)

:-(fails in singular regions (shadow zones, caustics, critical regions, etc.)

Table 1: Qualitative comparison of the FDM and the standard zero-order RM. (Note: asterisk denotes waves that could be modeled by the RM, provided higher-order terms would be considered).

be **smooth**, not changing rapidly with respect to the wavelength. To be more precise, the model suitable for the RM can contain a reasonable number of boundaries (interfaces), separating relatively thick layers or larger blocks, across which the model parameters are discontinuous. However, fine layering and rapid model parameter changes inside layers and blocks as well as rapid changes in the shape of interfaces are undesirable. The presence of these structural features may easily lead to a significant accuracy decrease or to chaotic behavior of rays which usually results in total break-down of the method.

The most important difference between FDM and RM concerns the completeness of the resulting synthetic wavefield. FDM yields a complete wavefield which is sometimes called the 'exact solution'. Of course, it suffers from various numerical problems and artifacts of the method, so that it may be far from being exact. Nevertheless, the FDM solution should contain all the possible waves propagating in the given structure within the given time window. In contrast, the RM yields only the **high-frequency approximation** of the wavefield which is, in principle, **incomplete**. (In this respect, the FDM wavefield is closer to reality than the RM wavefield).

Let us clarify, in what sense the RM wavefield is incomplete. It contains only those parts of the wavefield which correspond in their form (and properties) to the ray ansatz (the form of the trial solution, see later). As it is shown in Tab. 1, when dealing with the standard zero-order ray wavefield, the solution does not include:

- any near-field terms (similar to those known from the Stokes solution in homogeneous isotropic medium)

- any surface waves, leaky waves and other waves of interference character (waves in waveguides, etc.)

- any head-waves and other types of higher-order waves (e.g., reflections from higher-order interfaces, etc.)

- any inhomogeneous (evanescent) waves or waves originated from these waves, e.g. at some structural interface (postcritically transmitted waves, tunneling waves in a high-velocity layer, pseudospherical waves, etc.)

- waves in dissipative media

- diffracted waves.

There are possibilities to model, at least in part, some of the above types of waves using higher-order ray method or certain generalized approaches.

However, in the standard zero-order RM, the wavefield consists of **far-field body waves** only. Moreover, in practice, we can always consider only a finite number of a priori chosen the so-called elementary waves (individual reflected or transmitted waves, possibly converted from one type to another). Thus, in complex structures with layers and blocks, even the body-wavefield is incomplete.

Finally, the RM fails in certain singular regions like shadow zones (mainly in the vicinity of the boundary between illuminated and shadow regions), at caustic points (where the ray amplitude is infinite) and in the vicinity of caustics, in critical regions where rays reflected with the angle close to the critical one emerge at the surface, etc. In anisotropic media, there are moreover certain singular directions, characterized by the coupling of the quasi-shear waves, in which the RM breaks down. These singular situations are briefly discussed in this book.

Most of the items mentioned in the above comparison between RM and FDM are explained in more details later. Let us illustrate some of them in the following simple numerical example. The calculations are performed in a 2D salt-dome structure and simulate a seismic exploration experiment for one selected shot-point. The model, called PICROCOL (see Brokešová et al., 1994), has been designed at the Institute Francais du Petrole (IFP) for testing and comparison of various imaging techniques as well as for theoretical studies of seismic wave propagation. The model, shown in Fig. 1, contains some geologically complex areas and it has been used to test the applicability of the RM and other ray-based methods on a prestack seismic data in a structure typical in seismic prospection. Velocities and densities are not provided here, since these quantities are not relevant for this illustrative example. Although rays have not been defined yet (being introduced in Sec. 3.2), the reader certainly has an intuitive notion of rays, based, e.g., on analogy with geometrical optics, which is sufficient to apprehend the example. Fig. 1 shows rays reflected from two selected interfaces (all the primarily reflected *P*-waves have been calculated, but only rays of two selected elementary waves are shown in this figure), captured at receivers spread evenly along a line profile.

When looking at these ray diagrams we see what part of the medium is 'illuminated' by the two selected waves. Nevertheless, we can already anticipate some problems concerning the ray solution – we see, for example, a relatively complex ray behavior due to the complex shape of the reflecting interface in the case of red rays (the rays even form some caustics there) and we also see some shadow zones with no rays, so no ray synthetic seismograms can be obtained there. Let us note that these shadows are either due to an unconformity (for red rays) or due to the step discontinuity of the reflector (in the case of blue rays) of which both are features violating the requirement
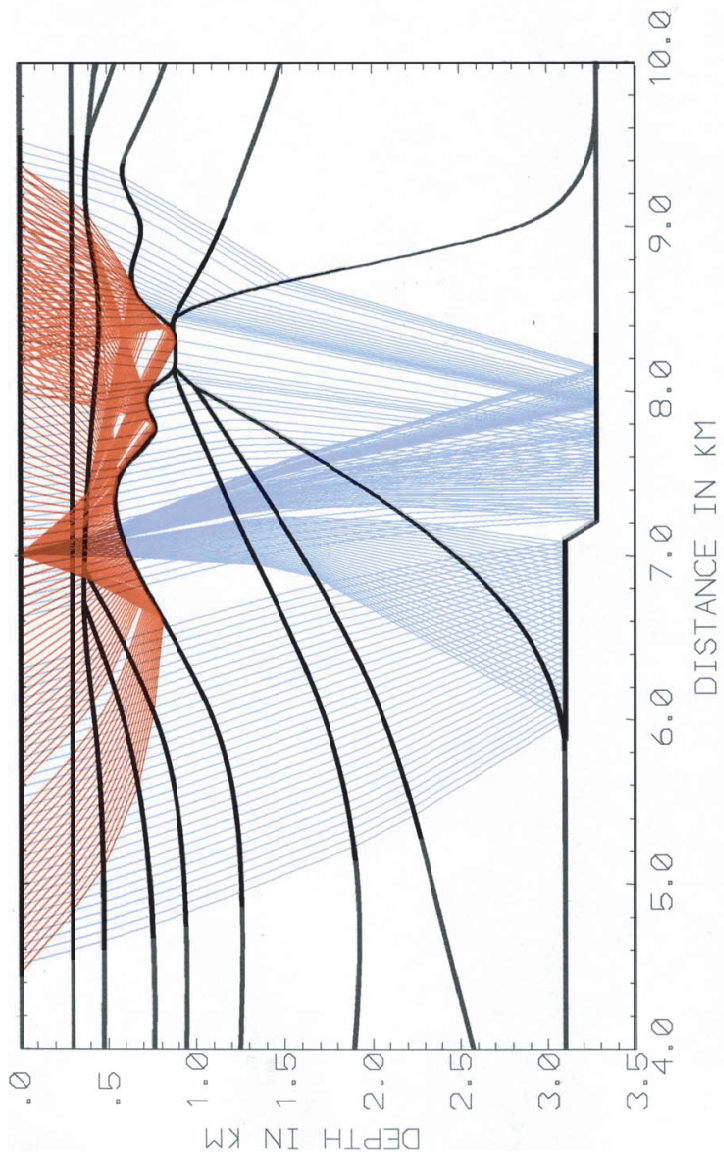
Figure 1: Rays of two reflected waves generated by one shot point in the PICROCOL model.
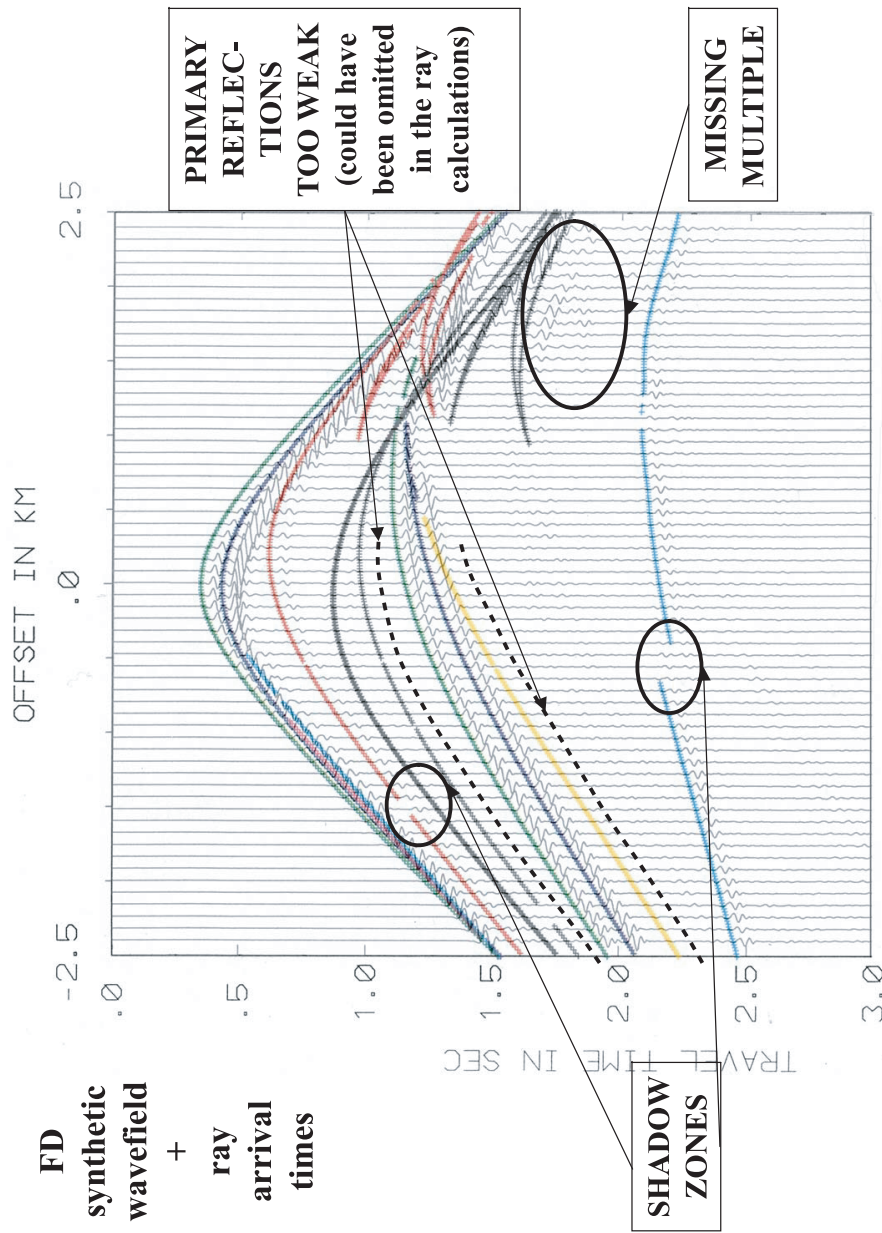
Figure 2: Example of one finite-difference shot gather plotted together with ray arrival times of all primarily reflected waves in the PICROCOL model.
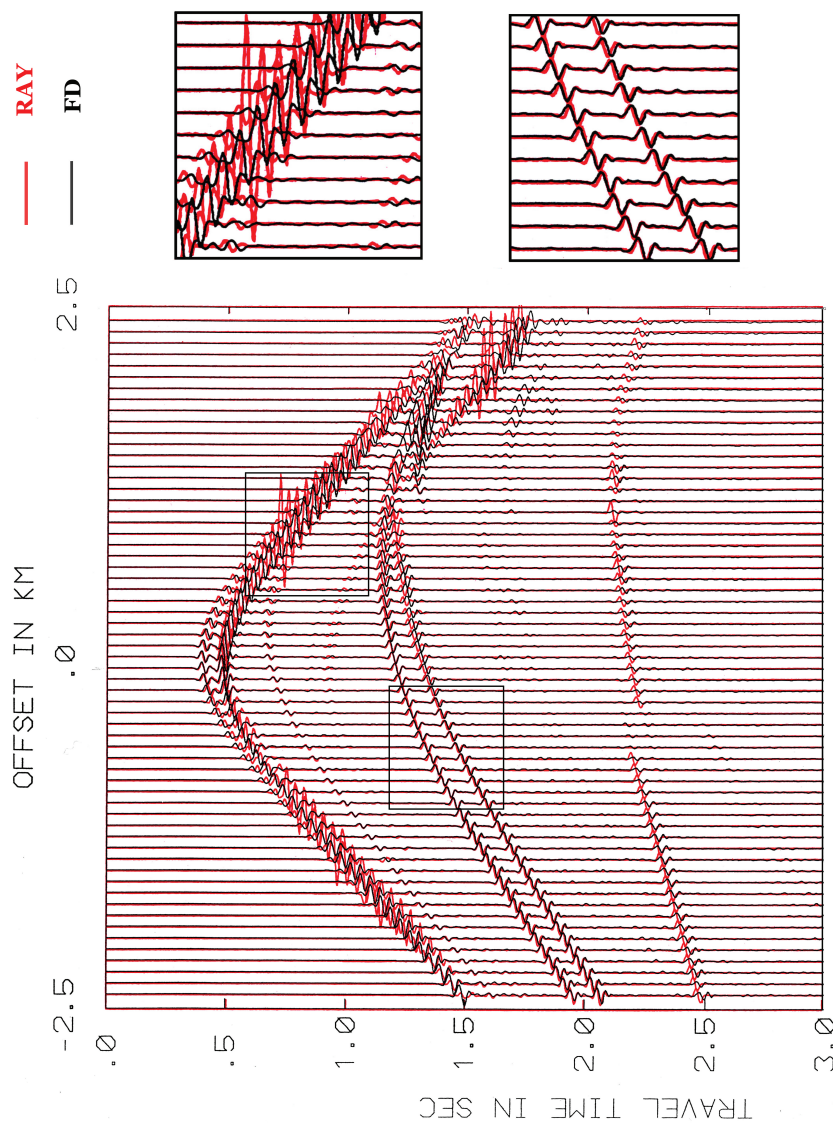
Figure 3: Comparison of RM (red) and FDM (black) synthetic seismograms for one shot-point in the PICROCOL model.

of the smoothness of the model.

Figure 2 shows an example of the FDM synthetic wavefield (pressure) corresponding to the selected shot-point. The FDM wavefield is used as a reference in this example. In the figure, the FDM wavefield is plotted together with ray arrival times of individual primarily reflected waves distinguished by colors (the red and light-blue points correspond to the red and light-blue rays in Fig. 1). Some drawbacks of RM are seen already in this figure (before comparing the corresponding synthetic seismograms). They are namely:

- shadow zones – we see that the FDM wavefield penetrates smoothly into the shadows, where there are no rays, and so the standard RM will result in zero seismograms

- missing waves in the ray calculation – although being created by some multiple reflections (all the primary reflections have been included in the ray calculation), they are important in the FDM wavefield

- in contrast to the preceding item, some ray travel times of primary reflections are calculated, but practically no corresponding arrivals are seen in the FDM wavefield because the corresponding waves are very weak in amplitude

The last two problems are basically due to the fact that we may not be able to estimate in advance, when selecting elementary waves included in the RM calculations, which waves will be strong in amplitude and which could be omitted.

The last figure concerning this numerical example, Fig. 3, compares ray (in red) and finite-difference (black) synthetic seismograms for the given shot-point. Here we see that in some regions the fit is very good, almost perfect (see, e.g., the right bottom detail figure), but there are also regions where there may be considerable differences in amplitudes and waveforms (e.g., in the vicinity of critical distance, the detail at the upper right; this phenomenon is explained later).

The RM can be computationally very efficient compared to full-wavefield methods. For example, in this particular model, to generate one RM shot gather took less than 5 % of the computer time required to obtain the FDM gather.

In this example we have seen that RM may be very useful when we want to identify individual waves in the wavefield and it gives the approximation of the seismograms which may be very good in some cases, or only rough in certain regions, or much distorted in others. Thus, we have to be careful in choosing the model suitable for the RM.

The limits of applicability of the RM are discussed briefly later. They concern the variations of the model parameters with respect to wavelength. Through this there are, in principle, some restrictions for minimum frequency in a given structure model. Moreover, the propagation distances and/or time window of interest also play an important role in evaluating the applicability of the RM. For example, from what has been said so far it is clear that the standard ray solution would fail at distances or times where surface waves play an important role in the wavefield, etc. In models in which only a part of the structure is not suitable for the RM there is a possibility to apply the RM (with an advantage) in a hybrid combination with some other suitable technique, e.g. FDM (Opršal et al., 2002). Such an approach finds applications for models containing a complex local structure embedded in a large, but considerably simpler, regional structure.

Finally let us note that the approximative character of the ray wavefield is not only a disadvantage, but sometimes it may be seen also as an advantage – it allows us to separate individual phases and to follow the energy flux trajectories of these waves. Thus, within the limits of its applicability, RM may provide a better insight into the wavefield.

2 Equation of motion and its ray solution

Traditionally, the ray method has been used in seismology in analogy to optics. The basic concept of rays as certain geometric trajectories, along which high-frequency seismic waves propagate, has been adopted in a more or less intuitive way. When dealing with more complex structures, it is sometimes not clear how to generalize the method. Another possibility is to derive rays from certain variational principles (e.g., the Fermat's principle) or some basic energy concepts. Nevertheless, in these approaches some assumptions have to be accepted 'ad hoc' and they are not clearly justified (e.g., separation of the wavefield to P- and S-waves in inhomogeneous isotropic media).

Seismic wave propagation through a structural model is described by equation of motion. In seismology the medium is considered as an elastic continuum and the corresponding equation of motion is known as the elastodynamic equation (EDE). In these course notes we present the so-called asymptotic ray theory (ART). In elastodynamics the ART has been introduced by Babich (1956) and Karal and Keller (1959) and it represents the most solid base for the RM.

In the ART all the equations are strictly derived from the equation of motion. There are no 'mysterious' approximations nor 'ad hoc' assumptions except one, which is in the very basis of the theory: it is the form of the solution itself. We have to adopt the ansatz solution, the form of which is discussed in this chapter. Once we accept this solution, all the succeeding formulas leading step by step to the final expressions for ground motions are derived in a very clear, straightforward and mathematically strict way.

2.1 Elastodynamic equations

In this chapter we explain in brief the basis of the asymptotic theory underlying the ray method. Most of the theory (and formulas) is exactly the same for both anisotropic and isotropic media. However, some of the equations are different. When necessary, we graphically distinguish the equations corresponding to the isotropic and anisotropic cases by framing them with an empty frame ☐ and a gray-filled frame ▨, respectively. Note that the case of an acoustic medium, important in many applications used in seismic prospection, is not explicitly treated throughout these course notes. Nevertheless, in many respects it can be regarded as a special case of an isotropic medium in which only P-waves can propagate.

Equation (2.1) represents the time domain EDE valid for general anisotropic media (see Aki and Richards, 1980):

$$[c_{ijkl}(\mathbf{x})u_{k,l}(\mathbf{x},t)]_{,j} - \rho(\mathbf{x})\ddot{u}_i(\mathbf{x},t) = -f_i(\mathbf{x},t) \ . \qquad (2.1)$$

Equation (2.2) is EDE in an isotropic medium:

$$[\lambda(\mathbf{x})u_{j,j}(\mathbf{x},t)]_{,i} + \{\mu(\mathbf{x})[(u_{i,j}(\mathbf{x},t) + u_{j,i}(\mathbf{x},t)]\}_{,j} - \rho(\mathbf{x})\ddot{u}_i(\mathbf{x},t)$$
$$= -f_i(\mathbf{x},t) \ . \qquad (2.2)$$

In the equations, ρ means the mass density, c_{ijkl} are general elastic stiffnesses (elements of the 4th-rank elastic tensor), λ and μ are the Lame's elastic parameters used to describe an isotropic medium, $c_{ijkl} = \lambda\delta_{ij}\delta_{kl} + \mu(\delta_{ik}\delta_{jl} + \delta_{il}\delta_{jk})$ (μ has the meaning of rigidity or shear modulus), δ_{ij} is the Kronecker's symbol, $\mathbf{u}$ denotes particle displacement and $\mathbf{f}$ is a body force per unit volume. Derivatives over time and space coordinates are denoted using dots above the letter (e.g., $\ddot{u}_i = \frac{\partial u_i^2}{\partial t^2}$) and comma in lower index (e.g., $u_{i,j} = \frac{\partial u_i}{\partial x_j}$), respectively. Einstein's summation convention is adopted for repeated indices. The reader is expected to be familiar with these equations as well as the basics of the continuum mechanics so it is not necessary to discuss these equations in detail.

In the frequency domain, the above EDE's (2.1) and (2.2) attain the form

$$[c_{ijkl}(\mathbf{x})u_{k,l}(\mathbf{x},\omega)]_{,j} + \rho(\mathbf{x})\omega^2 u_i(\mathbf{x},\omega) = -f_i(\mathbf{x},\omega) \ , \qquad (2.3)$$

and

$$[\lambda(\mathbf{x})u_{j,j}(\mathbf{x},\omega)]_{,i} + \{\mu(\mathbf{x})[(u_{i,j}(\mathbf{x},\omega) + u_{j,i}(\mathbf{x},\omega)]\}_{,j} + \rho(\mathbf{x})\omega^2 u_i(\mathbf{x},\omega)$$
$$= -f_i(\mathbf{x},\omega) \ , \ (2.4)$$

respectively, with ω being angular frequency. In these equations, ω in the argument of a quantity indicates that the quantity is represented by its Fourier spectrum, e.g. $\mathbf{u}(\mathbf{x},\omega) = \mathcal{F}[\mathbf{u}(\mathbf{x},t)]$, where the symbol $\mathcal{F}$ means the temporal Fourier transform.

In earthquake ground motion modeling, the displacement in the above equations means incremental quantity due to seismic motions, connected with an incremental (presumably small) deformation of seismic origin. The

11

body force is just due to a seismic source (not including, e.g., gravitation, etc.). In the RM it is common to consider the above equations of motion as **homogeneous equations**, i.e. **without the body forces**. Seismic source is introduced in an alternative way, via additional boundary conditions along a boundary surrounding the source. This corresponds to the concept of radiation pattern (Aki and Richards, 1980) as explained in Sec. 5.8.

2.2   Ray series solution

Now we come to the most important and crucial point of the whole theory: the assumed form of the solution of equations (2.1) – (2.4). It is well known that in homogeneous media, a monochromatic plane wave represents the simplest solution of the equation of motion. In an inhomogeneous medium, provided it is smooth, changing only insignificantly over the wavelength of the propagating wave, it seems to be reasonable to assume the wavefield to be in some sense locally similar to a plane wave. Let us clarify in what sense the solution we seek is assumed as a generalization of the monochromatic plane wave solution:

1. The amplitude $\mathbf{U}$ of the solution is no more constant, but it is allowed to vary slowly (with respect to the wavelength) with position.

2. The phase of the solution is no longer a linear function of position. However, the phase gradient (normal to the wavefront) is assumed to change only slowly in space.

3. In general, the solution is assumed in the form of an asymptotic series expansion. In the zero-order ray method, we consider only one (the zero-order) term of the expansion. Nevertheless to elucidate why to restrict to the zero-order term and what conditions should be satisfied to make this possible we need to start the explanation from the series expansion and evoke basic properties of asymptotic expansions, see Sec. 2.3.

4. We do not consider just monochromatic (time-harmonic) waves. Instead of an exponential function we use the analytic signals $F(t)$ to define the time behavior of the solution. The analytic signal is any complex-valued function whose real and imaginary parts form a Hilbert pair (the imaginary part is a Hilbert's transform $\mathcal{H}$ of the real one), i.e.,

$$F(t) = f(t) + \mathrm{i}\mathcal{H}[f(t)] = f(t) + \mathrm{i}\frac{1}{\pi}\mathrm{P.V.}\int\limits_{-\infty}^{\infty} \frac{f(\xi)}{t-\xi}\mathrm{d}\xi \ , \qquad (2.5)$$

where $f(t)$ is a real-valued function and P.V. means that the integral is taken in the sense of the Cauchy principal value. Note that the exponential function $\exp(\mathrm{i}t) = \cos(t) + \mathrm{i}\sin(t)$ is the special case of the analytic signal. The advantage of the analytic signal is that it has a one-sided spectrum, i.e., its Fourier transform vanishes for negative frequencies. By a high-frequency signal we understand a signal with $|F(\omega)| = |\mathcal{F}[F(t)]| = 0$ for $0 \leq \omega \leq \omega_0$, where ω_0 is high. Note that the sign of the imaginary part in the definition of analytic signal is closely related to the sign convention used for Fourier transform: $+$ sign would correspond to the $+$ sign of the exponent in Fourier transform.

The analytic signals in wave propagation problems are just the way to allow for a suitable compact notation and to make the mathematics simpler. However, at the end of an analytic-signal computation one must take only the real-part of it to obtain the physically meaningful quantity for which the problem is solved (e.g., displacement).

The displacement we seek is assumed in the form of the so-called **ray series** (see, e.g., Červený, 2001, Chapman, 2004, etc.).

In the time domain, the solution of (2.1) or (2.2) at a point $\mathbf{x}$ and time t is usually written in the form of the time series

$$\mathbf{u}(\mathbf{x}, t) = \sum_{k=0}^{\infty} \mathbf{U}_k(\mathbf{x}) F_k(t - \tau(\mathbf{x})) \;, \tag{2.6}$$

where $\mathbf{U_k}$ (vectorial amplitude coefficients, complex-valued functions) and τ (the so-called eikonal, a real-valued function) are functions to be determined under the condition (2.1) (or (2.2)) in anisotropic (or isotropic) media. These quantities are assumed to change only slowly in space. We discuss these quantities later. Now, let us only mention that the eikonal, which can be interpreted as travel time, is independent of frequency so that the solution (2.6) is, in principle, non-dispersive. In (2.6), F_k's are high-frequency analytic signals (depending on the source) satisfying

$$\frac{\mathrm{d}}{\mathrm{d}t} F_k(t) = \dot{F}_k(t) = F_{k-1}(t) \;, \tag{2.7}$$

which can be, alternatively, written as

$$F_k(t) = \int_{-\infty}^{t} F_{k-1}(t')\mathrm{d}t' \;. \tag{2.8}$$

These relations can be used to compute recursively F_k's if one of them, e.g., F_0, is known.

For ω_0 nominally high ($\omega_0 \gg 1$) it follows from (2.8) that

$$|F_{k-1}(0)| \gg |F_k(0)| . \tag{2.9}$$

However, this does not yet imply convergence of (2.6) in the vicinity of wavefront. Moreover, a high frequency ω_0 may not mean that it is high nominally. By a high frequency we mean the frequency for which wavelength is small with respect to characteristic dimensions of the model (scale lengths of inhomogeneities, propagation distances, etc.). Depending on the model, such a 'high' frequency may be even less than unity so that (2.9) does not hold and the higher-order terms in the ray series cannot be neglected with respect to the lower-order ones.

The ray series (2.6) can be generalized in terms of distributions. Since $F_0(t) = F_0(t) * \delta(t)$ (with $*$ symbol used for convolution), any $F_k(t)$ in the series can be written as $F_k(t) = F_0(t) * \delta_k(t)$, where $\delta_k(t)$ is the k-th integral of the Dirac delta function, i.e. $\delta_0(t) = \delta(t), \delta_1(t) = h(t), ..., \delta_k(t) = t^{k-1}h(t)/(k-1)!$ for $k > 1$, where h is the Heaviside step function ($h(t) = 0$ or 1 for negative or positive t, respectively). Four lowest-order δ_k's are shown in Figure 4.
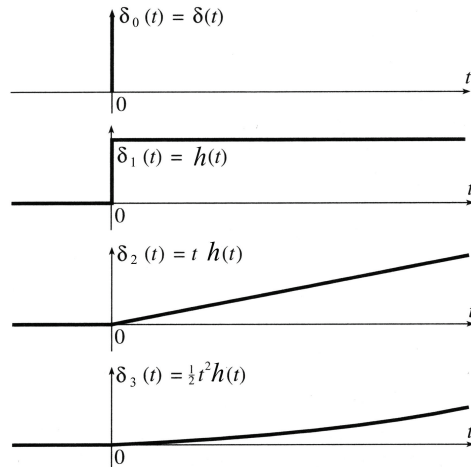
Figure 4: First four integrals of the Dirac delta function (after Červený, 2001).

By the use of distributions, the series (2.6) can be rewritten into the form

$$\mathbf{u}(\mathbf{x}, t) = F_k(t) * \sum_{k=0}^{\infty} \mathbf{U}_k(\mathbf{x})\delta_k(t - \tau(\mathbf{x})) . \tag{2.10}$$

In this way the solution can be interpreted in terms of propagating discontinuities. One speaks of a j-th order discontinuity of a function at a

point if its $(j-1)$-th derivative is discontinuous while all lower-order derivatives are continuous there. From this point of view, the solution in (2.10) is represented in terms of discontinuities propagating with the wavefront $(t = \tau)$. The most distinct discontinuity is carried by the zero-order term. Higher-order terms are smoother and smoother because of the k-th order integration of the Dirac function. In the vicinity of wavefront (i.e., for times close to τ), the series (2.10) may be convergent and it is sometimes called the near-wavefront expansion. However, for large $(t - \tau(\mathbf{x}))$ it is generally divergent.

The intent of the equations (2.10) or (2.6) is not in summing the series up to a large number of terms but rather in taking into account only the first few of them while neglecting the remaining ones. This can be better understood when transforming the equations into the frequency domain and evoking the concept of asymptotic series (see Sec. 2.3).

In the frequency domain, the ray series corresponding to (2.6) or (2.10) has the form

$$\mathbf{u}(\mathbf{x}, \omega) = 2h(\omega)f(\omega)\exp[-i\omega(\tau(\mathbf{x}))]\sum_{k=0}^{\infty}\mathbf{U}_k(\mathbf{x})(-i\omega)^{-k} \ , \tag{2.11}$$

where $f(\omega) = \mathcal{F}[f(t)]$, but $h(\omega)$ here means the Heaviside function of the variable ω. Note that $2h(\omega)f(\omega)$ is the spectrum of the analytic signal corresponding to the function $f(t)$.

The frequency-domain ray series are assumed to be an **asymptotic power series** for high ω. Thus we are concerned with what happens as ω tends to ∞ rather than what happens as the number of terms grows. The asymptoticity allows us to approximate the solution retaining only a few lowest-order terms and mostly even the zero-order one, as it is explained in the next section. The question whether (2.11) is really an asymptotic series in general structures is very difficult and it is beyond scope of this book. The asymptotic character of the series has been proved in many special cases.

2.3 Asymptotic power series and their basic property

Let us assume a sequence of inverse integer powers of ω, ω^{-k}, constituting a series with ω-independent coefficients a_k

$$\sum_{k=0}^{\infty}a_k\omega^{-k} \ . \tag{2.12}$$

For $k > 0$, the inverse powers ω^{-k} decay with $\omega \to \infty$. Moreover, the higher is the power, the faster its reciprocal decays with ω increasing. It holds

$$\lim_{|\omega|\to\infty}\frac{\omega^{-(n+k)}}{\omega^{-n}} = 0 \ , \tag{2.13}$$

for any $k > 0$ and any n. Utilizing the well known concept of "small-o estimate", the equation (2.13) can be written as

$$\omega^{-(n+k)} = o(\omega^{-n}) . \tag{2.14}$$

Any sequence $\{\zeta_n\}$ satisfying the condition $\zeta_{n+1} = o(\zeta_n)$ is called the **asymptotic sequence**, i.e. the inverse powers of ω form an asymptotic sequence.

The asymptoticity of the sequence, however, is not sufficient for the series (2.12) to represent the asymptotic expansion of a function x, $x(\omega) \approx \sum_{k=0}^{N} a_k \omega^{-k}$. For this the series must satisfy the condition given, e.g., by the Poincare's definition of asymptotic series. According to this definition, for all N the series must satisfy

$$|\omega^N [x(\omega) - \sum_{k=0}^{N} a_k \omega^{-k}]| < \epsilon , \tag{2.15}$$

for arbitrarily small ϵ. This condition is equivalent to

$$|x(\omega) - \sum_{k=0}^{N} a_k \omega^{-k}| = o(\omega^{-N}) , \tag{2.16}$$

or, alternatively, due to (2.14)

$$|x(\omega) - \sum_{k=0}^{N} a_k \omega^{-k}| \leq K \omega^{-(N+1)} , \tag{2.17}$$

for some positive constant K which may depend on N (but not on ω). For those familiar with the Landau's order estimates, the last equation can be rewritten by the use of the "large-O symbol"

$$|x(\omega) - \sum_{k=0}^{N} a_k \omega^{-k}| = O(\omega^{-(N+1)}) . \tag{2.18}$$

The conditions (2.15) or (2.16) mean that the error of the expansion up to N is less in order then ω^{-N}. Due to (2.17) – (2.18) we can further state that the error is of the exactly same order as $\omega^{-(N+1)}$, the first term of the sequence $\{\zeta_n = \omega^{-n}\}$ not included in the expansion. Moreover, since $\omega^{-(N+1)}$ decays to zero as ω approaches infinity, the condition (2.17) means that the error estimate of the expansion up to N can be made arbitrarily small, provided ω is sufficiently high. This is true for all N, including $N = 0$, in which case we keep only one term in (2.12), the one with a_0. This term is called the **leading term** of the expansion.
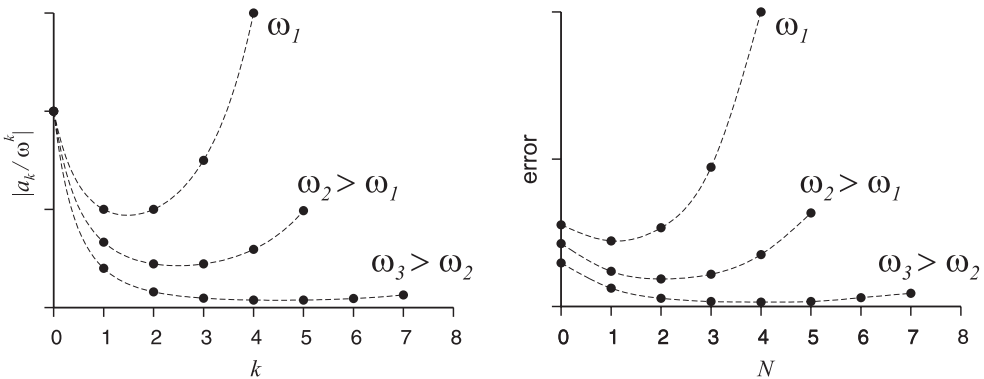
Figure 5: Typical behavior of individual terms in an asymptotic power series (left) and of the error of the expansion up to N (right).

The conditions (2.15) to (2.17) hold for all N. Thus we can even replace the upper limit of the sums by ∞ and write formally

$$x(\omega) \approx \sum_{k=0}^{\infty} a_k \omega^{-k} \ . \tag{2.19}$$

However, this does not imply convergence of the series (2.12)! Indeed, asymptotic series are often divergent. It definitely makes no sense to sum them up to some high N's, we usually take into account just the first few terms or even the leading term only. In the concept of asymptotic series the question of convergence is irrelevant as their major importance consists in the conditions (2.15) to (2.17), valid for any (even small) integer N.

Fig. 5 illustrates qualitatively how the individual terms of the series and the error of the expansion may behave with increasing ω and N. Typically, the error decreases with growing ω for any fixed number of terms in the series (even for the leading term itself). On the other hand, when ω is fixed, the error may grow with N for N greater than a certain value. It is therefore useless to add more terms into the expansion, when the error has passed its minimum.

As it has already been said, the series in (2.11) is assumed to be asymptotic. Since we deal with analytic signals in our solution, we can consider only non-negative frequencies in the expansion. The coefficients in the expansion have to be evaluated, for a given model setting, to make (2.11) be the solution of the equation of motion. In practice it is common to consider only the leading term in the series. From (2.12) we see that this term is just a constant a_0. It means that in (2.11) we retain only one term, the one with frequency-independent amplitude.

2.4 Zero-order ray solution

Let us start with several notes on the accuracy of the expansion (2.19). The parameter ω signifies angular frequency. It has been said that the error of the asymptotic expansion in inverse integer powers of ω can be made arbitrarily small, provided ω is sufficiently high. In physical reality, however, there are some natural limits for ω so that it cannot be higher than a certain maximum value and thus the estimate of the error of the expansion may not be, in general, small enough.

We speak here about the error estimate, not about the error itself. The error estimate is rather a general bound of the error; it does not mean that the error cannot be, in some specific case, smaller. There are known even certain canonical situations when the ray series is finite (i.e. it terminates at $n = N_{max}$, $\mathbf{U}_k(\mathbf{x}) = 0$ for $k > N_{max}$) and exact (the error for any $k > N_{max}$ is zero). For example, it has been shown by Vavryčuk and Yomogida (1995) that if the series (2.14) is written for the Green's function in a homogeneous isotropic medium it has only three non-zero terms for *P*- and three for *S*-waves. Altogether these six terms constitute the solution equivalent to the well known Stoke's solution for the Green's function (Aki and Richards, 1980), including the near-field term.

In the modeling of seismic wavefields in inhomogeneous media, the higher-order terms of the ray series have been considered rather exceptionally. In most of the practical seismic applications, only the zero-order ray approximation (taking into account the leading term only) is traditionally used.

In the following text we restrict ourselves only to the zero-order ray solution. In the time domain, omitting the index "0" in F_0 and $\mathbf{U}_0$, we write the trial solution as

$$\mathbf{u}(\mathbf{x}, t) = \mathbf{U}(\mathbf{x})F(t - \tau(\mathbf{x})) \ . \tag{2.20}$$

This expression is very general, useful also for transient signals. Specifying $F(t) = \exp(-\mathrm{i}\omega t)$, for some fixed frequency, we obtain the so-called time-harmonic solution

$$\mathbf{u}(\mathbf{x}, t, \omega) = \mathbf{U}(\mathbf{x}) \exp[-\mathrm{i}\omega(t - \tau(\mathbf{x}))] \ . \tag{2.21}$$

In its form this solution reminds the zero-order ray solution in the frequency domain (if we would fix t and allow ω to vary)

$$\mathbf{u}(\mathbf{x}, \omega) = \mathbf{U}(\mathbf{x}) \exp[\mathrm{i}\omega\tau(\mathbf{x})]2h(\omega)f(\omega) \ , \tag{2.22}$$

obtained from (2.11) retaining the leading term. Indeed, considering ω as a variable and t as a parameter, (2.21) represents a special case of

(2.22). Sometimes, if we are not interested much in the source spectrum, the frequency-domain zero-order ray ansatz is written as

$$\mathbf{u}(\mathbf{x}, \omega) = \mathbf{U}(\mathbf{x}) \exp[\mathrm{i}\omega\tau(\mathbf{x})] \ . \tag{2.23}$$

Typically ω is large enough that the leading term of the ray series sufficiently approximates the solution of (2.1) – (2.4). According to (2.17), the error estimate satisfies

$$|\mathbf{u}(\mathbf{x}, \omega) - \mathbf{U}(\mathbf{x}) \exp[\mathrm{i}\omega\tau(\mathbf{x})]| \leq K\omega^{-1} \ . \tag{2.24}$$

However, this condition cannot be used to study the accuracy of the solution and the applicability of RM in a quantitative way because it is difficult to find an analytic expression for the constant K. The validity conditions of the RM are mentioned in Chapter 7.

Let us discuss the zero-order ray solution and introduce related terminology. We call the function $\mathbf{U}$ the **ray amplitude**. It does not depend on frequency. It may be, in general, a complex-valued function of position $\mathbf{x}$.

The function τ is the so-called **eikonal**. In the standard RM it is assumed to be real-valued and it is independent of frequency. It is interpreted as **travel-time** of the elementary wave for which the solution is constructed. Surfaces $\tau(\mathbf{x}) = const$ represent wavefronts.

A very important quantity is the gradient of τ. It is a vector perpendicular to the wavefront. This vector, called the **slowness vector**, is given as

$$p_i(\mathbf{x}) = \tau_{,i}(\mathbf{x}) = \frac{\partial\tau(\mathbf{x})}{\partial x_i} = \frac{n_i^{\tau}(\mathbf{x})}{c(\mathbf{x})} \ , \tag{2.25}$$

where $\mathbf{n}^{\tau}$ is the unit vector perpendicular to the wavefront and c is the phase velocity. From (2.25) we see that the magnitude of $\mathbf{p}$ is inversely proportional to the phase velocity — that is why $\mathbf{p}$ is called the slowness vector.

Note that (2.20), (2.21), (2.22) and (2.23) describe a non-dispersive wavefield, progressing with a position-dependent phase speed $c(\mathbf{x})$, with wavefronts of general shape at surfaces of equal $\tau(\mathbf{x})$ and with position-dependent amplitude. In certain features such a solution represents a generalization of plane waves, the well known exact solution in homogeneous media. The quantities $\mathbf{U}$ and $\mathbf{p}$ are assumed to be **slowly varying functions of position x** over the wavelength under consideration (this requirement can also be used, among others, as a criterion of applicability of the RM in the given structure, see Sec. 7). This assumption makes good sense because we are dealing with a high-frequency asymptotic approximation of the wavefield. The higher the frequency is the less the medium is locally (within a wavelength) inhomogeneous and the wavefield propagation should locally resemble the propagation in a homogeneous medium. In other words, when

the wavelength is short compared with the scale of medium heterogeneities as well as the propagation distances, the solution can be expected to behave locally as plane waves.

2.5 Basic asymptotic ray theory equations for the zero-order solution

In order to determine the functions $\mathbf{U}(\mathbf{x})$ and $\tau(\mathbf{x})$, the parameters of our trial solution, we require the solution to fit asymptotically the corresponding equation of motion. Substituting the zero-order ray ansatz (2.20) in the equation (2.1) or (2.2) (without the body forces) and recombining the terms in the equation to gather those with the same time derivative of F yields

$$\ddot{F} N_i(\mathbf{U}, \nabla\tau) - \dot{F} M_i(\mathbf{U}, \nabla\tau) + F L_i(\mathbf{U}) = 0 , \qquad (2.26)$$

where the vectorial coefficients $\mathbf{N}$, $\mathbf{M}$ and $\mathbf{L}$ differ for anisotropic and isotropic cases. More specifically, for anisotropic media we get from (2.1)

$$
\begin{aligned}
N_i(\mathbf{U}, \nabla\tau) &= c_{ijkl}\tau_{,l}\tau_{,j}U_k - \rho U_i & (2.27)\\
M_i(\mathbf{U}, \nabla\tau) &= c_{ijkl}\tau_{,j}U_{k,l} + (c_{ijkl}\tau_{,l}U_k)_{,j} & (2.28)\\
L_i(\mathbf{U}) &= (c_{ijkl}U_{k,l})_{,j} , & (2.29)
\end{aligned}
$$

while, in isotropic structures, (2.2) yields

$$
\begin{aligned}
N_i(\mathbf{U}, \nabla\tau) &= (\lambda+\mu)U_j\tau_{,i}\tau_{,j} + \mu U_i\tau_{,j}\tau_{,j} - \rho U_i & (2.30)\\
M_i(\mathbf{U}, \nabla\tau) &= (\lambda+\mu)[U_{j,i}\tau_{,j} + U_{j,j}\tau_{,i} + U_j\tau_{,ij}] + \mu[2U_{i,j}\tau_{,j} + U_i\tau_{,jj}]\\
&\quad +\lambda_{,i}U_j\tau_{,j} + \mu_{,j}(U_i\tau_{,j} + U_j\tau_{,i}) & (2.31)\\
L_i(\mathbf{U}) &= (\lambda+\mu)U_{j,ij} + \mu U_{i,jj} + \lambda_{,i}U_{j,j} + \mu_{,j}(U_{i,j} + U_{j,i}) , & (2.32)
\end{aligned}
$$

In both cases, $\mathbf{N}$, $\mathbf{M}$ and $\mathbf{L}$ are vectorial functions of $\mathbf{U}$, and $\mathbf{N}$ and $\mathbf{M}$ depend also on the gradient of τ (slowness).

In the frequency domain, by inserting (2.23) (or (2.22)) into (2.3), away from body forces, and gathering the terms with the same power of ω we obtain

$$(\mathrm{i}\omega)^2 N_i(\mathbf{U}, \nabla\tau) - (\mathrm{i}\omega)^1 M_i(\mathbf{U}, \nabla\tau) + (\mathrm{i}\omega)^0 L_i(\mathbf{U}) = 0 , \qquad (2.33)$$

where the components of $\mathbf{N}$, $\mathbf{M}$ and $\mathbf{L}$ are again given by equations (2.27) to (2.29). The same equation (2.33) would result when inserting our frequency domain zero-order trial solution into the homogeneous equation (2.4) for isotropic media, with the exception that in isotropic media the coefficients would be given by (2.30) to (2.32) instead of (2.27) to (2.29). Note that we would obtain exactly the same when inserting the time-domain harmonic solution (2.21) into the corresponding time-domain equations of motion.

Note also that the equation (2.26) represents the equation of motion under the assumption of our trial solution. Thus it must be satisfied at any time and any point. Because of different orders of derivatives of F, this cannot be accomplished without setting all the coefficients $\mathbf{N}$, $\mathbf{M}$ and $\mathbf{L}$ to zero. Similarly, (2.33) could not be fulfilled for arbitrary frequency without setting the coefficients to zero. Thus, the equation of motion yields three conditions, $\mathbf{N} = \mathbf{0}$, $\mathbf{M} = \mathbf{0}$ and $\mathbf{L} = \mathbf{0}$, to be satisfied by the solution. Note that the conditions are exactly the same both in the frequency and the time domains and they remain unchanged also when dealing with the time-harmonic solution. Henceforth we need not distinguish these cases.

Clearly, under general circumstances, all of the conditions cannot be satisfied exactly (neither in anisotropic, nor in isotropic media) since they represent nine equations while there are only four parameters (three components of $\mathbf{U}$ and τ) in our ansatz. However, in high-frequency approximation, the conditions are of different importance.

Only the first two conditions are used to determine the eikonal and the ray amplitude. Note that if frequency is high, the first two terms in (2.33), having the multipliers ω^2 and ω, dominate over the third one. Thus, the conditions for $\mathbf{N}$ and $\mathbf{M}$ are more important to be satisfied. The same holds in the time domain, since due to the high-frequency character of F the terms with higher-order derivatives of F prevail, see (2.9). In general, the second and third terms in (2.26) and (2.33) do not vanish. Thus, our zero-order solution may not satisfy the equation of motion completely. In high-frequency approximation the error is presumably small.

The first condition, $\mathbf{N} = \mathbf{0}$, results in the so-called **eikonal equation**, nonlinear partial differential equation for $\tau(\mathbf{x})$. As it is explained in Sec. 3.1, besides τ it constrains also the direction (polarization) of $\mathbf{U}$. The magnitude of $\mathbf{U}$ (one scalar quantity) can be determined from the so-called **transport equation**. This equation is derived by projecting the vector $\mathbf{M}$ into the direction of the amplitude $\mathbf{U}$ (for details see Sec. 5.5).

After solving the eikonal and transport equations for τ and $\mathbf{U}$ we obtain a zero-order ray solution for one elementary wave. This is to be superposed with solutions for all the elementary waves under study. As explained above, the wavefield obtained in this way is not exact (except for a few canonical examples) but it provides a useful and widely applicable approximation.

3 Ray kinematics

In this chapter, we derive the eikonal equation, both for isotropic as well as anisotropic media. We show that in isotropic structures, the high-frequency wavefield separates into two independent waves, P and S, propagating at different speeds and differently polarized. In anisotropic media, the eikonal equation yields that, in any direction, three independent linearly polarized waves can propagate.

The eikonal equation is solved by the use of characteristic curves of the equation, that we call rays. We derive the so-called ray tracing system: differential equations allowing to calculate rays (and travel times along rays) in smooth media from known initial conditions. It has been already mentioned that there are some alternative possibilities to define rays. We show that rays introduced in this chapter as a tool for solving the eikonal equation are exactly the same curves as those satisfying Fermat's principle and those obtained from energy considerations as energy flux trajectories. Note that the approach presented here, i.e., defining rays as characteristics of the eikonal equation, is the most general among the mentioned alternatives.

At the end of this chapter we explain how to calculate rays across structural interfaces, specifically how to calculate slowness vectors of reflected and transmitted rays from the one of the incident ray. The slowness vectors of the waves generated at the interface represent the new initial conditions for the ray tracing system and allow us to continue with the ray calculation after interaction with the interface. In this way, rays and travel times along rays can be evaluated in a layered/blocky medium.

3.1 Eikonal equation

The eikonal equation comes from setting the first term, N_i for $i = 1, 2, 3$, in (2.26) or (2.33) to zero. In anisotropic media this condition reads

$$N_i(\mathbf{U}, \nabla \tau) = c_{ijkl}\tau_{,l}\tau_{,j}U_k - \rho U_i = 0 \ , \tag{3.1}$$

while for isotropic structures we have

$$N_i(\mathbf{U}, \nabla \tau) = (\lambda + \mu)U_j\tau_{,i}\tau_{,j} + \mu U_i\tau_{,j}\tau_{,j} - \rho U_i = 0 \ . \tag{3.2}$$

By introducing the so-called Christoffel matrix with elements Γ_{ik} as follows

$$\Gamma_{ik} = \frac{c_{ijkl}}{\rho}\tau_{,j}\tau_{,l} = \frac{c_{ijkl}}{\rho}p_j p_l \; , \tag{3.3}$$

or

$$\Gamma_{ik} = \frac{\lambda + \mu}{\rho}\tau_{,i}\tau_{,k} + \frac{\mu}{\rho}\delta_{ik}\tau_{,l}\tau_{,l} = \frac{\lambda + \mu}{\rho}p_i p_k + \frac{\mu}{\rho}\delta_{ik}p_l p_l \; , \tag{3.4}$$

we can rewrite (3.2) and (3.1) into the simple and compact form

$$(\Gamma_{ij} - \delta_{ij})U_j = 0 \; , \tag{3.5}$$

the same both for the isotropic and anisotropic media.

We have introduced here the Christoffel matrix $\mathbf{\Gamma}$ just as an useful notation to simplify the equations (3.1) and (3.2). The matrix, however, plays an important role in wave propagation problems and it has many interesting properties (see Červený, 2001). For what follows let us only mention that it is obviously symmetric, $\Gamma_{ij} = \Gamma_{ji}$, because of the well known symmetry of the elements of the elastic tensor c_{ijkl}. From the definition of the matrix it is clear that its elements are homogeneous functions of the second order in $p_i = \tau_{,i}$. This means that $\Gamma_{ik}(ap_j) = a^2\Gamma_{ik}(p_j)$, for any non vanishing a. Furthermore, the matrix is positively definite. Its eigenvalues are real and positive. Thanks to the symmetry of the Christoffel matrix, the eigenvectors corresponding to the different eigenvalues are orthogonal (independent from each other).

Representing the ray amplitude $\mathbf{U}$ by the use of a scalar amplitude factor A and the corresponding unit polarization vector $\mathbf{g}$, $U_i = Ag_i$, $|\mathbf{g}| = 1$ the equation (3.5) yields

$$(\Gamma_{ij} - \delta_{ij})g_j = 0 \; . \tag{3.6}$$

This equation can be viewed as an eigenvalue problem of the matrix $\mathbf{\Gamma}$. Indeed, the standard equation,

$$(\Gamma_{ij} - G\delta_{ij})g_j = 0 \; , \tag{3.7}$$

with G being a general eigenvalue, is equivalent to (3.6), under the condition

$$G = 1 \; . \tag{3.8}$$

As G is the eigenvalue of the Christoffel matrix, (3.8) constraints gradient of τ. Thus, by determining the eigenvalues of the matrix $\mathbf{\Gamma}$ and equating them to unity we obtain the eikonal equation (partial differential equation of the second order for τ) we look for.

The eigenvalues are determined standardly from the condition

$$\det(\Gamma_{jk} - G\delta_{jk}) = 0 \ . \tag{3.9}$$

This leads to the cubic equation for G's

$$G^3 - PG^2 + QG - R = 0 \ , \tag{3.10}$$

where the coefficients are given as follows: P is the trace of the Christoffel matrix $\boldsymbol{\Gamma}$

$$P = \Gamma_{ii} \ , \tag{3.11}$$

R is the determinant of $\boldsymbol{\Gamma}$

$$R = \det \Gamma_{ij} \ , \tag{3.12}$$

and Q is composed from 2×2 subdeterminants of $\boldsymbol{\Gamma}$ as

$$Q = \det \begin{pmatrix} \Gamma_{11} & \Gamma_{12} \\ \Gamma_{12} & \Gamma_{22} \end{pmatrix} + \det \begin{pmatrix} \Gamma_{22} & \Gamma_{23} \\ \Gamma_{23} & \Gamma_{33} \end{pmatrix} + \det \begin{pmatrix} \Gamma_{11} & \Gamma_{13} \\ \Gamma_{13} & \Gamma_{33} \end{pmatrix} \ . \tag{3.13}$$

Due to the symmetry and positive definiteness of the Christoffel matrix, the eigenvalues (roots of (3.10)) are real-valued and positive.

In anisotropic media, (3.10) yields, in general, **three different eigenvalues**

$$G_1 \neq G_2 \neq G_3 \ . \tag{3.14}$$

As soon as the eigenvalues are evaluated, we can easily find the corresponding eigenvectors from (3.7). These are three unit mutually perpendicular vectors. They represent polarization vectors of three independent linearly polarized waves, which can propagate in the given anisotropic model specified by c_{ijkl}. Their amplitudes are given as

$$\mathbf{U}^{(m)}(\mathbf{x}) = A^{(m)}(\mathbf{x})\mathbf{g}^{(m)}(\mathbf{x}) \ , \tag{3.15}$$

and their travel times $\tau^{(m)}$ must satisfy the eikonal equation

$$G_m(\tau_{,1}^{(m)}, \tau_{,2}^{(m)}, \tau_{,3}^{(m)}, x_1, x_2, x_3) = G_m(p_1^{(m)}, p_2^{(m)}, p_3^{(m)}, x_1, x_2, x_3) = 1 \ , \tag{3.16}$$

where $m = 1$, or 2 or 3, according to the type of the wave under consideration. In general anisotropy, there are no analytical expressions; everything has to be solved numerically.

To summarize, in a given anisotropic structure, only those waves of which the slowness vectors satisfy (3.16) may fulfill the equation of motion and thus represent the solution we seek. More specifically, only those waves make the first term in (2.26) and (2.33) zero (i.e., satisfy (3.1)). For a fixed $\mathbf{x}$ and a fixed $\mathbf{n}^\tau$ (the unit vector orthogonal to wavefront), the equation (3.16) poses a constraint on the phase velocity (see (2.25)). Thus, in a given point and a given direction, there are three possible waves propagating with three different phase speeds. They are polarized linearly along the three mutually perpendicular vectors $\mathbf{g}$ representing the eigenvectors of the Christoffel matrix. Their polarization vectors are not, in general, related to the wavefront (none of these is perpendicular or tangent to the wavefront, etc.). We usually call these waves as 'quasi-P'(qP) and 'quasi-S' (qS_1 and qS_2) waves. Note that for quasi-S waves it often occurs that their phase velocities are close in their magnitudes so that the waves are coupled, traveling with nearly the same phase speeds. In such a case, the zero-order ray solution as such breaks down as it is designed to describe separately propagating waves and not interference or coupled waves.

In isotropic media we solve the same equation (3.9), but here, when substituting (3.4) it can be shown (after simple algebra) that (3.10) factorizes into

$$(\frac{\mu}{\rho}p_i p_i - G)^2(\frac{\lambda + 2\mu}{\rho}p_i p_i - G) = 0 . \tag{3.17}$$

This means that two of the eigenvalues (let us say G_1 and G_2) coincide and only the third one (G_3) differs from them. Using the notation

$$\alpha = \sqrt{\frac{\lambda + 2\mu}{\rho}} , \tag{3.18}$$

and

$$\beta = \sqrt{\frac{\mu}{\rho}} , \tag{3.19}$$

this equation becomes

$$(\beta^2 p_i p_i - G)^2(\alpha^2 p_i p_i - G) = 0 . \tag{3.20}$$

This holds if either

$$G = \beta^2 p_i p_i \ , \qquad (3.21)$$

which, together with the condition $G = 1$, yields the following analytical expressions for the square of the slowness vector magnitude

$$p_i p_i = \frac{1}{\beta^2} \ , \qquad (3.22)$$

or if

$$G = \alpha^2 p_i p_i \ , \qquad (3.23)$$

yielding

$$p_i p_i = \frac{1}{\alpha^2} \ . \qquad (3.24)$$

Both (3.22) and (3.24) represent the eikonal equations in isotropic media. The equations constraint gradient of τ of the two waves, satisfying (3.2), which can propagate in a given isotropic model. We call these waves P and S, respectively. From (3.22) and (3.24) we also see that the magnitudes of their slowness vectors are α^{-1} and β^{-1}, respectively. The quantities α and β thus represent phase velocities of the two waves (compare (2.25)).

In isotropic media, only one of the eigenvectors of the Christoffel matrix can be determined uniquely (from (3.7)) — the one corresponding to the P-wave. As regards the remaining two, corresponding to the coinciding eigenvalues, we only know that they must be mutually perpendicular and orthogonal to the P-wave polarization vector. From this point of view, an isotropic medium is sometimes regarded as a degenerate case with respect to general anisotropic media.

Let us determine the eigenvector corresponding to the P-wave (i.e., to the eigenvalue G_3), $\mathbf{g}^{(3)}$. By multiplying the equation (3.7), for G_3 and $\mathbf{g}^{(3)}$, by $g_i^{(3)}$, substituting (3.4) for the elements of the matrix $\mathbf{\Gamma}$ and taking into account that $p_i = n_i^\tau / \alpha$ and $G_3 = 1$ we obtain

$$\left[\frac{\lambda + \mu}{\rho} \frac{n_i^\tau n_k^\tau}{\alpha^2} + \frac{\mu}{\rho} \delta_{ik} \frac{n_l^\tau n_l^\tau}{\alpha^2} - \delta_{ik} \right] g_k^{(3)} g_i^{(3)} = 0 \ . \qquad (3.25)$$

From this it follows that $(n_i^\tau g_i^{(3)})^2 = 1$ which yields $\mathbf{g}^{(3)} = \pm\mathbf{n}^\tau$. We conclude, that the P-wave, with the amplitude

$$\mathbf{U}^{(P)}(\mathbf{x}) = A(\mathbf{x})\mathbf{g}^{(3)}(\mathbf{x}) \ , \tag{3.26}$$

is linearly polarized perpendicularly to its wavefronts. The P-wave is also called the compressional or the longitudinal wave.

The eigenvectors $\mathbf{g}^{(1)}$ and $\mathbf{g}^{(2)}$ cannot be determined uniquely from (3.7), as the corresponding eigenvalues G_1 and G_2 coincide. We only know that they complement $\mathbf{g}^{(3)}$ into an orthonormal set. Thus, the S-wave is polarized in the plane tangent to the wavefronts. It is also called the shear wave. Its polarization is, in general, elliptical. For its amplitude we have the expression

$$\mathbf{U}^{(S)}(\mathbf{x}) = B(\mathbf{x})\mathbf{g}^{(1)}(\mathbf{x}) + C(\mathbf{x})\mathbf{g}^{(2)}(\mathbf{x}) \ . \tag{3.27}$$

Let us note that, in our high-frequency approximation, we have obtained separation of the wavefield into P- and S- waves in inhomogeneous isotropic media. This is a very important finding. The P- and S-wavefields are fully separated in homogeneous structures, but generally not in inhomogeneous structures. Only, provided that the frequency is high, they are separated approximately (we have derived the separation for our approximate solution). Let us emphasize that in the approach we follow in this book, the separation is not assumed 'ad hoc', but it follows from the equation of motion as a consequence of our trial solution.

3.2   Solution of the eikonal equation by the use of characteristics

The eikonal equation, both for isotropic as well as anisotropic models, represents a non-linear constraint for the slowness vector $\mathbf{p}$. Recall in mind that

$$p_i(\mathbf{x}) = \tau_{,i}(\mathbf{x}) = \frac{\partial \tau(\mathbf{x})}{\partial x_i} \ . \tag{3.28}$$

Thus, the eikonal equation is a non-linear partial differential equation of the first order for τ (the eikonal).

To find the eikonal, we must know how to solve eikonal equations. There are different approaches to this problem. One possibility is to evaluate the eikonal directly by the use of certain grid-based methods, called usually as eikonal solvers. For example, the FDM approach by Vidale (1990), or Podvin and Lecomte (1991), and, on the other hand, the so-called fast marching

method (Sethian, 1999), fall into this category. However, stability and accuracy represent a serious problem of these techniques. Moreover, the eikonal solvers do not take into account the multi-valuedness of the solution, physically corresponding to the wavefront folding and triplications of hodochrons (relatively frequent situations in seismology). In these course notes, an alternative, ray-based, approach is applied. To solve the eikonal equation we use the method of characteristic curves (e.g., Bleistein, 1984). In this method, the multi-valued solution can be easily obtained by the so-called ray multipathing. Moreover, rays (obtained as the characteristic curves, see below) provide a good base to evaluate ray amplitudes, necessary to complement the ray solution.

To explain the concept of characteristics it is convenient to rewrite the eikonal equation into the form of the static Hamilton-Jacobi equation, known from classical mechanics,

$$H(x_i, \frac{\partial \Psi}{\partial x_i}) = 0 \ , \tag{3.29}$$

or

$$H(x_i, p_i) = 0 \quad \text{with} \quad p_i = \frac{\partial \Psi}{\partial x_i} \ . \tag{3.30}$$

Here $\Psi = \Psi(x_j)$ is the generating function to be determined (in our case $\psi = \tau$), and p_j are the generalized momenta. It is important to emphasize that here we do not interpret the 'Hamiltonian' H as a total energy of the system. In the following, we just use the Hamilton formalism to solve the equation. In this formalism, p_i's an x_i's are treated as independent variables.

The equation (3.30) is usually solved by the use of characteristics which satisfy the so-called canonical equations. What is the meaning of these curves? These are the curves (in 6D phase space, (p_i, x_i)), along which the eikonal equation is satisfied and along which τ (the generating function) can be easily computed by simple quadrature (a curve integral). The canonical equations for the characteristic curves read

$$\frac{\mathrm{d}x_i}{\mathrm{d}u} = \frac{\partial H}{\partial p_i} \ , \quad \frac{\mathrm{d}p_i}{\mathrm{d}u} = -\frac{\partial H}{\partial x_i} \ , \quad \frac{\mathrm{d}\tau}{\mathrm{d}u} = p_i \frac{\partial H}{\partial p_i} \ , \quad i = 1, 2, 3, \tag{3.31}$$

with u being a flow parameter along the curve. In this way, the eikonal equation (nonlinear partial differential equation) is replaced by a system of seven ordinary differential equations (3.31) which are usually much easier to solve. They allow us to determine the characteristic curve in 6D phase space (x_i, p_i), parameterized by the flow parameter u: $x_i = x_i(u)$, $p_i = p_i(u)$. It is obtained from the first six coupled equations of the system. The projection of this 6D curve into the 3D space (x_i), i.e., the geometrical trajectory of the characteristic curve, we call the **seismic ray**. As it results from the first six equations of the system (3.31), the equations are called the **ray tracing**

system (RTS). The ray tracing system provides, along with the geometrical trajectories (rays), the distribution of the slowness along these trajectories, $p_i = p_i(u)$.

The seventh equation of (3.31), not coupled with the other six, allows us to determine the eikonal $\tau = \tau(u)$ by a simple quadrature along the ray. To summarize, in this approach we are able to calculate travel times, but not at any point in space but only at the points through which some rays pass.

3.3 Ray tracing system in isotropic media

In isotropic structures, the eikonal equation to be solved is of the form

$$p_i p_i = \frac{1}{v^2} \; , \tag{3.32}$$

the same for both *P*- ($v = \alpha$) and *S*- ($v = \beta$) waves.

In the Hamilton-Jacobi form, the above equation reads $H(p_i, x_i) = 0$, where

$$H = (p_i p_i - v^{-2}) \; . \tag{3.33}$$

We can consider, with advantage, the function H in a more general form

$$H(x_i, p_i) = \frac{1}{\eta} [(p_i p_i)^{\eta/2} - v^{-\eta}] \; , \tag{3.34}$$

which corresponds to taking the power $\eta/2$ of the equation (3.32) and multiplying it by $1/\eta$. For $\eta = 0$ the above expression is not defined and must be replaced by the limit for $\eta \to 0$. Using the l'Hospital rule we obtain for H in the limit

$$H(x_i, p_i) = \frac{1}{2} \ln(p_i p_i) + \ln v = \frac{1}{2} \ln(v^2 p_i p_i) \; . \tag{3.35}$$

If we insert (3.34) into the canonical equations (3.31), we obtain the following general six RTS equations

$$\frac{\mathrm{d}x_i}{\mathrm{d}u} = v^{2-\eta}p_i \quad \frac{\mathrm{d}p_i}{\mathrm{d}u} = \frac{1}{\eta}\frac{\partial}{\partial x_i}\Big(\frac{1}{v^\eta}\Big) \ , \tag{3.36}$$

and for τ the equation

$$\frac{\mathrm{d}\tau}{\mathrm{d}u} = (p_k p_k)^{\frac{\eta}{2}} = \frac{1}{v^\eta} \ , \tag{3.37}$$

Note that the equations for x_i's and those for p_i's are coupled, so that they must be solved together. Alternatively, we can write the six equations of (3.36) in the form of the three second-order RTS equations

$$\frac{\mathrm{d}}{\mathrm{d}u}\Big(v^{\eta-2}\frac{\mathrm{d}x_i}{\mathrm{d}u}\Big) = \frac{1}{\eta}\frac{\partial}{\partial x_i}\Big(\frac{1}{v^\eta}\Big) \ . \tag{3.38}$$

The parameter η is usually considered as an integer. It controls the physical meaning of the parameter u in the RTS equations. Let us specify the RTS for different special choices of η, useful for seismological applications:

1. For $\eta = 0$, u equals directly the travel time τ, which follows from the seventh equation of the system (3.31) with (3.35) inserted for H. In this case, the equation like (3.37) for τ need not be solved — the travel time is known at any point at which the ray is calculated. This is the main advantage of this choice. The RTS has the form

$$\frac{\mathrm{d}x_i}{\mathrm{d}\tau} = v^2 p_i \quad \frac{\mathrm{d}p_i}{\mathrm{d}\tau} = -\frac{\partial \ln v}{\partial x_i} = -\frac{1}{v}v_{,i} \ . \tag{3.39}$$

2. For $\eta = 1$, u has the meaning of the arclength along the ray (denoted s henceforth), see (3.37). It is easy to imagine how the rays are traced point by point in terms of the arclength. The RTS in this case reads

$$\frac{\mathrm{d}x_i}{\mathrm{d}s} = v p_i \quad \frac{\mathrm{d}p_i}{\mathrm{d}s} = \frac{\partial}{\partial x_i}\Big(\frac{1}{v}\Big) = -\frac{1}{v^2}v_{,i} \ , \tag{3.40}$$

and τ can be easily obtained from

$$\frac{\mathrm{d}\tau}{\mathrm{d}s} = \frac{1}{v} \; .$$

(3.41)

3. For $\eta = 2$, the simplest form of the RTS is obtained (it does not contain v in the equations for x_i's)

$$\frac{\mathrm{d}x_i}{\mathrm{d}\sigma} = p_i \quad \frac{\mathrm{d}p_i}{\mathrm{d}\sigma} = \frac{1}{2}\frac{\partial}{\partial x_i}(\frac{1}{v^2}) = \frac{1}{2}(v^{-2})_{,i} \; ,$$

(3.42)

and for τ we have

$$\frac{\mathrm{d}\tau}{\mathrm{d}\sigma} = \frac{1}{v^2} \; .$$

(3.43)

4. Finally, for $\eta = -1$ we write the RTS

$$\frac{\mathrm{d}x_i}{\mathrm{d}\varsigma} = v^3 p_i \quad \frac{\mathrm{d}p_i}{\mathrm{d}\varsigma} = -\frac{\partial v}{\partial x_i} \; ,$$

(3.44)

and τ is given by

$$\frac{\mathrm{d}\tau}{\mathrm{d}\varsigma} = v \; .$$

(3.45)

This form of the RTS is particularly useful for gradient media in which v depends linearly on space coordinates.

There are possibly other choices of η in (3.34) or possibly other choices for the Hamiltonian itself, leading to alternative forms of the RTS. These are, however, beyond the scope of this book.

Let us note that to calculate rays and travel times along rays in an isotropic medium, the model is fully described by distribution of velocities $v = \alpha$ or $v = \beta$. None of the ray tracing equations depend on the density of the medium. In ray kinematics, the density is not used as a medium parameter despite the fact that it stands in the equation of motion. It is relevant only when dealing with ray amplitudes.

In order to calculate rays using the RTS, initial conditions for x_i's, p_i's and τ must be specified. Thus, we have to specify the point $x_{i0} = x_i(u_0)$ (source) from which the rays are emitted, the initial slowness $p_{i0} = p_i(u_0)$ which must satisfy $p_{i0}p_{i0} = v^{-2}(x_{i0})$ for the given type of wave (either P- or S-, i.e., we take $v = \alpha$ or $v = \beta$ in the condition as well as in the RTS), and the initial time $\tau_0 = \tau(u_0)$. Alternatively, instead of p_{i0} we can specify only the direction of the initial slowness, since its magnitude is constrained by the eikonal equation at x_{i0}. One such possibility, used often in applications, is to employ two angles, declination ψ and azimuth ϑ as follows: $p_{10} = v^{-1}(x_{i0}) \sin\psi(x_{i0}) \cos\vartheta(x_{i0})$, $p_{20} = v^{-1}(x_{i0}) \sin\psi(x_{i0}) \sin\vartheta(x_{i0})$, and $p_{30} = v^{-1}(x_{i0}) \cos\psi(x_{i0})$.

Note that not all of the equations in the RTS (3.36) (and the corresponding equations for specific choices of the flow parameter along the ray) are independent. Because of the eikonal equation (3.32), being satisfied (by definition) along rays, and constraining p_i's, only two slowness components can be calculated using the RTS. When all three slowness components are obtained from the RTS, the constraint condition can be used to check the accuracy or to correct the solution at each step Δu in the case of the numerical solution of the RTS equations.

The number of the RTS equations decreases further in certain simpler situations, namely in the case of lower dimensionality of the structure model. Let us first consider a 2D model, in which velocity does not vary along one coordinate direction. Without loss of generality let this coordinate be x_2. We then call the plane x_1-x_3 the plane of the symmetry of such a model. For general initial conditions (general initial direction of a ray, not related in any sense to the plane of the model symmetry) we compute a 3D ray in the 2D model. Such computations are usually called as $2\frac{1}{2}$-dimensional. In this case the RTS reduces to four equations for x_1, x_3, and p_1, p_3 of exactly the same form as above ((3.36), (3.39) – (3.44)), generally requiring a numerical solution, plus two equations for x_2 and p_2, for which we have a straightforward 'analytical' solution. In its simplest form it can be written for the parameter σ (for which x_i's does not depend explicitly on velocity) as

$$x_2 = x_{20} + p_{20}(\sigma - \sigma_0), \quad p_2 = p_{20} , \tag{3.46}$$

i.e., p_2 is a constant and x_2 grows linearly with σ. For any other flow parameter we would also obtain the constant p_2 (thanks to vanishing derivative of the corresponding power of velocity in the equation for p_2), but equation for x_2 would moreover contain some power of velocity in its linear term. Since velocity varies with x_1 and x_3, to solve the equation for x_2 would require

to perform a simple quadrature. To summarize, in the case of $2\frac{1}{2}$D computations of rays, we solve (usually numerically) exactly the same equations as in the general 3D case in the plane x_1-x_3. These equations are supplemented by a very simple equation for x_2. The p_2 slowness component need not be calculated as it remains constant along the whole ray. Similarly as in a general 3D case, one of the equations for p_1 and p_3 can be optionally replaced by the constraint for p_i's — the eikonal equation (3.32). The initial slowness must also satisfy this constraint. Thus, $p_{10}^2 + p_{30}^2 = 1/v_0^2 - p_{20}^2$, where $v_0 = v(x_{10}, x_{30})$. In this way, via initial conditions, p_{20} influences the solution of the equations in the x_1-x_3 plane. Let us add finally that, as it can be shown easily from (3.46), the projection of a ray into the x_1-x_2 plane (the map view) is not a straight line. It means that, eventhough the model is only 2D, the ray represents a 3D curve.

For special choice of the initial slowness conditions such that $p_{20} = 0$, the situation simplifies even further. The p_2 component remains equal to zero along the whole ray. Therefore the x_2 ray coordinate remains equal to its initial value x_{20}, see (3.46). Thus the ray is an in-plane ray, situated in the plane perpendicular to x_2-axis, i.e., the plane x_1-x_3. The ray calculation is fully two-dimensional (a 2D ray is computed in 2D medium), described completely by the four RTS equations for x_1, x_3, and p_1, p_3, with corresponding initial conditions $x_{10}, x_{30}, p_{10}, p_{30}$ with $p_{10}^2 + p_{30}^2 = 1/v_0^2$.

Further simplification is possible in 1D models in which velocity varies in one direction only. Let this direction be the direction of the x_3-axis (usually vertical). Then, if we rotate the coordinate system along the x_3-axis axis to make the initial slowness vector being situated in the plane x_1-x_3, the p_{20} component will vanish, similarly as in the previous case. Thus, $p_2 = p_{20} = 0$ along the whole ray (thanks to the velocity independence on x_2) and $x_2 = x_{20}$. The whole ray is situated in the plane x_1-x_3. However, in contrast to the 2D model, we have moreover $p_1 = p_{10}$ (thanks to the velocity independence on x_1) and $x_1 = x_{10} + p_{10}(\sigma - \sigma_0)$. The horizontal slowness p_1, remaining constant along the whole ray, is often called the ray parameter and denoted traditionally as p ($p \neq |\mathbf{p}|$). Provided we use other flow parameter than σ, the equation for x_1 contains the corresponding power of velocity in the linear term, but this does not complicate the situation in a principal way; the equation can still be solved by a simple quadrature. From the RTS, only the two equations for x_3 and p_3 retain their original form and must be, in general, solved by standard numerical solvers under the initial conditions $x_{30}, p_{30} = \pm(1/v_0^2 - p_{10}^2)^{1/2}$. Despite the model is 1D, the problem of the ray computation is 2D, since we need two coordinates (x_1 and x_3) to describe rays, 2D in-plane curves. The problem would become fully 1D only for $p_{10} = 0$, in which case the ray would be a vertical straight line.

In certain simple structures (simple velocity distributions) the RTS can

be solved analytically. Let us name here only two examples: the case of a homogeneous medium and that of a medium with velocity increasing linearly in one direction (1D gradient model). The reader is encouraged to derive in detail the following equations.

In homogeneous media, described by the velocity v_0, the slowness preserves its initial value and from the equation for $\mathrm{d}x_i/\mathrm{d}u$ in (3.36) we have

$$x_i = x_{i0} + v_0^{2-\eta} p_{i0}(u - u_0) \tag{3.47}$$

which is the parametric equation of a straight line. The rays in homogeneous isotropic media are thus straight lines starting from the source in a direction prescribed by the initial conditions for p_i. (The analogous conclusion about rays we will be able to make even for anisotropic homogeneous media, see Sec. 3.6.) The wavefronts are spheres. In the plane x_1-x_3, we obtain from the RTS (3.36), with $x_{20} = p_{20} = 0$, by substituting $\tau - \tau_0$ from (3.37) instead of $u - u_0$, the parametric equation of a circle with its center at $[x_{10}, x_{30}]$ and radius $v_0(\tau - \tau_0)$:

$$(x_1 - x_{10})^2 + (x_3 - x_{30})^2 = [v_0(\tau - \tau_0)]^2 \ . \tag{3.48}$$

For $\tau = const$ this represents the equation of wavefront in the plane x_1-x_3. Wavefronts together with a family of rays shot from a point source with evenly spaced declination are plotted in Fig. 6.

It can be easily shown, using the RTS (3.44), that in a gradient model the rays are segments of circles. For example, in the model with linearly increasing velocity in the vertical direction (x_3), $v(x_i) = v_0 + a_3(x_3 - x_{30})$, where v_0 is the velocity value at the source depth, $v_0 = v(x_{i0}) = v(x_{30})$ (v does not depend on x_1, x_2), (3.44) yields in the plane x_1-x_3 (i.e., for $x_{20} = p_{20} = 0$) that

$$(x_1 - x_{10} - \frac{p_{30}v_0}{a_3}p_{10})^2 + (x_3 - x_{30} - \frac{v_0}{a_3})^2 = [\frac{1}{a_3 p_{10}}]^2 \ , \tag{3.49}$$

which is the equation of a circle with the center $[x_{10} + \frac{p_{30}v_0}{a_3}p_{10}, x_{30} - \frac{v_0}{a_3}]$ and the radius $\frac{1}{a_3 p_{10}}$. It can be shown that the wavefronts are again spheres like in the previous example of a homogeneous structure. However, in the model with the vertical gradient of velocity, the center of the spheres is not fixed — it moves along a vertical line downwards. The expression for the sphere
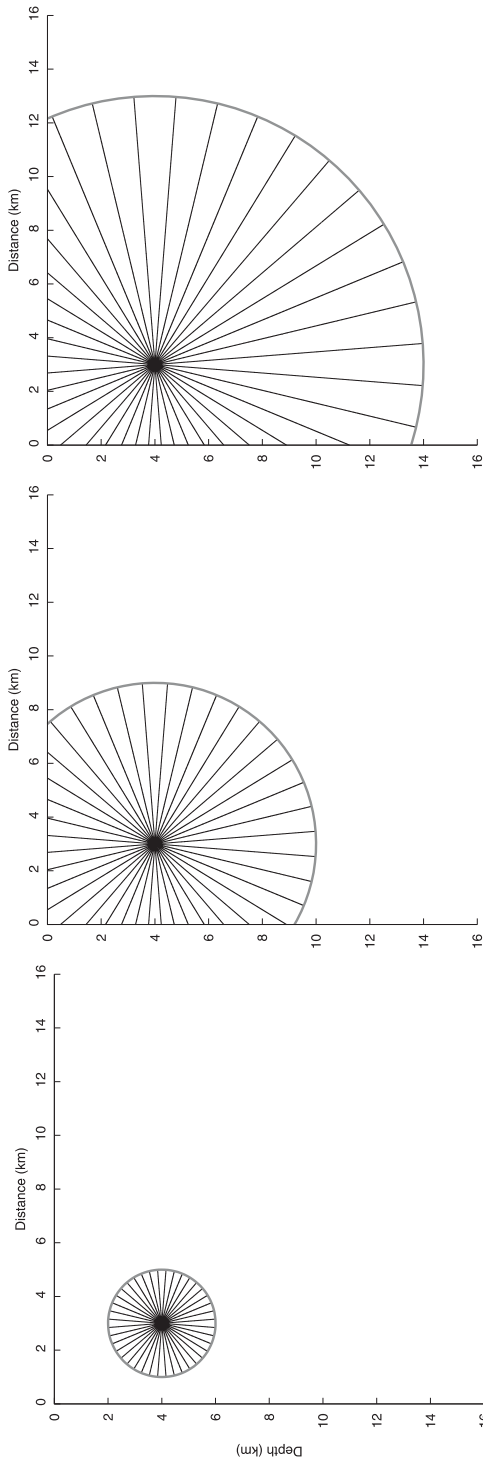
Figure 6: Rays (black) and wavefronts (gray) at three different time instants (1s, 3s and 5s) in the homogeneous structure $v(x_i) = v_0$, $v_0 = 2$ kms^{-1}. The rays are emitted from a point source at depth of 4 km.
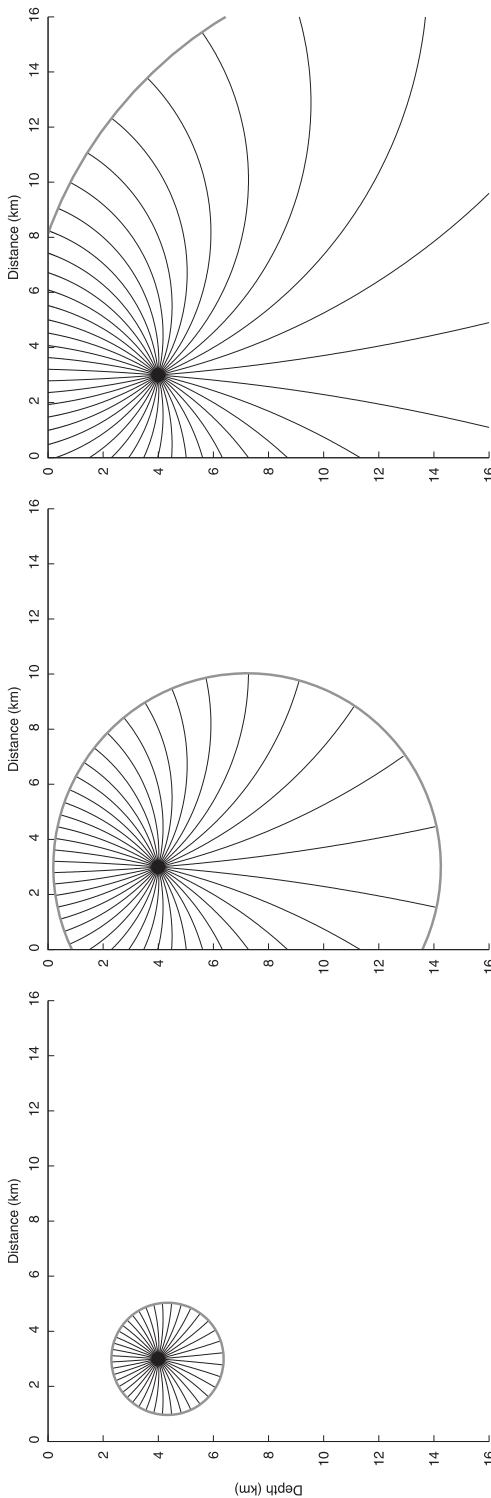
Figure 7: The same as in Fig. 6, but for the structure with constant vertical gradient of velocity: $v(x_i) = v_0 + a_3(x_3 - x_{30})$, $v_0 = 3.33 \text{ kms}^{-1}$, $a_3 = 1/3 \text{ s}^{-1}$, $x_{30} = 4 \text{ km}$.

radius is also different from that in homogeneous media. In the plane x_1, x_3, the wavefronts are circles given by the equation

$$[x_1 - x_{10}]^2 + [x_3 - x_{30} + \frac{v_0}{a_3}(1 - \cosh(a_3(\tau - \tau_0)))]^2 = [\frac{v_0}{a_3}\sinh(a_3(\tau - \tau_0))]^2,$$

$$(3.50)$$

with $\tau = const$. The family of rays and corresponding wavefronts in a particular gradient model are depicted in Fig. 7.

For general (realistic) models, however, an analytical solution of the RTS is not available. The equations have to be solved numerically by the use of a suitable standard procedure (e.g., the Runge-Kutta method or the predictor-corrector method, etc., see Červený et al., 1988). The step Δu in the integration (affecting the numerical efficiency of the computations) depends on the smoothness of the structure. The accuracy is kept under a prescribed limit by successive local halving of the step wherever it is necessary. For details the interested reader is referred to arbitrary textbooks on numerical methods (see also Press et al., 1996).

Instead of the Cartesian coordinates, it would be also useful to rewrite the eikonal equation and the RTS into some curvilinear (orthogonal) coordinates, e.g. the spherical coordinates which are of great importance in global seismology. This can be done by the use of the well known Lame's scale factors h_i, determined from the expression for the square of the infinitesimal length element $\mathrm{d}s^2$. The spherical coordinates r (radius), θ (colatitude) and ϕ (longitude) are defined by the relations $x_1 = r\sin\theta\cos\phi, x_2 = r\sin\theta\sin\phi, x_3 = r\cos\theta$. Then, $\mathrm{d}s^2 = \mathrm{d}r^2 + r^2\mathrm{d}\theta^2 + r^2\sin^2\theta\mathrm{d}\phi^2$ from which we have the scale factors for the spherical coordinates $h_r = 1$, $h_\theta = r$ and $h_\phi = r\sin\theta$. The spherical components of the slowness vector read

$$p_r = \tau_{,r}, \quad p_\theta = \frac{1}{r}\tau_{,\theta}, \quad p_\phi = \frac{1}{r\sin\theta}\tau_{,\phi} . \qquad (3.51)$$

The RTS can be written in various forms, for various flow parameters along the ray. For detailed derivation see Červený (2001). Here let us present the simplest form for the parameter σ

$$
\begin{aligned}
\frac{\mathrm{d}r}{\mathrm{d}\sigma} &= \tau_{,r} & \frac{\mathrm{d}\tau_{,r}}{\mathrm{d}\sigma} &= \frac{1}{2}\frac{\partial}{\partial r}(\frac{1}{v^2}) + \frac{1}{r}(\frac{1}{v^2} - \tau_{,r}^2) , \\
\frac{\mathrm{d}\theta}{\mathrm{d}\sigma} &= \frac{\tau_{,\theta}}{r^2} & \frac{\mathrm{d}\tau_{,\theta}}{\mathrm{d}\sigma} &= \frac{1}{2}\frac{\partial}{\partial\theta}(\frac{1}{v^2}) + \frac{1}{r^2}\frac{\tau_{,\phi}^2\cos\theta}{\sin^3\theta} , \\
\frac{\mathrm{d}\phi}{\mathrm{d}\sigma} &= \frac{\tau_{,\phi}}{r^2\sin^2\theta} & \frac{\mathrm{d}\tau_{,\phi}}{\mathrm{d}\sigma} &= \frac{1}{2}\frac{\partial}{\partial\phi}(\frac{1}{v^2}).
\end{aligned}
\qquad (3.52)
$$

The travel time is given by

$$\frac{d\tau}{d\sigma} = \frac{1}{v^2} \ . \tag{3.53}$$

The system (3.52) can be modified into a very suitable form by introducing a new variable ϱ instead of the radial distance r by the relation $\varrho = \ln r$, and by taking a new flow parameter κ instead of σ: $d\kappa = r^{-2}d\sigma$. The new form of the RTS then reads

$$
\begin{aligned}
\frac{d\varrho}{d\kappa} &= \tau_{,\varrho} & \frac{d\tau_{,\varrho}}{d\kappa} &= \frac{1}{2}\frac{\partial w^2}{\partial \varrho} \ , \\
\frac{d\theta}{d\kappa} &= \tau_{,\theta} & \frac{d\tau_{,\theta}}{d\kappa} &= \frac{1}{2}\frac{\partial w^2}{\partial \theta} + \frac{\tau_{,\phi}^2 \cos\theta}{\sin^3\theta} \ , \\
\frac{d\phi}{d\kappa} &= \frac{\tau_{,\phi}}{\sin^2\theta} & \frac{d\tau_{,\phi}}{d\kappa} &= \frac{1}{2}\frac{\partial w^2}{\partial \phi} \ ,
\end{aligned}
\tag{3.54}
$$

with $w = r/v$. For travel time we have

$$\frac{d\tau}{d\kappa} = w^2 \ . \tag{3.55}$$

The advantage and importance of this modified RTS in the spherical coordinates will become clear if we deal with less dimensional media. When considering, e.g., a 2D medium, not depending on the longitude ϕ, and an initial slowness direction in the plane $\phi = const$, the RTS (3.54) simplifies to

$$
\begin{aligned}
\frac{d\varrho}{d\kappa} &= \tau_{,\varrho} & \frac{d\tau_{,\varrho}}{d\kappa} &= \frac{1}{2}\frac{\partial w^2}{\partial \varrho}, \\
\frac{d\theta}{d\kappa} &= \tau_{,\theta} & \frac{d\tau_{,\theta}}{d\kappa} &= \frac{1}{2}\frac{\partial w^2}{\partial \theta} \ .
\end{aligned}
\tag{3.56}
$$

This system is of the exactly same form as the 2D RTS (for calculation a 2D ray in a 2D medium) in Cartesian coordinates, provided we transform

$$
\begin{aligned}
x_1 &\rightarrow \theta, & x_3 &\rightarrow \varrho = \ln r, & 1/v^2 &\rightarrow w^2 = r^2/v^2 \ , \\
p_1 &\rightarrow \tau_{,\theta}, & p_3 &\rightarrow \tau_{,\varrho}, & d\sigma &\rightarrow d\kappa = 1/w^2 d\tau.
\end{aligned}
\tag{3.57}
$$

This transformation, called the **Earth flattening transformation** (EFT, see Miller, 1977, Jobert and Jobert, 1987, or Červený, 2001) finds a lot of practical use. Thanks to this transformation, any computer program for 2D ray tracing in Cartesian coordinates can be directly used for 2D ray tracing in polar coordinates r and θ (and vice versa) by a simple modification of the input and output data. Also any analytic solution in the plane $x_1 - x_3$ can be easily taken into coordinates r, θ by the use of this transformation. The transformation is also utilized in the program ZRAYAMP, designed for calculations in a spherically symmetric Earth. The program is described and documented in Chap. 8.

3.4 Rays as extremals of Fermat's functional

It can be easily shown that the rays, defined as characteristics of the eikonal equation, are identical with the curves defined by the Fermat principle. The Fermat's principle is sometimes used for an alternative definition of rays, but such an approach is less general in certain aspects than that applied in the previous section. For example, when using the Fermat's principle to derive rays, the separation of P- and S-waves must be assumed a priori without clear physical justification. In the approach adopted in this book, the separation of the P- and S- wavefields has been derived under the assumption of our form of the solution (i.e., in high-frequency approximation). It has been derived when obtaining the eikonal equations (see Sec. 3.1), so that it is natural to calculate rays for the P- and S- waves separately from the corresponding eikonal equations.

Let us consider the so-called Fermat's functional

$$I = \int\limits_S^R d\tau \ , \tag{3.58}$$

with τ being the travel time of a signal (in our case seismic) that it needs to propagate from a fixed point S to another fixed point R. The travel time is integrated along a curve connecting the two points.

In the Fermat's principle we seek a curve (integration path) connecting the points S and R along which the value of this integral is stationary. This condition means that the variance of the integral, δI, vanishes:

$$\delta I = \delta \int\limits_S^R d\tau = 0 \ . \tag{3.59}$$

The integration path corresponding to the stationary value of the Fermat's integral is called the extremal of the Fermat's functional. In general, there

may be more than one stationary value and, consequently, more than one extremal connecting the two points S and R. This case corresponds to the so-called multipathing – a common situation in seismology accompanied by multi-valuedness of the travel time between S and R.

Let u be a general monotonic flow parameter along such a curve. It is convenient to rewrite the functional (3.58) in a parametric form

$$I = \int_S^R \frac{\mathrm{d}\tau}{\mathrm{d}u}\mathrm{d}u = \int_S^R L(x_i, x_i')\mathrm{d}u \ , \tag{3.60}$$

where $x_i = x_i(u)$ and $x_i' = \frac{\mathrm{d}x_i(u)}{\mathrm{d}u}$. In analogy to Hamiltonian mechanics, the travel time τ plays the role of the action and its derivative along the curve, $L(x_i, x_i')$, can be identified as the Lagrangian of the system. As $\delta I = 0$, the Lagrangian satisfies the well known Euler-Lagrangian equations

$$\frac{\mathrm{d}}{\mathrm{d}u}\left(\frac{\partial L}{\partial x_i'}\right) - \frac{\partial L}{\partial x_i} = 0 \ . \tag{3.61}$$

Therefore, solving the Euler-Lagrangian equations we can find the extremal $x_i = x_i(u)$ of the Fermat's principle.

In isotropic media, the functional can be simply written as

$$I = \int_S^R \frac{\mathrm{d}s}{v} \ , \tag{3.62}$$

where v is either α or β (being a function of position: $v = v(x_i)$) and s is the arclength along the integration path. In Cartesian coordinates, the infinitesimal length element $\mathrm{d}s$ satisfies

$$\mathrm{d}s^2 = \mathrm{d}x_i\mathrm{d}x_i = (\mathrm{d}x_1)^2 + (\mathrm{d}x_2)^2 + (\mathrm{d}x_3)^2 \ . \tag{3.63}$$

Thus, $\mathrm{d}s$ can be expressed in terms of x_i''s as

$$\mathrm{d}s = (x_i'x_i')^{1/2}\mathrm{d}u \ , \tag{3.64}$$

and the functional (3.62) reads

$$I = \int_S^R \frac{1}{v(x_i)}(x_i'x_i')^{1/2}\mathrm{d}u \ . \tag{3.65}$$

This equation is already in the parametric form (3.60) with the Lagrangian $L(x_i, x_i') = v^{-1}(x_i)(x_i'x_i')^{1/2}$. Expressing the derivatives of L in equations (3.61) we obtain

$$\frac{\mathrm{d}}{\mathrm{d}u}\left(\frac{1}{v}\frac{x_i'}{(x_i'x_i')^{1/2}}\right) - \frac{\partial}{\partial x_i}\left(\frac{1}{v}\right)(x_i'x_i')^{1/2} = 0 \ . \qquad (3.66)$$

These are the equations for an extremal of the Fermat's functional in an isotropic media written using a general flow parameter along the curve. If we choose specially $u = s$ (i.e., the flow parameter equals the arclength) we obtain from (3.64) $(x_i'x_i')^{1/2} = 1$, so that

$$\frac{\mathrm{d}}{\mathrm{d}s}\left(\frac{1}{v}\frac{\mathrm{d}x_i}{\mathrm{d}s}\right) = \frac{\partial}{\partial x_i}\left(\frac{1}{v}\right) \ . \qquad (3.67)$$

This equation is exactly in the form of the second-order RTS (3.38) for $u = s$ (i.e., $\eta = 1$). Thus, we have proved that the extremals of the Fermat's principle are identical with the rays derived as characteristics of the eikonal equation.

3.5 Rays as energy flux trajectories

In this section we first prove that in isotropic media, rays are orthogonal to wavefronts. Then it will be easy to prove that rays represent trajectories along which the high-frequency part of energy flows because, in isotropic media, the direction of the energy flux is perpendicular to wavefronts.

Let us assume an orthogonal curve to a wavefront, parameterized by arclength s, $x_i = x_i(s)$. The unit vector $\mathbf{t}$, tangent to the curve ($t_i = \mathrm{d}x_i/\mathrm{d}s$), must be parallel to the slowness vector, since the slowness is perpendicular to the wavefront by definition. Therefore, it is given by

$$t_i = \frac{\mathrm{d}x_i}{\mathrm{d}s} = vp_i \ . \qquad (3.68)$$

The last equality in the above equation is due to the requirement of unit magnitude of the vector and of its direction parallel to $\mathbf{p}$. The equation (3.68) represents the first part of the RTS with s as the parameter along the ray, see (3.40). To derive a complete set of differential equations for the orthogonal trajectories we must also find equations for $\mathrm{d}p_i/\mathrm{d}s$. Utilizing the eikonal equation $p_ip_i = v^{-2}$ we have

$$\begin{aligned}
\frac{\mathrm{d}p_i}{\mathrm{d}s} &= \frac{\partial p_i}{\partial x_j}\frac{\mathrm{d}x_j}{\mathrm{d}s} = vp_j\frac{\partial}{\partial x_j}\left(\frac{\partial\tau}{\partial x_i}\right) = vp_j\frac{\partial}{\partial x_i}\left(\frac{\partial\tau}{\partial x_j}\right) \\
&= vp_j\frac{\partial p_j}{\partial x_i} = \frac{1}{2}v\frac{\partial}{\partial x_i}(p_jp_j) = \frac{1}{2}v\frac{\partial}{\partial x_i}\left(\frac{1}{v^2}\right) = \frac{\partial}{\partial x_i}\left(\frac{1}{v}\right) \ .
\end{aligned}$$

This represents the second part of the RTS for flow parameter s, compare (3.40). Thus, the conclusion is that **in isotropic media rays are orthogonal to wavefronts**. This also means that the slowness vector is tangent to a ray at any point of the ray.

Further let us show that the group velocity vector $\mathbf{v}^g$, pointing in direction of energy flux, is perpendicular to wavefronts. The group velocity is given as the ratio between the energy flux vector $\mathbf{S}$ (analogous to the Poynting vector known from the theory of electromagnetism) and the total elastic energy E, which is the sum of the strain energy E_W and kinetic energy E_K. The expressions for these quantities are well known from continuum mechanics:

$$v_i^g = \frac{S_i}{E} \ , \tag{3.69}$$

$$S_i = -c_{ijkl}u_{k,l}\dot{u}_j \ , \tag{3.70}$$

$$E = E_W + E_K = \frac{1}{2}c_{ijkl}\varepsilon_{ij}\varepsilon_{kl} + \frac{1}{2}\rho\dot{u}_i\dot{u}_i \ , \tag{3.71}$$

where ε_{ij} are strain tensor elements which can be expressed in terms of displacement $\mathbf{u}$ as $\varepsilon_{ij} = \frac{1}{2}(u_{i,j} + u_{j,i})$.

We have to insert our zero order ray solution for $\mathbf{u}$ into above energy-related quantities. However, since the energy expressions are nonlinear in $\mathbf{u}$, we cannot use the complex-valued form of the solution. We should use only the real part of it, written in a compact form as $\mathbf{u} = \frac{1}{2}(\mathbf{U}F + \mathbf{U}^*F^*)$, where the asterisk denotes complex-conjugate quantities. When inserting for $\mathbf{u}$ the corresponding expression for isotropic media ((3.26) for P- and (3.27) for S-waves), we easily show that the group velocity satisfies (both for P- and S-waves)

$$v_i^g = vn_i^\tau \ , \tag{3.72}$$

where $\mathbf{n}^\tau$ is the unit vector perpendicular to the wavefront and v is either α or β. This means that the group velocity vector is parallel to the slowness vector, i.e., similarly as $\mathbf{p}$, the group velocity vector is tangent to a ray at any point of the ray. Thus, in isotropic media, **rays represent the energy**

flux trajectories under the high-frequency approximation. In other words, the high-frequency part of the elastic energy flows along rays.

3.6   Ray tracing system in anisotropic media

In anisotropic media, rays can be defined in the same way as we have done in isotropic models, i.e. as characteristic curves of the eikonal equation. The eikonal equation can be written in the form (see (3.16))

$$G_m(x_i, p_i) = 1 \ , \tag{3.73}$$

where $m = 1$ or 2 or 3.

   We rewrite it in the form of the Hamilton-Jacobi equation

$$H(x_i, p_i) = 0 \ ,$$

by assigning, e.g.,

$$H = \frac{1}{2}(G_m - 1) \ . \tag{3.74}$$

As we will see later, the factor $\frac{1}{2}$ in H is closely connected with the choice of the specific parameter along the ray (in this case the travel time τ). When another flow parameter would be more suitable for a particular application, the Hamiltonian H should have to be properly modified. The canonical equations for characteristics then yield

$$
\begin{aligned}
\frac{\mathrm{d}x_i}{\mathrm{d}u} &= \frac{\partial H}{\partial p_i} = \frac{1}{2}\frac{\partial G_m}{\partial p_i} \ , \\
\frac{\mathrm{d}p_i}{\mathrm{d}u} &= -\frac{\partial H}{\partial x_i} = -\frac{1}{2}\frac{\partial G_m}{\partial x_i} \ , \\
\frac{\mathrm{d}\tau}{\mathrm{d}u} &= p_i\frac{\partial H}{\partial p_i} = \frac{1}{2}p_i\frac{\partial G_m}{\partial p_i} \ .
\end{aligned}
\tag{3.75}
$$

   It is not difficult to show that, similarly to the elements of the Christoffel matrix Γ_{ij}, also its eigenvalues G_m are homogeneous functions of the second order in p_i and they satisfy (due to the Euler's theorem)

$$p_i\frac{\partial G_m}{\partial p_i} = 2G_m \ . \tag{3.76}$$

Thus, from the last equation in (3.75) we obtain

$$\frac{\mathrm{d}\tau}{\mathrm{d}u} = G_m = 1 \tag{3.77}$$

(the last equality being the consequence of the eikonal equation (3.73)). Thus, for our particular choice of H, the flow parameter along the ray is equal to τ and the RTS reduces to six equations

$$\frac{\mathrm{d}x_i}{\mathrm{d}\tau} = \frac{1}{2}\frac{\partial G_m}{\partial p_i} \ , \quad \frac{\mathrm{d}p_i}{\mathrm{d}\tau} = -\frac{1}{2}\frac{\partial G_m}{\partial x_i} \ . \tag{3.78}$$

In general anisotropic media, it is not possible to find analytic expressions for G's; the eigenvalues are to be found numerically. Nevertheless, we can make the ray tracing equations (3.78) more explicit by expressing G_m in terms of Γ_{ij} (3.3) and components of the corresponding eigenvector $\mathbf{g}^{(m)}$. When multiplying (3.6) by g_i (for a given m) and taking into account that the eigenvectors are unit vectors we immediately obtain

$$G_m = \Gamma_{ik}g_i^{(m)}g_k^{(m)} = a_{ijkl}p_jp_lg_i^{(m)}g_k^{(m)} \ , \tag{3.79}$$

where a_{ijkl} are density normalized elastic parameters, $a_{ijkl} = c_{ijkl}/\rho$. Substituting this G_m into the Hamiltonian in (3.75) or directly to the equations (3.78) we come to the RTS in the form

$$\frac{\mathrm{d}x_i}{\mathrm{d}\tau} = a_{ijkl}p_lg_j^{(m)}g_k^{(m)}, \quad \frac{\mathrm{d}p_i}{\mathrm{d}\tau} = -\frac{1}{2}\frac{\partial a_{jkln}}{\partial x_i}p_kp_ng_j^{(m)}g_l^{(m)}. \tag{3.80}$$

Likewise in the case of isotropic media, the equations for x_i's and p_i's are coupled and must be solved together with proper initial conditions x_{i0} and p_{i0}. To be physically relevant, the p_{i0} must be chosen to satisfy the eikonal equation $G_m(x_{i0}, p_{i0}) = 1$ at the initial point x_{i0}. If the eikonal equation is satisfied for the initial conditions, it is satisfied anywhere along the ray given by the equations (3.80).

It would be possible to rewrite the RTS (3.80) into an alternative form by expressing analytically the products of $g_i^{(m)}$ or by the use of a certain other flow parameter, e.g. the arclength s. For details the reader is referred to Červený (2001).

3.7 Notes on the ray tracing system in anisotropic media

In this section we make several comments on rays and the RTS in anisotropic media.

First, let us realize that the RTS is exactly the same for all the three waves which can propagate in the given anisotropic model. The type of the wave must be specified by initial conditions, satisfying the eikonal equation $G_m = 1$ for a given m. Thus, in this respect, the initial conditions play even a more important role in anisotropic than in isotropic media. When the eikonal equation is satisfied at the initial point of the ray, the RTS keeps it satisfied along the whole ray, i.e. the type of wave does not change along the ray. This holds, of course, in smooth media only, for which the RTS has been derived. At structural interfaces the type of wave may change, see Sec. 3.8.

Second, on the right-hand sides of the RTS equations there are, besides the elastic moduli (model parameters) and slowness components (RTS solutions), the components of the eigenvectors, corresponding to the given type of wave. These vectors must therefore be known at each point of the ray. At each point we have to determine them (numerically) from the equations

$$(\Gamma_{ij} - G_m \delta_{ij})g_j^{(m)} = 0, \quad g_j^{(m)}g_j^{(m)} = 1 , \tag{3.81}$$

which, however, does not represent a numerical problem.

Next, let us concentrate on the first part of the RTS — the equations for $\frac{\mathrm{d}x_i}{\mathrm{d}\tau}$, the i-th component of a vector tangent to the ray. Compare the indices of the tangent vector component and of the slowness component on both sides of the equations: it is i (free index) in $\frac{\mathrm{d}x_i}{\mathrm{d}\tau}$ versus l in p_l in the right-hand side expression $a_{ijkl}p_l g_j^{(m)} g_k^{(m)}$. From this we can immediately conclude that, in general anisotropic media, the **tangent vectors to rays are not generally parallel to the slowness vectors along the rays**. But the slowness is always orthogonal to the wavefront by definition, thus, in anisotropic media, the **rays are not orthogonal to wavefronts** like in the isotropic case. From this it moreover follows that the initial conditions for p_i's, possibly translated into initial directional angles of the slowness, do not represent the initial direction of the ray.

Similarly to the isotropic case, even in anisotropic media the rays are identical with extremals of the Fermat principle, i.e. they are the curves rendering the Fermat functional stationary. However, in anisotropic models, the proof requires to take into account the so-called second-degree Langrangian, satisfying the same Euler-Lagrange equations. The modified Lagrangian allows to apply the Legendre transform between the Lagrangian and the relevant Hamiltonian and to find directly the Hamiltonian canonical system of six ordinary differential equations of the first order (Hamiltonian ray

equations (3.75)) as a consequence of the Fermat principle. For a detailed treatment the reader is referred to the paper by Červený (2002).

Further, let us recall the general expressions for the energy-related quantities, see equations (3.69) – (3.71). If we substitute for **u** the corresponding (real-valued) anisotropic solution we can easily show that the group velocity is given as

$$v_i^g = a_{ijkl} p_l g_j^{(m)} g_k^{(m)} \ . \tag{3.82}$$

But this is exactly what stands in the right-hand sides of the equations (3.80) for $\frac{dx_i}{d\tau}$, having the meaning of components of a vector tangent to ray. We may thus conclude that in anisotropic media, similarly to the isotropic case, **energy of high-frequency elastic waves flows along rays**. However, in general, the energy does not flow perpendicularly to wavefronts; it may happen only locally, or for certain special symmetries of the elastic parameters.

From the numerical point of view, the RTS in anisotropic structures fails provided two eigenvalues coincide or are close to each other in their values. In such a case the eigenvectors in the right-hand sides of the RTS are not determined uniquely from (3.81). This can happen for the two qS-waves (and the corresponding eigenvalues G_1 and G_2) either globally or locally. Globally it means throughout the whole model like in isotropic or weakly anisotropic media (close to isotropic). In the case of a weak anisotropy a difficulty arises due to qS-wave coupling and can be avoided by, e.g., various perturbation approaches (for details see Červený, 2001). However, even in the case of a stronger anisotropy, G_1 may coincide with or be close to G_2 locally, in the vicinity of quasi-shear wave singular directions. Let us explain this using the concept of the so-called slowness surface, see Fig. 8, comparing the slowness surfaces in an anisotropic (transversally isotropic) and isotropic model.

At a given point in the model, the slowness surface is represented by the endpoints of all slowness vectors pointing in all directions

$$p_i = c^{-1} n_i^\tau \ , \tag{3.83}$$

(compare (2.25)), where $\mathbf{n}^\tau$ is the unit normal to wavefront. When we specify directions of $\mathbf{n}^\tau$ in terms of two take-off angles, the slowness surface can be regarded as a spherical graph of the phase velocity reciprocal as $\mathbf{n}^\tau$ ranges over the unit sphere. The slowness (and, consequently, the phase velocity) is constrained by the condition (3.9). This reduces to cubic equations for the eigenvalues G (see Sec. 3.1), so, in general, there are three slowness
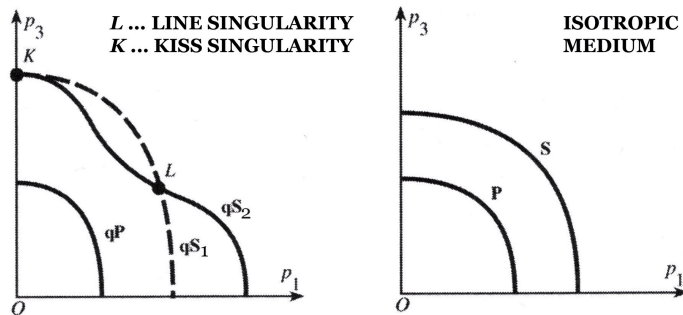
Figure 8: An example of slowness surfaces in a typical transversally isotropic (left) and isotropic medium (right), the p_1-p_3 cross-section (after Červený, 2001).

surfaces: one for the quasi-P and two for the quasi-S waves. Since the condition (3.9) is quadratic in p_i, the solutions are the same for $\pm\mathbf{p}$ and the slowness surfaces have the point symmetry. The slowness surfaces cannot be folded. Nevertheless, the quasi-S wave surfaces may touch or intersect each other for certain directions of $\mathbf{n}^\tau$ (so-called singular directions). In these directions, the eigenvalues G_1 and G_2 coincide. There are several types of such singularities, for details see, e.g., Červený (2001). Fig. 8 illustrates such a situation for a vertical transversally isotropic medium (anisotropic medium with vertical rotational symmetry). For comparison we see also slowness surfaces in an isotropic medium (two surfaces, for P- and S- waves).

3.8   Rays across interfaces

Now we know how to calculate rays and travel times in smooth media, both isotropic and anisotropic. To complete the basics of the ray kinematics it remains to explain how to calculate rays across structural interfaces (material discontinuities).

Let us assume two solid halfspaces in welded contact, separated by an interface Σ which is slightly curved (with radii of curvature much larger than the prevailing wavelength under study), see figure 9.

Assume a ray incident to this interface. At the point of incidence we define the unit normal $\boldsymbol{\nu}$ to the interface. The requirement of only slight curvature of the interface ensures that variations of the normal $\boldsymbol{\nu}$ to the interface within the distance of a prevailing wavelength λ are substantially smaller than unit: $\lambda|\nabla\nu_i| \ll 1$.

At the point of incidence, the slowness vector of the incident ray, $\mathbf{p}^\mathrm{I}$, is known. The normal may be oriented to either side of the interface; let us
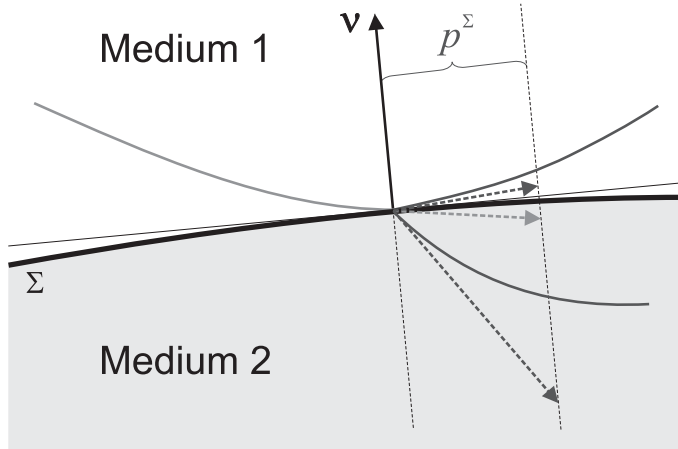
Figure 9: A ray incident to a slightly curved interface, separating two homogeneous halfspaces, gives rise to rays of a reflected and transmitted wave. The arrows represent the slowness vectors tangent to the corresponding rays at the point of incidence.

choose its orientation in such a way that $(\mathbf{p}^{\mathrm{I}}\cdot\boldsymbol{\nu}) < 0$, i.e., it is oriented into the first medium (the medium from which the wave incidents). The task is to calculate rays of generated waves (reflected and transmitted), which requires knowing their slowness vectors at the point.

We employ the boundary conditions (BC) at the interface. Let us assume both halfspaces, separated by the interface, to be solid and welded. In such a case, the BC require the continuity of displacement u_i and traction $T_i = c_{ijkl}\nu_j u_{k,l}$ across the interface. For another type of the interface (solid-fluid, solid-vacuum, etc.), the BC should be properly modified, but the basic idea explained in the following would be the same.

At the point of incidence, the incident wave gives rise to the reflected and transmitted waves. More specifically, in isotropic media there are, in general, four generated waves (two reflected and two transmitted), while in anisotropic media we can have 6 generated waves (three reflections and three refractions). The BC have to be satisfied by all the waves involved in the reflection/transmission (R/T) problem. Using the upper indices I, R and T for the incident, reflected, and transmitted waves respectively, we can write the boundary conditions in the form of six equations (for $i = 1, 2, 3$)

$$
\begin{aligned}
u_i^{\mathrm{I}} &= \sum_{n=1}^{K} u_i^{\mathrm{T}n} - \sum_{n=1}^{K} u_i^{\mathrm{R}n} \\
T_i^{\mathrm{I}} &= \sum_{n=1}^{K} T_i^{\mathrm{T}n} - \sum_{n=1}^{K} T_i^{\mathrm{R}n} ,
\end{aligned}
\tag{3.84}
$$

where K is either 2, in the case of an isotropic medium, or 3, for an

anisotropic structure.

The boundary conditions have to be satisfied at any time and at any point on the interface Σ. The only way to satisfy all the BC universally is that F and τ in its argument are exactly the same for both the incident wave as well as for all the generated waves. Following this argument further we find, that since τ as a function of $\mathbf{x}$ must be continuous across Σ (although τ itself may change along Σ), the same must hold for its derivative in any direction tangential to Σ. Thus we conclude that tangent slowness components p^{Σ} of all the generated waves are the same as that of the incident wave, see Fig. 9.

Tangent slowness component, however, is not enough to determine the complete slowness vector of a generated wave. For this we need to recall the eikonal equation, constraining the magnitude of the slowness vector.

More specifically, in isotropic media, utilizing the condition $p_i p_i = v^{-2}$ we can easily derive complete expressions for the slowness vectors $\mathbf{p}^{\mathrm{T}_n}$, $\mathbf{p}^{\mathrm{R}_n}$, of a transmitted and reflected wave, respectively

$$
\begin{aligned}
p_k^{\mathrm{T}_n} &= p_k^{\mathrm{I}} - (p_m^{\mathrm{I}}\nu_m)\nu_k + \left[\tfrac{1}{(v^{\mathrm{T}_n})^2} - \tfrac{1}{(v^{\mathrm{I}})^2} + (p_m^{\mathrm{I}}\nu_m)^2\right]^{1/2}\nu_k \\
p_k^{\mathrm{R}_n} &= p_k^{\mathrm{I}} - (p_m^{\mathrm{I}}\nu_m)\nu_k - \left[\tfrac{1}{(v^{\mathrm{R}_n})^2} - \tfrac{1}{(v^{\mathrm{T}_n})^2} + (p_m^{\mathrm{I}}\nu_m)^2\right]^{1/2}\nu_k \ .
\end{aligned}
\tag{3.85}
$$

Here, $v^{\mathrm{I}}, v^{\mathrm{R}_n}$ and v^{T_n} denote the propagation velocity of the incident and the reflected and transmitted wave we consider, either P- or S- (n equals 1 or 2). Note that the first two terms in the right-hand side of the equations (3.85), the subtraction of the incident slowness and its component normal to the interface, represent the tangential component of the slowness of the R/T waves (known due to the BC). The last term is the normal component of the slowness vector of the generated wave. The sign in front of this term is connected with the orientation of the normal $\boldsymbol{\nu}$ with respect to the propagation direction of the considered R/T wave. It is different for the reflected wave, going back to the first medium, and the transmitted wave, propagating into the second medium. For the orientation convention we adopted in the beginning of this section, we have to take the '+' sign in case of the transmitted wave and the '-' sign for the reflected wave.

It is evident, that the square-bracketed expressions in (3.85) may be of a negative value yielding a purely imaginary square root. The square root in (3.85) represents the slowness component normal to the interface. If the slowness is complex-valued we speak on the so-called inhomogeneous waves. From (3.85) it follows that such waves can be generated at the interface, for certain range of the angle of incidence (the acute angle between $\mathbf{p}^{\mathrm{I}}$ and $\boldsymbol{\nu}$),

if v^{T_n} (or v^{R_n}) is greater than v^{I}. In these course notes we deal only with real-valued slowness vectors and we have not defined rays corresponding to a complex-valued travel time. In the theory explained here, the rays of inhomogeneous waves are not calculated. Henceforth, we restrict ourselves to waves (and rays) with real-valued slownesses.

Alternatively, instead of using the general expressions (3.85) for the complete slowness of the generated waves, we can determine the slownesses $\mathbf{p}^{\mathrm{T}_n}$ and $\mathbf{p}^{\mathrm{R}_n}$ from their magnitudes (given by the corresponding eikonal equations) and their directions. The directions, expressed in terms of the angles of reflection and transmission (defined as acute angles between the normal $\boldsymbol{\nu}$ and the slowness of the corresponding R/T wave), can be found knowing the magnitudes and the tangential components. The equality of the tangential components of a transmitted wave and the incident wave, can be written in the form of the well known Snell's law

$$\frac{\sin i^{\mathrm{T}_n}}{v^{\mathrm{T}_n}} = \frac{\sin i^{\mathrm{I}}}{v^{\mathrm{I}}} \ . \tag{3.86}$$

The same formula would arise equating the tangential components of a reflected wave and the incident one except the upper index T_n would be replaced by R_n. Snell's law, yielding the direction, together with the eikonal equation, giving the magnitude, can be used equivalently to (3.85) to find the complete slowness vector of any wave generated at the interface. Both approaches involve the cases of possible wave conversions (P to S or S to P) by specifying the proper velocity of the generated wave.

The equality of the tangential components of the slownesses of all the generated waves and that of the incident wave is a universal principle valid both in isotropic as well as in anisotropic models. We can write a formula analogical to (3.86) even for anisotropic media

$$\frac{\sin i^{(m)}}{v^{(m)}(i^{(m)})} = \frac{\sin i^{\mathrm{I}}}{v^{\mathrm{I}}(i^{\mathrm{I}})} \ , \tag{3.87}$$

where the given generated wave is specified by $m = 1, 2, \ldots, 6$. However, in contrast to the isotropic case, this formula cannot be used to determine direction of the slowness vectors of generated waves, since in anisotropic media velocity is directionally dependent.

In anisotropic structures the only way how to find complete slownesses of generated waves is to constrain the normal components by the use of the condition of solvability of the eigenvalue problem (3.9). In the condition, let

us substitute for Γ_{ij} the corresponding expression quadratic in slowness, and decompose the slowness of the generated wave into its tangential component $\mathbf{p}^\Sigma$, which is known (common for all the involved waves), and the normal component $\mathbf{p}^\nu = |\mathbf{p}^\nu|\boldsymbol{\nu}$, which we seek. Then, assigning $G = 1$, the condition (3.9) becomes a sixth-order algebraic equation for $|\mathbf{p}^\nu|$

$$\det[a_{ijkl}(p_j^\Sigma + |\mathbf{p}^\nu|\nu_j)(p_l^\Sigma + |\mathbf{p}^\nu|\nu_l) - \delta_{ik}] = 0 \ . \qquad (3.88)$$

The density normalized medium parameters a_{ijkl} in (3.88) are specified either to correspond to the first halfspace, in case we are interested in reflected waves, or to the second halfspace, if we want to trace the rays of transmitted waves. In both cases, only three solutions for the slowness normal $|\mathbf{p}^\nu|$ are physically relevant. Nevertheless, from (3.88) we generally get six roots. The selection criterion for the solution is the direction of wave propagation (into the correct halfspace) away from the interface. Physically, the direction of propagation is the direction in which energy of the wave flows. This is also the direction tangent to ray. Thus, we select the correct solutions according the corresponding group velocity (3.82): for reflections it must point into the first halfspace, while for transmitted waves into the second one. Since, in general anisotropy, the direction of the group velocity differs from the direction of the phase velocity (i.e., direction of the slowness vector), it may happen that, for example, the slowness of a reflected wave points into the second halfspace what we could intuitively expect rather for transmitted waves. Such situations, quite common in anisotropic models, never happen in isotropic media in which directions of the group and phase velocities (and also that of the slowness vector) coincide.

   For a given elementary wave, knowing the formulas and rules to find slowness vectors of the waves generated by the wave incident at some slightly curved interface, we can continue tracing rays after interaction with the interface by setting the slowness of the required R/T wave as a new initial condition for the RTS at the point of incidence. In this way we are able to calculate rays (and travel times) not only throughout smooth continuous models, but also in models containing smooth layers or blocks separated by sharp structural discontinuities, both in isotropic and anisotropic media.

4 Two important ray-based coordinate systems

Before proceeding to the ray dynamics, based on the solution of the transport equations, see Sec. 2.5, we have to introduce two new coordinate systems, related to rays, which are extremely useful when computing ray amplitudes. These are namely the ray-centered coordinates and the ray coordinates. Despite similar names, their definition and properties are considerably different. The ray-centered coordinates are defined and discussed in section 4.1 for isotropic models in which they are used with advantage to simplify the evaluation of amplitudes, as the corresponding coordinate basis vectors are closely related to the ray amplitude polarization vectors. For completeness, analogous coordinates in anisotropic media are briefly mentioned at the end of Sec. 4.1. In the following text, however, they are not applied to calculate amplitudes in anisotropic media. The second of the coordinate systems presented in this chapter, the ray coordinates, is introduced in the section 4.2. It is defined in exactly the same way both in isotropic as well as anisotropic structures and in both these cases it is equally important for ray dynamics (see Chap. 5).

4.1 Ray-centered coordinates

The ray-centered coordinates (RCC) are very useful in a close vicinity of the ray. This ray, which can be considered as one axis of the RCC system, is called the central ray. Let us assume a central ray Ω and a point M in its vicinity, the position of which we want to describe using the RCC q_1, q_2, q_3, see figure 10.
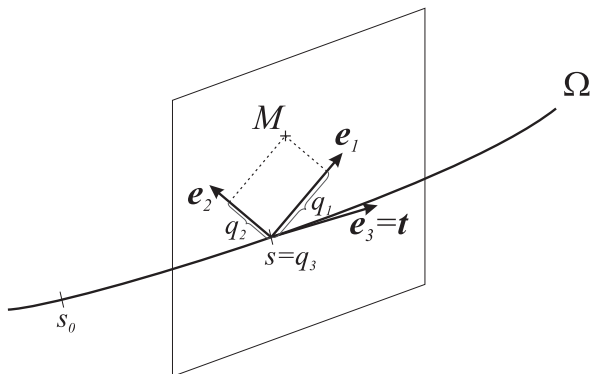
Figure 10: Ray-centered coordinate system.

A principal role in the RCC system is played by the plane perpendicular to the central ray, which passes through the point M. Having such a plane it is very simple to explain the physical meaning of the coordinates. The

last of the three numbers, q_3, has the meaning of a flow parameter along the ray u (mostly the arclength s). We have to specify an initial reference point u_0 on the central ray from which we can determine uniquely the position of any point on the ray. In the RCC, $q_3 = u - u_0$ determines the position of the point being a perpendicular projection of the point M to the central ray, i.e., the cross-section of the perpendicular plane and the central ray. The other two coordinates, q_1 and q_2 are the Cartesian coordinates of M in this perpendicular plane with the origin on the ray, see Fig. 10.

It is clear from how the coordinate system is constructed that it is regular only provided there is only one possible perpendicular plane from M to the central ray. Therefore, when using the RCC, we restrict ourselves to a small vicinity of the central ray (small in terms of q_1 and q_2), i.e. to distances much smaller than the radius of curvature of the central ray, so that there cannot be more than one perpendicular projection of M to the ray.

We define the RCC basis vectors in such a way that they represent an orthogonal right-handed triplet of unit vectors $\mathbf{e}_1, \mathbf{e}_2, \mathbf{e}_3$ at any point on the central ray specified by q_3. Note that along the ray, their position in space generally change, but in an exactly defined way. The vector $\mathbf{e}_3$, corresponding to the coordinate q_3, is the unit vector tangent to the ray (which we know from the RTS). The remaining two vectors are not only arbitrary unit vectors, mutually perpendicular and perpendicular to $\mathbf{e}_3$, but they are defined under the requirement of orthogonality of the coordinate system. This requirement is equivalent to the requirement of the so-called parallel transport of the vectors $\mathbf{e}_1, \mathbf{e}_2$ along the central ray. It means that a change of these vectors along the ray is parallel to a vector tangent to the ray. In other words, the two vectors do not rotate around the ray (more specifically: around the tangent to the ray). Using the flow parameter s this can be written as

$$\frac{\mathrm{d}\mathbf{e}_I(s)}{\mathrm{d}s} = a_I(s)\mathbf{p}(s) \ , \tag{4.1}$$

where a_I is a continuous function of s, $I = 1, 2$ (henceforth we keep the following index convention: an upper-case index is of values 1 or 2 while a lower-case index ranges from 1 to 3) and $\mathbf{p}$ is the slowness vector. This is the condition the RCC basis vectors $\mathbf{e}_I$ satisfy, but without knowing a_I, the equation (4.1) cannot be used to compute the vectors along the ray.

The factor of proportionality a_I in (4.1) can be easily found. By multiplying (4.1) with $\mathbf{p}$, and using the eikonal equation (3.32), we come to

$$a_I(s) = v^2 \frac{\mathrm{d}\mathbf{e}_I(s)}{\mathrm{d}s} \cdot \mathbf{p} \ . \tag{4.2}$$

This can be rewritten realizing that, in isotropic media, $\mathbf{e}_I$ is perpendicular to $\mathbf{p}$, so that $\mathbf{e}_I(s) \cdot \mathbf{p}(s) = 0$. Taking the derivative of this scalar vectorial product with respect to s, which must also be equal to zero, we immediately obtain the equality $\mathrm{d}\mathbf{e}_I/\mathrm{d}s \cdot \mathbf{p} = -\mathbf{e}_I \cdot \mathrm{d}\mathbf{p}/\mathrm{d}s$. When substituting this into (4.2), the equation becomes

$$a_I(s) = -v^2 \mathbf{e}_I(s) \cdot \frac{\mathrm{d}\mathbf{p}(s)}{\mathrm{d}s} \ . \tag{4.3}$$

Taking further into account the RTS equations $\mathrm{d}\mathbf{p}(s)/\mathrm{d}s = \nabla(1/v) = -v^2 \nabla v$ we obtain finally (4.1) in the form

$$\frac{\mathrm{d}\mathbf{e}_I}{\mathrm{d}s} = (\mathbf{e}_I \cdot \nabla \mathbf{v})\mathbf{p} \ . \tag{4.4}$$

Note that this equation is invariant with respect to a change of the flow parameter along the ray — it can be written in exactly the same form for any other suitable parameter, e.g., τ.

To summarize, the vectors $\mathbf{e}_I$ are defined to be unit, mutually perpendicular, attached to the central ray, belonging to the plane orthogonal to the central ray at any point of this ray, forming a right-handed triplet with $\mathbf{e}_3$, and subject to the equation (4.4). At a given reference point of the central ray, the vectors can be chosen to be rotated arbitrarily in the perpendicular plane. Then, at all the other points $\mathbf{x}(s)$ of the ray, their direction is uniquely determined by (4.4). In practice, the equation (4.4) is usually solved for only one of the two vectors $\mathbf{e}_I$; the other one is determined to complement (together with $\mathbf{e}_3 = \mathbf{t}$) the right-handed triad of unit mutually perpendicular vectors.

As it has been already mentioned above, an important consequence of the equation (4.4) is that it guarantees the RCC being orthogonal. The orthogonality of a coordinate system is defined in such a way that its metric tensor g_{ij} is diagonal. The metric tensor relates the square of the length element $\mathrm{d}l$ with the relevant coordinates (in our case q_i): $(\mathrm{d}l)^2 = \mathrm{d}\mathbf{r} \cdot \mathrm{d}\mathbf{r} = g_{ij}\mathrm{d}q_i\mathrm{d}q_j$ with $\mathbf{r}$ being radiusvector. It can be shown, see Červený (2001), that, provided (4.4) is satisfied, the only non-vanishing elements of g_{ij} are those for $i = j$.

Employing differential geometry of rays, one could take into account an-
other important right-handed triplet of mutually perpendicular unit vectors,
attached to the ray, known as the Frenet trihedral (see, e.g., Pujol, 2003).
The trihedral consists of the unit tangent vector $\mathbf{t}$ and the so-called nor-
mal $\mathbf{n}$ and binormal $\mathbf{b}$. For those familiar with this concept let us clarify
the difference between the two mentioned vector triplets: the RCC basis $\mathbf{e}_i$
and the trihedral $\mathbf{n}, \mathbf{b}, \mathbf{t}$. It may help to elucidate even more the properties
and behavior of the RCC basis. The vectors $\mathbf{e}_3$ and $\mathbf{t}$ coincide. In contrast
to $\mathbf{e}_I$, the normal and binormal rotates around ray. The variation of $\mathbf{b}$ is
perpendicular both to $\mathbf{b}$ and $\mathbf{t}$, so that it is parallel to $\mathbf{n}$

$$\frac{\mathrm{d}\mathbf{b}}{\mathrm{d}s} = -T(s)\mathbf{n} \; , \tag{4.5}$$

where T is known as the torsion of the curve (ray, in our case). The torsion
is related to the so-called Rytov angle φ, $\mathrm{d}\varphi/\mathrm{d}s = T(s)$, see also figure 11
comparing the two triplets along ray. Let us emphasize that a coordinate
system based on the Frenet trihedral would not be, in general, orthogonal.
Nevertheless, it would be always possible to calculate easily $\mathbf{e}_I$ knowing the
Frenet trihedral, for details see Čerevný (2001) or Pujol (2003).
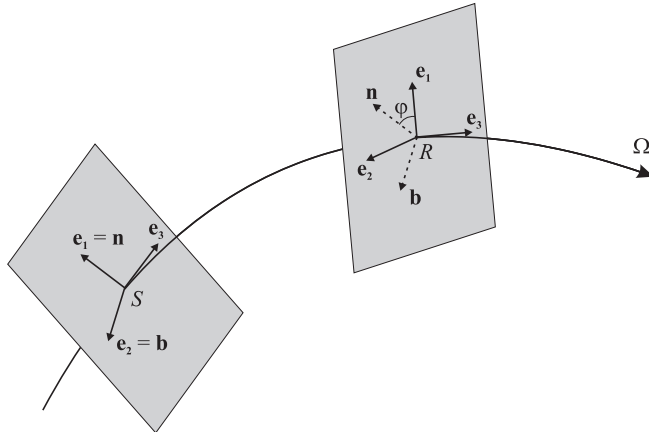
Figure 11: Ray-centered basis vectors and the Frenet trihedral (after
Červený, 2001).

For in-plane rays (in 2D and 1D ray modeling) the vectors $\mathbf{e}_I$ can be
evaluated easily without solving the equations (4.4), since the rays have
zero torsion. In smooth media, if we specify one of the vectors, for example
$\mathbf{e}_2$, to be perpendicular to the plane of the ray at one reference point, it
remains perpendicular to it along the whole ray. Thus, knowing the ray
we automatically know, besides the vector $\mathbf{e}_3$, also the vector $\mathbf{e}_2$ at each
point of the ray. The third RCC basis vector is then computed easily to

complement the right-handed triplet of mutually orthogonal vectors. At structural interfaces we can, in principle, specify the vectors $\mathbf{e}_I$ arbitrarily and use them as 'initial conditions' for computations continuing in the next smooth part of the medium. Nevertheless, it is useful to specify them in a consistent way. For example, in the case of in-plane calculations mentioned above it is useful to consider $\mathbf{e}_2$ being perpendicular to the plane of the ray also at the interfaces.

The importance of the RCC system in the ray-based modeling of seismic wavefields in isotropic structures is two-fold. First, they are useful in the so-called paraxial seismics when the wavefield is approximated not exactly on the ray but also in a close vicinity of such a ray. Restricting our considerations to a close vicinity of the ray ensures the regularity of the RCC (see above) and enables small values of q_1, q_2 only. This allows the omission of terms of a higher than second-order in q_I's in relevant equations both in ray kinematics as well as in ray dynamics. Second, in isotropic media, the RCC basis vectors are used as a frame to describe the direction of the displacement vector, i.e., the direction of the ray amplitude $\mathbf{U}$, at a point on the ray. More specifically, the vector $\mathbf{e}_3 = \mathbf{t}$ determines the amplitude direction of the linearly polarized P- wave, while the vectors $\mathbf{e}_1$ and $\mathbf{e}_2$ determine the polarization of an S- wave. The ray amplitudes, expressed in the RCC system, then read

$$
\begin{aligned}
\mathbf{U}^P &= (0, 0, A)^T \\
\mathbf{U}^S &= (B, C, 0)^T \ ,
\end{aligned}
\tag{4.6}
$$

where the symbol T indicates that the vectors are transposed. The quantity A is the magnitude of the P-wave amplitude $|\mathbf{U}^P| = A$, while B and C can be viewed as Cartesian coordinates of the S- wave amplitude vector in the plane perpendicular to the ray, with respect to the basis $\mathbf{e}_I$. Later it is shown that the direction of the S-wave amplitude vector remains fixed with respect to $\mathbf{e}_1$ and $\mathbf{e}_2$ along the entire ray, i.e., $\mathbf{U}^S$ is transported parallel along the ray in the same way as the vectors $\mathbf{e}_I$.

In seismological calculations the amplitudes are commonly expressed in Cartesian coordinates related to the structure and not in the RCC. Let us introduce the transformation matrix $\mathbf{H}$ from the RCC to the general Cartesian coordinates x_1, x_2, x_3, with the basis vectors $\mathbf{i}_1, \mathbf{i}_2$ and $\mathbf{i}_3$. The elements of the transformation matrix

$$
H_{kl} = \frac{\partial x_k}{\partial q_l}
\tag{4.7}
$$

are, in general, relatively difficult to express. However, on the central ray (i.e., for $q_I = 0$) the corresponding expressions are simple. At a point R, situated on the central ray, the transformation matrix from the RCC to the general Cartesian coordinates is given by

$$H_{kl}(R) = \mathbf{i}_k \cdot \mathbf{e}_l(R) \ . \tag{4.8}$$

It can be shown (see Červený, 2001) that $\mathbf{H}$ is orthonormal along the central ray, i.e.

$$\mathbf{H}^{-1}(R) = \mathbf{H}^T(R), \quad \det \mathbf{H}(R) = 1 \ . \tag{4.9}$$

Instead of the RCC defined and discussed above, it is sometimes useful (and sufficient) to introduce a local Cartesian system with its origin at a specified point (for example, the receiver) on the central ray Ω and with the basis vectors coinciding with the RCC basis vectors at this point. Such a coordinate system is called the local ray-centered Cartesian coordinate system. Note the basis vectors of this Cartesian system and the RCC basis vectors coincide mutually only at the point at which the local system is introduced; in any other point they depart from each other. The RCC basis vectors vary along the ray while the basis vectors of the local ray-centered Cartesian system remain constant in space.

In this section we have up to now assumed an isotropic model. In anisotropic media, analogous coordinate systems to the above-mentioned could be introduced as well. Probably the most important are the so-called **wavefront orthogonal coordinates** (WOC) which are at any point of a given ray analogous to the local ray-centered Cartesian system specified at that point. More specifically, the third coordinate axis (the third basis vector) is parallel to the slowness vector at any point on the ray and the remaining two basis vectors are analogous to the vectors $\mathbf{e}_I$, i.e. they are tangent to the wavefront and satisfy equations similar to (4.4). Note that the system is orthogonal, but the important difference to the RCC in isotropic media is, that the basis vector parallel to the slowness is not, in general, tangent to the ray. In contrast to the RCC in isotropic models, the ray Ω is no longer a coordinate line in the WOC in anisotropic structures. Note that the basis vectors of this system are not, in general, related in any way to the amplitude polarization vectors which are uniquely determined by solving the eigenvalue problem (3.7). Thus the importance of these coordinates is not in a simple way to express the ray amplitudes, like in the case of isotropy.

Nevertheless, the system is useful in paraxial seismic and it allows to calculate easily some other quantities related to amplitudes, like for example, the so-called geometrical spreading of rays (see Sec. 5.1 and 5.3).

4.2   Ray coordinates

Up to now we have treated, implicitly or explicitly, only a single ray. It was a ray specified by its initial conditions and calculated by the use of the RTS in a smooth structure, or possibly transformed across an interface in a layered/blocky structure. Such a single ray may also represent one axis (the so-called central ray) in the RCC system introduced in the previous section. In this section we extend our considerations to the so-called **ray fields**: the sets of rays, belonging to a certain elementary wave, that correspond to a continuous range of initial conditions.

In general 3D problems, the initial conditions can be parameterized by two parameters, say γ_1, γ_2. The physical meaning of the two parameters may be various; for example, in the case of a point source, γ_I parameterize the initial slowness (in terms of take-off angles from the source, two slowness components, etc.). Note that the so-called ray parameter introduced in Sec. 3.3 as the horizontal slowness component, being constant along ray in 1D structures, can be understood as a special case of such a parameter γ_I ($I = 1$ for in plane rays). Let us emphasize that the parameters γ_I specify uniquely the ray in a given ray field by parameterizing the initial conditions. There are also other alternatives, how to specify the ray by the parameters γ_I. For example, when the position of the initial point of the ray may vary along a certain surface while the direction of the ray is fixed (e.g., rays orthogonal to wavefronts or to a structural interface in the so-called 'exploding reflector' approaches), the parameters γ_I can be coordinates of the point on the surface. In any case it is important that the parameters uniquely determine the ray in the ray field. This is why we call them the **ray parameters**.
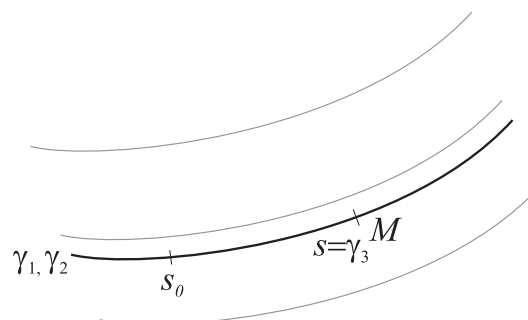
Figure 12: Ray coordinates $\gamma_1, \gamma_2, \gamma_3$.

Let us assume a ray field and a point M, the position of which we want to describe using the ray coordinates $\gamma_1, \gamma_2, \gamma_3$, see figure 12. The first two coordinates, γ_I, have the meaning of the ray parameters specifying the ray passing through the point M. The third one, γ_3, represent a flow parameter u (common choices are $u = s$, $u = \tau$, etc.) specifying the position of the point M on the given ray.

In general, the RC system is not orthogonal. Moreover, it cannot be used in shadow zones of the ray field (regions not illuminated by rays), or, on the contrary, if more than one ray passes through a given point M (the case of multipathing). In such situations the RC system is not regular.

From what has been said so far it is clear that the ray travel time τ, one of the two quantities determining the zero-order ray solution (see Sec. 2.4), is in fact calculated as a function of γ_i, rather then x_i. In the next chapter we will see that the same holds also for the second of the two quantities, the ray amplitude. Nevertheless, the regularity of the RC system means that the mapping between x_i's and γ_i's is regular. Then $\mathbf{x}$ can be expressed parametrically in terms of the RC: $\mathbf{x} = \mathbf{x}(\gamma_1, \gamma_2, \gamma_3)$. This can be viewed as the parametric equation of the ray specified by the ray parameters γ_1, γ_2 (i.e., for γ_I fixed), or the equation of the surface of constant γ_3 with variable γ_I (e.g., the wavefront in the case of $\gamma_3 = \tau = const$).

Let us denote by $\mathbf{Q}$ the transformation matrix from the RC to general Cartesian coordinates: $Q_{ij} = \frac{\partial x_i}{\partial \gamma_j}$. The regularity of the RC system can be defined by the use of the Jacobian of this transformation

$$
J^{(u)} = \frac{D(x_1, x_2, x_3)}{D(\gamma_1, \gamma_2, \gamma_3)} = \det \mathbf{Q} = \begin{vmatrix} \frac{\partial x_1}{\partial \gamma_1} & \frac{\partial x_1}{\partial \gamma_2} & \frac{\partial x_1}{\partial \gamma_3} \\ \frac{\partial x_2}{\partial \gamma_1} & \frac{\partial x_2}{\partial \gamma_2} & \frac{\partial x_2}{\partial \gamma_3} \\ \frac{\partial x_3}{\partial \gamma_1} & \frac{\partial x_3}{\partial \gamma_2} & \frac{\partial x_3}{\partial \gamma_3} \end{vmatrix} , \tag{4.10}
$$

i.e. the system is regular wherever this Jacobian does not vanish. In complex media, $J^{(u)}$ vanishes on so-called caustic surfaces, curves or points, see Sec. 5.4. Note that since $\gamma_3 = u$, the last column in (4.10), $\left(\frac{\partial x_1}{\partial u}, \frac{\partial x_2}{\partial u}, \frac{\partial x_3}{\partial u}\right)^T$, is given by solution of the relevant RTS. Several ways how to calculate the complete Jacobian are briefly discussed in section 5.2. One of them is explained in a greater depth in Sec. 5.3.

Specially, for $u = s$, we will denote the Jacobian by J and call it as the **ray Jacobian**. It plays a very important role in the calculation of ray amplitudes. The ray Jacobian can be also expressed as

$$
J = \left(\frac{\partial \mathbf{x}}{\partial \gamma_1} \times \frac{\partial \mathbf{x}}{\partial \gamma_2} \right)_{s=const} \cdot \mathbf{t} , \tag{4.11}
$$

where $\mathbf{t}$ is the unit vector tangent to ray. Note finally that the square root $\sqrt{J}$ is usually called the **geometrical spreading**.

5   Ray dynamics

In the previous chapter we defined certain quantities important in ray dynamics, namely the ray Jacobian and the geometrical spreading. How do these quantities relate to ray amplitudes? This can be explained by evoking the concept of the so-called ray tube. This concept allows us to find an analytical solution to the transport equation for scalar amplitude factors (see Sec. 5.5) along rays. This leads to the equation known as the continuation formula: it enables us to determine the scalar ray amplitude at a point on the ray provided the amplitude is known at some other (usually initial) point on the same ray. The initial amplitudes may be defined by introducing the so-called radiation function, as it is explained in the section 5.8. Special attention is devoted to the calculation of the ray amplitudes across structural interfaces by the use of proper reflection/transmission (R/T) coefficients. The chapter ends with expressions for the ray theory Green's function in a layered or blocky medium, both isotropic as well as anisotropic.

5.1   Ray tube

Let us consider a family of rays, belonging to a certain ray field, with the ray parameters γ_I being in the interval $(\gamma_1, \gamma_1 + \mathrm{d}\gamma_1) \times (\gamma_2, \gamma_2 + \mathrm{d}\gamma_2)$. This ray family, defined by the ray parameter perturbations $\mathrm{d}\gamma_1$ and $\mathrm{d}\gamma_2$, represents the so-called **elementary ray tube**. A part of such a tube, bounded by two wavefronts at times τ_0 and τ, is depicted in figure 13.
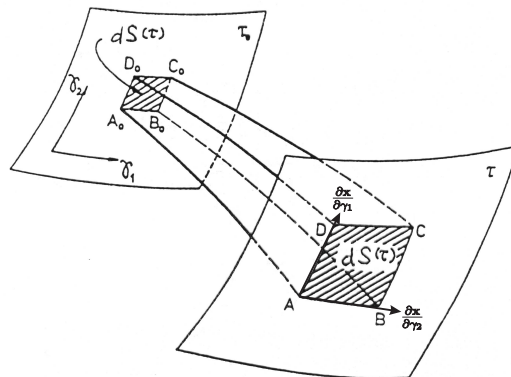
Figure 13: Section of an elementary ray tube (after Pšenčík, 1994).

Intuitively, it can be expected that in the parts of the model characterized by the focusing of rays, where the ray tube becomes narrow, the ray amplitude should increase in inverse proportion. On the contrary, where the rays spread, the amplitude is expected to decrease. This behavior is

a consequence of conservation of energy and the fact that energy (its high-frequency part) flows along rays. It is quantified by the continuation formula (see Sec. 5.6). For now, we just take into account that in evaluating the ray amplitudes the principal role is played by the cross-sectional area of the elementary ray tube. In the following we show how to express the cross-sectional area in terms of the ray Jacobian J.

Let us consider the area of that portion of the relevant wavefront, cut out by the given elementary ray tube – see the shaded areas in Fig. 13. From differential geometry, the vectorial surface element cut out from the wavefront is given by the vectorial product of two vectors tangent to the wavefront as

$$\mathrm{d}\mathbf{S}^{(\tau)} = \left(\frac{\partial \mathbf{x}}{\partial \gamma_1} \times \frac{\partial \mathbf{x}}{\partial \gamma_2} \right)_{\tau=const} \mathrm{d}\gamma_1 \mathrm{d}\gamma_2 . \tag{5.1}$$

This vector is, by definition, normal to the wavefront. In isotropic media it is moreover tangent to rays and its magnitude has the meaning of the cross-sectional area of the ray tube (in the direction perpendicular to the tube). In a general anisotropic case, however, the vector $\mathrm{d}\mathbf{S}^{(\tau)}$ differs in its direction from rays (i.e., from the direction of the group velocity, see Sec. 3.7). The cross-sectional (scalar) surface element can be obtained by projecting the vector $\mathrm{d}\mathbf{S}^{(\tau)}$ into the direction of $\mathbf{t}$ (the unit vector tangent to the ray at a point of interest)

$$\mathrm{d}S^{\perp} = \mathrm{d}\mathbf{S}^{(\tau)} \cdot \mathbf{t} . \tag{5.2}$$

Note that it is possible to apply the formula (5.2) even in isotropic media. There

$$\mathrm{d}S^{\perp} = \mathrm{d}\mathbf{S}^{(\tau)} \cdot \mathbf{t} = \pm |\mathrm{d}\mathbf{S}^{(\tau)}| , \tag{5.3}$$

where $\pm$ indicates that $\mathrm{d}\mathbf{S}^{(\tau)}$ may be oriented in or against the direction of $\mathbf{t}$ (it is controlled by mutual orientation of the vectors $\frac{\partial \mathbf{x}}{\partial \gamma_I}$, tangent to the wavefront, see (5.1)). In anisotropic media, the projecting of $\mathrm{d}\mathbf{S}^{(\tau)}$ does not only determine the sign but also modifies the magnitude of the resulting scalar cross-sectional surface element.

Let us quantify the difference in directions of the vectors $\mathbf{t}$ (the unit tangent to ray) and $\mathrm{d}\mathbf{S}^{(\tau)}$ in a general anisotropic structure by the angle Φ between these two vectors. The vector $\mathbf{t}$ is parallel to the group velocity vector $\mathbf{v}^g$, so that $\mathbf{t} = \mathbf{v}^g/|\mathbf{v}^g|$, while the vector $\mathrm{d}\mathbf{S}^{(\tau)}$, normal to wavefront, is parallel to the slowness vector $\mathbf{p}$, and the unit normal to wavefront $\mathbf{n}^\tau$, see the figure 14. Thus, Φ is given by

$$\cos \Phi = \mathbf{n}^\tau \cdot \mathbf{t} = c\mathbf{p} \cdot \frac{\mathbf{v}^g}{|\mathbf{v}^g|} = \frac{c}{v^g} \ , \tag{5.4}$$

where c denotes the phase velocity and $v^g = |\mathbf{v}^g|$ is the group velocity magnitude. In the above equation, the well known identity

$$p_i v_i^g = 1 \tag{5.5}$$

is used. This identity is obvious for isotropic models, but it is also valid in anisotropic structures. It can be simply derived as follows:

$$p_i v_i^g = p_i t_i |\mathbf{v}^g| = \frac{\partial \tau}{\partial x_i} \frac{\mathrm{d}x_i}{\mathrm{d}s} \frac{\mathrm{d}s}{\mathrm{d}\tau} = \frac{\partial \tau}{\partial x_i} \frac{\mathrm{d}x_i}{\mathrm{d}\tau} = \frac{\mathrm{d}\tau}{\mathrm{d}\tau} = 1 \ . \tag{5.6}$$

In the above equation we have used $\frac{\mathrm{d}s}{\mathrm{d}\tau} = v^g = (v_i^g v_i^g)^{1/2}$ which is a consequence of the RTS (3.80), namely $\frac{\mathrm{d}x_i}{\mathrm{d}\tau} = v_i^g$, see Sec. 3.7. Note that in isotropic models, $\Phi = 0°$.
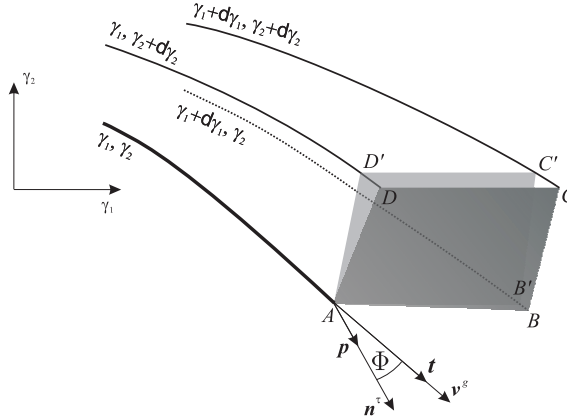
Figure 14: Vectors normal to the surfaces of constant s (AB'C'D') and τ (ABCD) differ by angle Φ.

Similarly to (5.2), the cross-sectional surface element can be obtained by the use of the projection of any other vectorial surface element $\mathrm{d}\mathbf{S}^{(u)}$, cut by the ray tube from a surface of constant u, into the vector $\mathbf{t}$. Especially, in the case of $u = s$ we have, similarly as for the wavefront in an isotropic medium, $\mathrm{d}S^\perp = \mathrm{d}\mathbf{S}^{(s)} \cdot \mathbf{t} = \pm|\mathrm{d}\mathbf{S}^{(s)}|$, since $\mathrm{d}\mathbf{S}^{(s)}$ is always parallel to ray (i.e., the relevant cross-section is perpendicular to ray).

It is easy to express $\mathrm{d}S^\perp$ in terms of the ray Jacobian J. From (4.11) we see that

$$\mathrm{d}S^\perp = \mathrm{d}\mathbf{S}^{(s)} \cdot \mathbf{t} = J\mathrm{d}\gamma_1 \mathrm{d}\gamma_2 \ . \tag{5.7}$$

However, $\mathrm{d}S^\perp$ can be expressed from (5.2) in terms of $J^{(\tau)}$ as well:

$$\mathrm{d}S^\perp = \mathrm{d}\mathbf{S}^{(\tau)} \cdot \mathbf{t} = J^{(\tau)}\frac{\mathrm{d}\tau}{\mathrm{d}s}\mathrm{d}\gamma_1\mathrm{d}\gamma_2 = J^{(\tau)}(v^g)^{-1}\mathrm{d}\gamma_1\mathrm{d}\gamma_2 \ . \tag{5.8}$$

Comparing the above two equations we also obtain the relationship between J and $J^{(\tau)}$

$$J^{(\tau)} = v^g J \ . \tag{5.9}$$

This formula is general, valid both for anisotropic and isotropic media. In the case of isotropic media we can moreover substitute v (α or β) for v^g.

5.2 How to calculate the ray Jacobian

There are several ways to evaluate J at a point on a ray in smooth media. Namely:

1. It is possible to use a relatively robust, approximate approach in which the differentials $\mathrm{d}\gamma_I$ and $\mathrm{d}S^\perp$ in (5.7) are substituted by finite differences $\Delta\gamma_I$ and $\Delta S^\perp$. The ray Jacobian at a point A on a ray Ω is then approximated as

$$J \doteq \frac{\Delta S^{(\perp)}}{\Delta\gamma_1\Delta\gamma_2} \ . \tag{5.10}$$

This approach requires us tracing additional rays, nearby to the ray of interest and differing in their ray parameters by $\Delta\gamma_I$, to simulate the ray tube (see Fig. 1). On these rays we find the points corresponding to the same wavefront as the point A – i.e. the points B, C and D. Then we in fact "measure" numerically the area of the rectangle $ABCD$ which yields approximately the scalar surface element $\Delta S^{(\tau)}$. It is also possible to trace only two nearby rays and approximate the area of the rectangle by taking twice the area of the triangle ABD, see Fig. 1.

In isotropic media, rays are orthogonal to wavefronts, so that $\Delta S^{(\tau)}$ represents $\Delta S^{(\perp)}$ in (5.10) and we can write

$$J \doteq \frac{\Delta S^{(\tau)}}{\Delta\gamma_1\Delta\gamma_2} \ . \tag{5.11}$$

In anisotropic models, $\Delta S^{(\tau)}$ differs, in general, from $\Delta S^\perp$. It should be recalculated using the angle Φ, introduced in the previous section (see (5.4)). Then
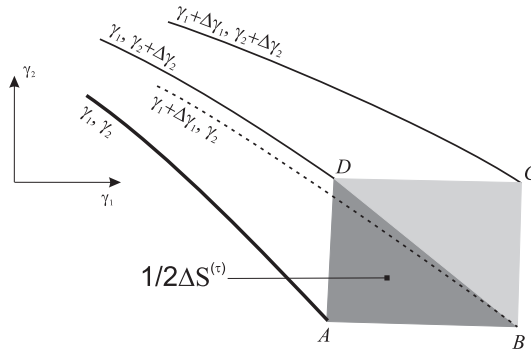
Figure 15: "Finite-difference" approximation of J at a point A on the ray of interest.

$$J \doteq \frac{c}{v^g} \frac{\Delta S^{(\tau)}}{\Delta \gamma_1 \Delta \gamma_2} \ . \tag{5.12}$$

Note that the above formulas allow us to determine only the absolute value of J. From (4.11) we see that the sign is given by mutual orientation of the vectors $\frac{\partial \mathbf{x}}{\partial \gamma_I}$. These vectors can be easily modeled using the nearby rays replacing the derivatives by finite differences.

In 2D and 1D structures, when dealing with in-plane rays, the situation is simpler. Instead of two or three neighboring rays only one is necessary to calculate. J is approximated by measuring the length of the straight line element connecting the point of interest and the point with the same travel time, situated on the neighboring ray.

2. Another possibility is to apply the so-called **dynamic ray tracing** (DRT) system. It is the system of additional linear differential equations solved along the ray of interest, so that no nearby rays are needed. The system yields, among others, the quantities $\partial x_i/\partial \gamma_I$, which, supplemented with $\partial x_i/\partial \gamma_3$, known from the RTS, are necessary to evaluate the complete matrix $\mathbf{Q}$ and therefore $J = \det \mathbf{Q}$. This approach is not only approximate like that of finite differences – it is exact. The DRT system is not difficult to derive (see Sec. 5.3). It is also easy to solve the system along the ray because the equations are linear. It should be noted that the DRT is not only a tool to obtain J along the ray, it has many other important applications, mainly in paraxial seismic (see, for example, Beydoun and Keho, 1987).

3. In homogeneous media, both isotropic and anisotropic, the ray Jacobian can be calculated analytically. Let us show this for the case of a

point source in an isotropic medium and the ray parameters representing take-off angles from the source, the declination ψ_0 and the azimuth ϑ_0: $\gamma_1 = \psi_0$ and $\gamma_2 = \vartheta_0$. Rays $\mathbf{x}(\gamma_1, \gamma_2)$ are straight lines

$$x_1 = l \sin \psi_0 \cos \vartheta_0, \quad x_2 = l \sin \psi_0 \sin \vartheta_0, \quad x_3 = l \cos \psi_0 \ , \tag{5.13}$$

where l denotes the distance from the source (length of the ray), so that it has the meaning of the arclength parameter s. Expressing the derivatives $\frac{\partial x_i}{\partial \gamma_I}$, and $\frac{\partial x_i}{\partial s}$ and evaluating the relevant determinant (4.10) we immediately obtain

$$J = l^2 \sin \psi_0 \ . \tag{5.14}$$

5.3 Dynamic ray tracing

Dynamic ray tracing (DRT) is a procedure that allows us to compute the first two columns of the matrix $\mathbf{Q}$ (see equation (4.10)) by solving a system of several linear ordinary differential equations of the first order along the ray. Together with solving the RTS, yielding the third column of the matrix, the DRT provides the possibility of direct evaluation of det $\mathbf{Q}$ and thus obtaining the geometrical spreading without the necessity of tracing any auxiliary nearby rays. Moreover, in this way the geometrical spreading is computed exactly in contrast to the approximate simulation of an elementary ray tube by the finite difference approach mentioned in the previous section.

The DRT equations can be expressed either in Cartesian, or RCC (WOC) coordinates. Probably the simplest it is to derive the DRT system of equations in Cartesian coordinates by differentiation of the RTS with respect to the ray parameters γ_I. We seek the elements of the transformation matrix from the RC to the general Cartesian coordinates

$$Q_{iJ} = \left(\frac{\partial x_i}{\partial \gamma_J} \right)_{\gamma_3 = const} . \tag{5.15}$$

(let us recall that the lower-case index runs from 1 to 3, while the upper-case one from 1 to 2). In analogy let us denote

$$P_{iJ} = \left(\frac{\partial p_i}{\partial \gamma_J} \right)_{\gamma_3 = const} = \left(\frac{\partial^2 \tau}{\partial x_i \partial \gamma_J} \right)_{\gamma_3 = const} . \tag{5.16}$$

The quantities Q_{iJ}, complemented by the elements $Q_{i3} = (\partial x_i/\partial \gamma_3)$ (with constant γ_I), which are known from the RTS as $\partial x_i/\partial u$ (with u being a flow parameter along the ray), constitute the matrix $\mathbf{Q}$. Differentiating $\mathrm{d}x_i/\mathrm{d}u$ with respect to γ_J yields the equation for the change of Q_{iJ} along the ray

$$\frac{\partial}{\partial \gamma_J} \left(\frac{\mathrm{d}x_i}{\mathrm{d}u} \right) = \frac{\mathrm{d}}{\mathrm{d}u} \left(\frac{\partial x_i}{\partial \gamma_J} \right) = \frac{\mathrm{d}}{\mathrm{d}u} Q_{iJ} \ , \tag{5.17}$$

where all the derivatives with respect to γ_J are considered for constant γ_3 (i.e., constant u). Similarly, by differentiating $\mathrm{d}p_i/\mathrm{d}u$ from the RTS with respect to γ_J results in the equation for the change of P_{iJ} along the ray.

In anisotropic media we have derived the RTS (3.78), with the flow parameter τ, so that we consider $\gamma_3 = u = \tau$. From (5.17), utilizing (3.78), we obtain

$$\frac{\mathrm{d}}{\mathrm{d}\tau} Q_{iJ} = \frac{\partial}{\partial \gamma_J} \left(\frac{\mathrm{d}x_i}{\mathrm{d}\tau} \right) = \frac{1}{2} \frac{\partial}{\partial \gamma_J} \left(\frac{\partial G}{\partial p_i} \right) = \frac{1}{2} \left(\frac{\partial^2 G}{\partial p_i \partial x_k} \frac{\partial x_k}{\partial \gamma_J} + \frac{\partial^2 G}{\partial p_i \partial p_k} \frac{\partial p_k}{\partial \gamma_J} \right) , \tag{5.18}$$

where we have omitted the index m (the type of wave). For $\frac{\mathrm{d}}{\mathrm{d}\tau} P_{iJ}$ we proceed analogously. Utilizing the notation (5.15) and (5.16) we finally obtain the DRT in the form of the system of twelve linear ordinary differential equations

$$\begin{aligned} \frac{\mathrm{d}}{\mathrm{d}\tau} Q_{iJ} &= \frac{1}{2} \left(\frac{\partial^2 G}{\partial p_i \partial x_k} Q_{kJ} + \frac{\partial^2 G}{\partial p_i \partial p_k} P_{kJ} \right) \\ \frac{\mathrm{d}}{\mathrm{d}\tau} P_{iJ} &= -\frac{1}{2} \left(\frac{\partial^2 G}{\partial x_i \partial x_k} Q_{kJ} + \frac{\partial^2 G}{\partial x_i \partial p_k} P_{kJ} \right) . \end{aligned} \tag{5.19}$$

The DRT equations for $\frac{\mathrm{d}}{\mathrm{d}u} Q_{iJ}$ and $\frac{\mathrm{d}}{\mathrm{d}u} P_{iJ}$ are coupled and must be solved together (in analogy to the coupled RTS equations for x_i's and p_i's). Among these twelve equations, only eight are independent because elements of Q_{iJ} and P_{iJ} are constrained by four additional conditions. Two of the constraint conditions are due to the fact that the slowness vector, orthogonal to wavefront by definition, must be perpendicular to the wavefront tangent vectors $\partial x_k/\partial \gamma_J$ (with constant τ). Thus we have

$$p_i Q_{iJ} = 0 \ . \tag{5.20}$$

The other two constraints can be obtained by differentiating the eikonal equation $G = 1$ with respect to γ_J while taking into account the RTS (3.78). Thus, we can write

$$\frac{\partial G}{\partial x_i} Q_{iJ} + \frac{\partial G}{\partial p_i} P_{iJ} = \frac{\mathrm{d}p_i}{\mathrm{d}\tau} Q_{iJ} - \frac{\mathrm{d}x_i}{\mathrm{d}\tau} P_{iJ} = 0 \ . \tag{5.21}$$

This allows us to reduce the DRT system for 2×2 matrices with elements Q_{IJ} and P_{IJ} and calculate the remaining Q_{3J}, P_{3J} from the constraints. Initial conditions for the system are briefly discussed later.

In isotropic media we can derive the DRT system analogously from the RTS (3.39). This is equivalent to specifying $G = v^2 p_i p_i$ with v written for α or β. Inserting the corresponding derivatives of our G into the system (5.19) leads to

$$
\begin{aligned}
\frac{\mathrm{d}}{\mathrm{d}\tau} Q_{iJ} &= \frac{\partial v^2}{\partial x_k} p_i Q_{kJ} + v^2 P_{iJ} \\
\frac{\mathrm{d}}{\mathrm{d}\tau} P_{iJ} &= -\frac{1}{2} \frac{\partial^2 v^2}{\partial x_i \partial x_k} v^{-2} Q_{kJ} - \frac{\partial v^2}{\partial x_i} p_k P_{kJ} \ .
\end{aligned}
\tag{5.22}
$$

The constraint conditions are the same as in anisotropic media, only (5.21) can be made more explicit substituting from the RTS and writing thus $v^{-3} v_{,k} Q_{kJ} = -p_k P_{kJ}$.

The equations of the DRT system are linear and it is not difficult to solve them for proper initial conditions. In homogeneous models, the system can even be solved analytically. Nevertheless, even in complex media in which the system has to be integrated numerically, the numerical effort exerted is usually much less than that put forth to solve the RTS.

The initial conditions depend on the parameterization of the ray field (i.e., the type of the ray parameters γ_I). They also differ in the case of a point source or the case of rays starting at a smooth initial surface. Let us present here an example of the **point source** initial conditions for their particular importance in practice. Let us derive them first in the easier case of an isotropic medium.

For the ray parameters chosen as the ray take-off angles at the source point (i.e., $\gamma_1 = \psi_0$, the declination, and $\gamma_2 = \vartheta_0$, the azimuth) we can specify the initial slowness vector as $\mathbf{p}(\tau_0) = v_0^{-1} \mathbf{n}^{\tau_0} = v_0^{-1}(\sin\psi_0 \cos\vartheta_0, \sin\psi_0 \sin\vartheta_0, \cos\psi_0)^T$, where v_0 denotes α or β at the source point and the upper index τ_0 indicates that the normal to wavefront, $\mathbf{n}^\tau$, also corresponds to the source point (specified by the parameter τ_0). Differentiating the slowness components $p_i(\tau_0) = v_0^{-1} n_i^{\tau_0}$ with respect to γ_I yields

$$
P_{iJ}(\tau_0) = v_0^{-1} \frac{\partial n_i^{\tau_0}}{\partial \gamma_J} \ .
\tag{5.23}
$$

Explicitly, it is

$$P_{11}(\tau_0) = v_0^{-1} \cos \psi_0 \cos \vartheta_0, \quad P_{12}(\tau_0) = -v_0^{-1} \sin \psi_0 \sin \vartheta_0,$$

$$P_{21}(\tau_0) = v_0^{-1} \cos \psi_0 \sin \vartheta_0, \quad P_{22}(\tau_0) = v_0^{-1} \sin \psi_0 \cos \vartheta_0, \qquad (5.24)$$

$$P_{31}(\tau_0) = -v_0^{-1} \sin \psi_0, \qquad P_{32}(\tau_0) = 0 .$$

The point source initial conditions for Q_{iJ} are simply

$$Q_{iJ}(\tau_0) = 0 , \qquad (5.25)$$

since all the rays start from the same point and thus the change of $x_i(\tau_0)$ from one ray to another is zero, so that $\frac{\partial x_i}{\partial \gamma_J}(\tau_0) = 0$. Note that these initial conditions for Q_{iJ} make the ray Jacobian and, consequently, the geometrical spreading vanish at the point source.

In anisotropic media we can use the same parameterization of the point source ray field, but the take-off angles determine the initial slowness direction which, in general, differs from the initial ray direction. Nevertheless, the initial take-off angles of the slowness uniquely determine the corresponding ray in the ray field. As above, for $Q_{iJ}(\tau_0)$ at a point source we can write

$$Q_{iJ}(\tau_0) = 0 . \qquad (5.26)$$

To obtain the initial conditions for P_{iJ} we need to consider the derivatives of $p_i(\tau_0) = c_0^{-1}(\mathbf{n}^{\tau 0})n_i^{\tau 0}$, with c_0 being the phase velocity of the considered wave at the source, with respect to γ_I. Compared to the isotropic case this is a little more complicated by the fact that the phase velocity depends on γ_I. Consequently, an extra term appears in $P_{iJ} = \partial p_i/\partial \gamma_J$. To find the derivative we consider the equality $c_0 = \mathbf{n}^{\tau 0} \cdot \mathbf{v}^g$ which follows from (5.5). Then,

$$
\begin{aligned}
P_{iJ}(\tau_0) &= c_0^{-1}\frac{\partial n_i^{\tau 0}}{\partial \gamma_J} - n_i^{\tau 0} c_0^{-2}\frac{\partial}{\partial \gamma_J}(n_k^{\tau 0} v_k^g) = \\
&= c_0^{-1}\left(\frac{\partial n_i^{\tau 0}}{\partial \gamma_J} - p_i(\tau_0)v_k^g(\tau_0)\frac{\partial n_k^{\tau 0}}{\partial \gamma_J} - p_i(\tau_0)n_k^{\tau 0}\frac{\partial v_k^g}{\partial \gamma_J} \right) .
\end{aligned}
\qquad (5.27)
$$

The last term in the above equation vanishes as the vector $\mathbf{n}^\tau$ is generally (not only in anisotropic media) perpendicular to the vector $\partial \mathbf{v}^g/\partial \gamma_J$.

Indeed, using the RTS equation $\mathrm{d}x_i/\mathrm{d}\tau = v_i^g$ (valid in anisotropy as well as in isotropy), we can write

$$\frac{\partial v_k^g}{\partial \gamma_J} = \frac{\partial}{\partial \gamma_J}\left(\frac{\mathrm{d}x_k}{\mathrm{d}\tau}\right) = \frac{\mathrm{d}}{\mathrm{d}\tau}\left(\frac{\partial x_k}{\partial \gamma_J}\right) , \tag{5.28}$$

where the derivatives with respect to γ_J are taken with constant τ. The vector $\partial x_k/\partial \gamma_J$ is always tangent to wavefront and the same holds for its change with τ (i.e., from one wavefront to the next one). Thus, for the initial P_{iJ} at a point source in general anisotropic media we have

$$P_{iJ}(\tau_0) = c_0^{-1}\left(\frac{\partial n_i^{\tau_0}}{\partial \gamma_J} - p_i(\tau_0)v_k^g(\tau_0)\frac{\partial n_k^{\tau_0}}{\partial \gamma_J}\right) . \tag{5.29}$$

In isotropic media, it is convenient to express the DRT system in the RCC in which the simplest form of the system can be obtained. Let us consider the 3×3 transformation matrix from the RC to the RCC

$$Q_{ij}^{(q)} = \frac{\partial q_i}{\partial \gamma_j} , \tag{5.30}$$

where the upper index (q) is used to emphasize the difference between this matrix and the transformation matrix $\mathbf{Q}$ from the RC to the general Cartesian coordinates x_i, introduced in Sec. 4.2. Let us assume, for the sake of consistency with the previous derivations, that γ_3 as well as q_3 is chosen equal to the flow parameter τ. Further let us consider the matrix only along the central ray of the RCC. Then the matrix has the form:

$$\mathbf{Q}^{(q)} = \begin{pmatrix} \frac{\partial q_1}{\partial \gamma_1} \equiv \bar{Q}_{11} & \frac{\partial q_1}{\partial \gamma_2} \equiv \bar{Q}_{12} & 0 \\ \frac{\partial q_2}{\partial \gamma_1} \equiv \bar{Q}_{21} & \frac{\partial q_2}{\partial \gamma_2} \equiv \bar{Q}_{22} & 0 \\ \frac{\partial \tau}{\partial \gamma_1} & \frac{\partial \tau}{\partial \gamma_2} & 1 \end{pmatrix} . \tag{5.31}$$

Note that the first two elements of the last column, $\frac{\partial q_1}{\partial \tau}$ and $\frac{\partial q_2}{\partial \tau}$, vanish due to the fact that $q_I = 0$ on the central ray. The determinant of the matrix is

$$\det \mathbf{Q}^{(q)} = \det \bar{\mathbf{Q}} , \tag{5.32}$$

where $\bar{\mathbf{Q}}$ is the 2×2 upper left submatrix of the matrix $\mathbf{Q}^{(q)}$. The ray tube cross-sectional area is, however, defined in terms of det $\mathbf{Q}$, the determinant of the transformation matrix from the RC to a general Cartesian coordinates. Nevertheless, on the central ray this does not make a difference, since (due to (4.9)) we can write

$$J^{(\tau)} = vJ = \det \mathbf{Q} = \det \mathbf{H} \det \mathbf{Q}^{(q)} = \det \bar{\mathbf{Q}} \; , \qquad (5.33)$$

with v denoting either α or β, the P- or S-wave velocity, respectively, and $\mathbf{H}$ is the transformation matrix from the RCC to general Cartesian coordinates (see Sec. 4.1).

Thus, to obtain the ray Jacobian and the geometrical spreading, we must know the elements of the 2×2 matrix $\bar{\mathbf{Q}}$. They are the solutions of the eight DRT equations expressed in RCC coordinates. For a detailed derivation of these equations let us refer to Červený (2001). In the matrix form this DRT system reads

$$\frac{d\bar{\mathbf{Q}}}{d\tau} = v^2\bar{\mathbf{P}}, \qquad \frac{d\bar{\mathbf{P}}}{d\tau} = -v^{-1}\bar{\mathbf{V}}\bar{\mathbf{Q}} \; , \qquad (5.34)$$

where bars over the letters indicate the 2×2 matrices. All the matrices are considered on the central ray. The matrix $\bar{\mathbf{P}}$ is defined by $\bar{P}_{IJ} = \partial p_I^{(q)}/\partial \gamma_J$ with $p_I^{(q)} = \partial\tau/\partial q_I$. The quantities $p_I^{(q)}$ represent the first two slowness components, expressed in the RCC. It should be mentioned that although $\partial\tau/\partial q_I$, the derivatives tangential to the wavefront (the surface of constant τ) equal zero on the central ray, their derivatives with respect to γ_J (i.e., $\bar{P}_{IJ}$), specified on the central ray, do not generally vanish. The same argumentation can be followed for $\bar{Q}_{IJ} = \partial q_I/\partial \gamma_J$ — in general it does not vanish on the central ray, even though q_I itself does. In the system (5.34), $\bar{\mathbf{V}}$ is the matrix of the second derivatives of velocity v with respect to q_I's: $\bar{V}_{IJ} = (\partial^2 v(q_1, q_2, \tau)/\partial q_I \partial q_J)_{q_1=q_2=0}$.

The equations (5.34) represent the simplest possible form of the DRT system. The system can be derived from the eikonal equation transformed into the RCC (for details see Červený, 2001). It can be easily solved numerically at much lower cost than the RTS, provided the proper initial conditions are specified. Let us present here, as an example, the initial conditions corresponding to a point source at the point τ_0. They can be found in a way analogous to that which we have used in the case of the DRT system (5.22), expressed in the Cartesian coordinates. The point source initial conditions are

$$\bar{\mathbf{Q}}(\tau_0) = 0, \quad \bar{\mathbf{P}}(\tau_0) = v^{-1}(\tau_0) \begin{pmatrix} 1 & 0 \\ 0 & \sin\psi_0 \end{pmatrix}, \tag{5.35}$$

where ψ_0 has the same meaning as in (5.24).

For general initial conditions, the system (5.34) can be solved with the advantage of using the so-called **propagator matrix**, the matrix of fundamental solutions. The topics related to the propagator matrix and its interesting properties are beyond the scope of these course notes as they are not essential for the reader to understand the following text. Details can be found in many textbooks on ray theory, like, for example, Červený (2001), or Chapman (2004).

Let us mention here also the analytical solution of the system (5.34) for a point source in a homogeneous isotropic medium:

$$\bar{\mathbf{Q}}(\tau) = vl\bar{\mathbf{P}}(\tau_0), \quad \bar{\mathbf{P}}(\tau) = \bar{\mathbf{P}}(\tau_0), \tag{5.36}$$

with $\bar{\mathbf{P}}(\tau_0)$ given by (5.35) and l meaning the length of the straight ray from the point τ_0 to the point τ, similarly as in the equation (5.14).

In anisotropic models, we can consider the DRT system in the wavefront orthonormal coordinates (WOC) analogous to the RCC in many respects. The coordinates are briefly mentioned at the end of Sec. 4.1. Performing the DRT in the WOC would also require us to solve eight linear ordinary differential equations (for details see Červený, 2001). However, for general anisotropy the DRT in the Cartesian coordinates is usually numerically more efficient than that written in the WOC, despite the fact that it consists of twelve equations.

5.4 Caustics

It has been mentioned in Sec. 4.2 that the RC system is regular as long as the Jacobian of the transformation from the RC to the general Cartesian coordinates does not vanish. We call a point at which the Jacobian is equal to zero the **caustic point**. Since the Jacobian is equal to the area of the cross-sectional surface element of the elementary ray tube, it is clear that at the caustic point the rays forming the tube cross each other so that the tube shrinks to zero. This may happen provided the medium is complex enough for the ray field to develop multipathing of rays, e.g., due to an inhomogeneous velocity. However, this may also happen in homogeneous media in the presence of an concave reflector.

The caustic points are not isolated in space, they form surfaces or lines in 3D or 2D cases. An example of the formation of a caustic in a 2D model is shown in figure 16.
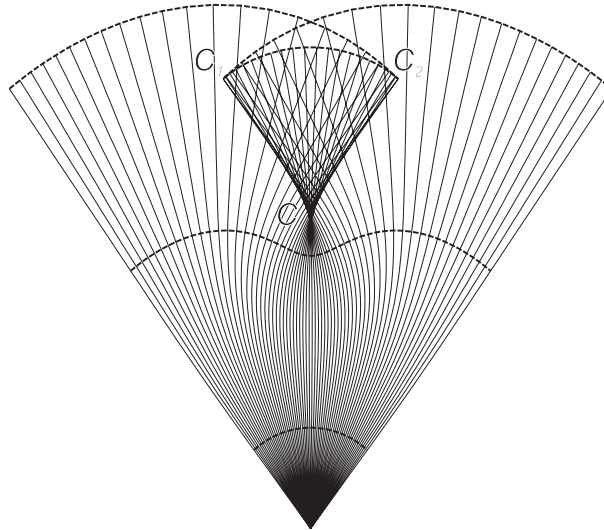
Figure 16: Example of the formation of a 2D cuspoidal caustic due to a low-velocity zone in the model. The caustic leads to folding in the ray field which is associated with a triplication of the wavefront. Note the ray envelopes CC_1 and CC_2 forming the caustic lines.

We have defined the caustic point by the condition $\det \mathbf{Q} = 0$. This means that the rank of $\mathbf{Q}$ is less than 3. We distinguish two types of caustic points, shown in the figure 17:

1. caustic of the first order (see Fig. 17, top), for which rank$\mathbf{Q} = 2$, and

2. caustic of the second order (see Fig. 17, bottom), for which rank$\mathbf{Q} = 1$.

Note that the caustic of the first order is associated with the flattening of the elementary ray tube to a line segment, while at the caustic of the second order the tube shrinks to a point.

Not only is the RC not regular at caustics, but also the ray solution as such breaks down at, and in the vicinity of, a caustic point. In Sec. 5.7 it is shown that the ray amplitude grows to infinity at a caustic and we speak about the caustic singularity of the RM. Away from caustics the ray solution is applicable (within the limits of the RM applicability, see Chap. 7), provided a proper phase shift due to the passage through a caustic is adopted.

The phase shift due to caustic can be easily explained in the case of an isotropic medium. After passing a caustic of the first order, J changes
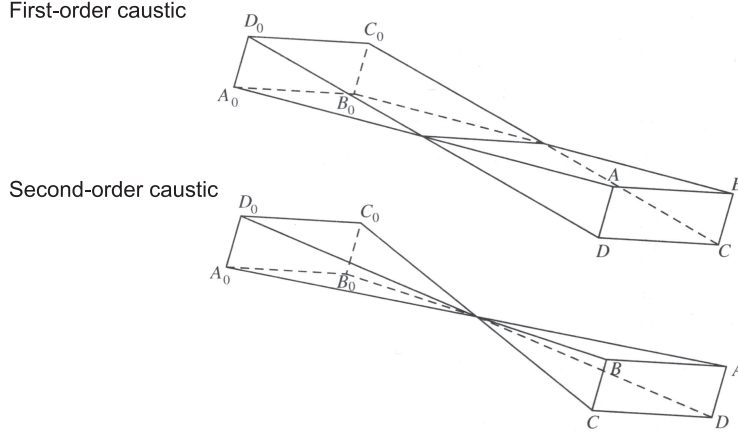
Figure 17: Caustics of the first and second order. Ray A_0A corresponds to ray parameters γ_1, γ_2, ray B_0B corresponds to $\gamma_1 + \mathrm{d}\gamma_1, \gamma_2$, ray C_0C corresponds to $\gamma_1 + \mathrm{d}\gamma_1, \gamma_2 + \mathrm{d}\gamma_2$, and ray D_0D corresponds to ray parameters $\gamma_1, \gamma_2 + \mathrm{d}\gamma_2$ (after Červený, 2001).

sign, which is associated with the change of the mutual orientation of the vectors $\frac{\partial \mathbf{x}}{\partial \gamma_I}$, tangent to the surface of constant s. This introduces a factor $\sqrt{-1}$ into the geometrical spreading and therefore the phase shift of $\pi/2$. In this respect, the caustic of the second order can be viewed as two first-order caustics in one, so that an additional phase shift of $\pi/2$ is necessary. To summarize, after passing through a caustic, the argument of the geometrical spreading $\sqrt{J}$ takes the shift $\Delta K \pi/2$, where ΔK equals 1 or 2 for the caustic of the first or second order, respectively.

In anisotropic media, the situation is more complicated. The quantity ΔK may also be negative, $\Delta K = -1$ or $\Delta K = -2$. This is related to the fact that in anisotropic media the local slowness surface need not be convex (see example in Fig. 8). For a discussion of this problem see Červený, 2001. A detailed derivation can be found in the paper by Bakker, 1998.

Note that the phase shift due to caustics is cumulative: as many times as the ray crosses or touches a caustic, that many times the proper phase shift must be added. More specifically, along a ray from a point S to a point R, the amplitude gains the term $\exp[-\mathrm{i}\frac{1}{2}\pi K(S, R)]$, where $K(S, R) = \sum_{i=1}^{i=N} \Delta K_i$ with N being the number of caustic points along the ray between the points S and R. The exponent K is sometimes called the "index of the ray trajectory". It is known also as the "KMAH index" (see Červený, 2001).

5.5 Calculation of ray amplitudes. Transport equation

Let us recall what we have derived up to now. We have assumed that the solution we seek is of the form (2.20)

$$\mathbf{u}(\mathbf{x}, t) = \mathbf{U}(\mathbf{x})F(t - \tau(\mathbf{x})).$$

We know how to calculate τ, the solution of the eikonal equation, along rays. Besides computing the eikonal, the eikonal equation allows us to determine also the eigenvectors of the Christoffel matrix, $\mathbf{g}^{(m)}, m = 1, 2, 3$. In anisotropic structures, these three vectors can be specified uniquely while, in isotropic media, this is possible only for one of them, that corresponding to the P-wave ($\mathbf{g}^{(3)}$, see Sec. 3.1). This eigenvector is the unit vector normal to wavefront, i.e., it is parallel to $\mathbf{n}^\tau$ (and also to the slowness vector $\mathbf{p}$, the group velocity vector $\mathbf{v}^g$, and the unit vector tangent to ray $\mathbf{t}$). The remaining two are mutually orthogonal unit vectors $\mathbf{g}^{(1)}, \mathbf{g}^{(2)}$, situated in the plane tangent to wavefront, making together with $\mathbf{g}^{(3)}$ a right-handed triplet, but their orientation within the plane may be arbitrary. To our advantage we can make them identical with the RCC basis vectors $\mathbf{e}_1, \mathbf{e}_2$ introduced in the section 4.1. Their orientation, being specified arbitrarily at one (initial) point of the ray, is determined uniquely along the whole ray solving (4.4).

As it has been explained in Sec 3.1, the Christoffel matrix eigenvectors represent also the ray amplitude polarization vectors. In anisotropic models, in which all three waves of the zero-order solution are linearly polarized in the direction of the corresponding eigenvectors, we can express the ray amplitude in the form of (3.15), i.e.

$$\mathbf{U}^{(m)}(\mathbf{x}) = A^{(m)}(\mathbf{x})\mathbf{g}^{(m)}(\mathbf{x}) \ .$$

In isotropic models we have such a simple expression only for the P-wave (equation (3.26))

$$\mathbf{U}^{(P)}(\mathbf{x}) = A(\mathbf{x})\mathbf{g}^{(3)}(\mathbf{x}) \ ,$$

while for the S-wave we have to use the form (3.27)

$$\mathbf{U}^{(S)}(\mathbf{x}) = B(\mathbf{x})\mathbf{g}^{(1)}(\mathbf{x}) + C(\mathbf{x})\mathbf{g}^{(2)}(\mathbf{x}) \ ,$$

where B and C are coordinates of the S-wave amplitude vector with respect to the basis vectors $\mathbf{g}^{(1)}, \mathbf{g}^{(2)}$. Note that the polarization of S-waves is, in general, elliptical. In can be linear only in certain special cases.

Since the polarization the amplitude we want to evaluate is implicitly given by the corresponding eigenvectors, the only quantities to be determined are the scalar amplitude factors $A^{(m)}$ (in anisotropic media) and A for the P-, and B and C for the S-wave (in isotropic media). For this we need to solve the so-called transport equation (TE), briefly mentioned in Sec. 2.5, governing the transport of the scalar ray amplitude along the ray. Note that the scalar ray amplitudes may be complex-valued.

The TE can be derived by inserting the zero-order ray solution into the EDE (see Sec. 2.5) and equating to zero the coefficient $\mathbf{M}$ of the first power of ω, or the first derivative of F, when working in the frequency or the time domain, respectively. Note that, in the equation, the coefficient $\mathbf{N}$ of the second power of ω (the second derivative of F) vanishes because τ satisfies the eikonal equation. Thus, in anisotropic media, we come to the condition:

$$M_i = c_{ijkl}\tau_{,j}U_{k,l} + (c_{ijkl}\tau_{,l}U_k)_{,j} = 0 \ , \quad \text{for} \quad i = 1,2,3 \ . \qquad (5.37)$$

Knowing τ (corresponding to the selected wave type m), one could consider this equation, after substituting (3.15) for $\mathbf{U}$, as the equation for the scalar amplitude of the zero-order solution. The problem is that, in general, the condition $\mathbf{M} = 0$ cannot be satisfied exactly (the vector $\mathbf{M}$ cannot be made zero taking into account only the leading term amplitude). In other words, it is not possible to find $A^{(m)}$ that makes the vector vanish. It should not be surprising since we know that our zero-order solution is only an approximation and cannot completely satisfy the equation of motion (otherwise it would be the exact solution). To explain this in greater depth it is useful to recall for the moment the concept of the ray series. Let us imagine that instead of the leading term we would insert the whole ray series into the EDE. Following the same procedure as that adopted in Sec. 2.5, i.e. gathering the terms of the same power of ω (or derivative of F), and keeping only the most singular terms up to ω^0 (F), we would obtain the equation analogous to (2.33) (or (2.26)) with $\bar{\mathbf{N}}, \bar{\mathbf{M}}, \bar{\mathbf{L}}$ instead of $\mathbf{N}, \mathbf{M}, \mathbf{L}$. Obviously, $\bar{\mathbf{N}} = \mathbf{N}$, since only the leading term can contribute to the highest power of ω (or the highest derivative of F). This is not the case of $\bar{\mathbf{M}}$: it differs from $\mathbf{M}$ due to a contribution from the first higher-order term, the term with the amplitude $\mathbf{U}_1$ (note that any other higher-order term does not contribute to $\bar{\mathbf{M}}$). To make it more clear, let us decompose $\bar{\mathbf{M}}$ as

$$\bar{\mathbf{M}}(\nabla\tau, \mathbf{U}, \mathbf{U}_1) = \mathbf{M}(\nabla\tau, \mathbf{U}) + \Delta\mathbf{M}(\nabla\tau, \mathbf{U}_1) \ . \qquad (5.38)$$

For the sake of simplicity, $\nabla\tau$ can be skipped from the list of variables in (5.38) as it is of no concern in the argument that follows. Since the first

higher-order term in the ray series contributes to $\bar{\mathbf{M}}$ in the same way as the leading term contributes to $\mathbf{N}$, the difference $\Delta\mathbf{M}$ is clearly

$$\Delta\mathbf{M}(\mathbf{U_1}) = \mathbf{N}(\mathbf{U_1}) = (\mathbf{\Gamma} - \mathbf{I})\mathbf{U_1} \ , \tag{5.39}$$

where $\mathbf{\Gamma}$ is the Christoffel matrix introduced in Sec. 3.1, and $\mathbf{I}$ denotes the 3×3 identity matrix.

Solving asymptotically the equation of motion, we require

$$\bar{\mathbf{M}}(\mathbf{U}, \mathbf{U}_1) = 0 \ . \tag{5.40}$$

However, the difference $\Delta\mathbf{M}$ does not vanish (so that neither $\mathbf{M}(\mathbf{U})$ which equals to $-\Delta\mathbf{M}(\mathbf{U}_1)$) eventhough τ satisfies the eikonal equation. $\Delta\mathbf{M} = \mathbf{N}$ would be zero only provided $\mathbf{U}$ would stand in it instead of $\mathbf{U}_1$, since $\mathbf{U}$ is parallel to the relevant eigenvector (corresponding to the selected type of wave) of the matrix $\mathbf{\Gamma}$. Nevertheless, we can utilize to our advantage the fact that $\Delta\mathbf{M}$ is perpendicular to the eigenvector. Multiplying $\bar{\mathbf{M}}$ with $\mathbf{g}^{(m)}$, we are left with the scalar condition

$$\bar{\mathbf{M}}(\mathbf{U}, \mathbf{U}_1) \cdot \mathbf{g}^{(m)} = \mathbf{M}(\mathbf{U}) \cdot \mathbf{g}^{(m)} = 0 \ , \tag{5.41}$$

solvable for the corresponding $A^{(m)}$ or A, B, C. Thus, taking the inner product of $\mathbf{M}$ with the relevant polarization vector and equating this product to zero leads to the transport equation for our zero-order solution. Note that the direction of the polarization vector is also called the principal direction (see Chapman, 2004) and the above linked procedure yields the so-called principal amplitude component.

Let us derive the TE in anisotropic media. For any of the three waves propagating there (the index $m = 1, 2, 3$ is omitted in the following derivation) we start with the equation $M_i(A\mathbf{g})g_i = 0$. After simple algebra, substituting (2.28) for M_i, utilizing the symmetry $c_{ijkl} = c_{klij}$ and writing $\mathbf{p}$ for $\nabla\tau$ we get

$$M_i(A\mathbf{g})g_i = 2c_{ijkl}p_jg_ig_kA_{,l} + A(c_{ijkl}p_lg_kg_i)_{,j} = 0 \ . \tag{5.42}$$

This equation can be simplified even further by writing v_i^g for $\frac{1}{\rho}c_{ijkl}p_lg_jg_k$, see (3.82)

$$2\rho v_i^g A_{,i} + A(\rho v_i^g)_{,i} = 0, \quad \text{i.e.} \quad 2\rho\mathbf{v}^g \cdot \nabla A + A\nabla \cdot (\rho\mathbf{v}^g) = 0 \ . \tag{5.43}$$

The first term in the above equations represents a directional derivative of A in the direction of $\mathbf{v}^g$. From Sec. 3.7 we know that $\mathbf{v}^g$ has the meaning of a group velocity and so (5.43) is an ordinary differential equation for A along a ray, the curve everywhere tangent to $\mathbf{v}^g$. The equation governs the evolution of the scalar ray amplitude along a ray and it is called the transport equation. An alternative and compact form of the above equation can be obtained by multiplying it by the complex conjugate quantity A^* and summing it with the TE written for A^* and multiplied by A. This gives rise to a conservation equation

$$(\rho A A^* v_i^g)_{,i} = 0, \quad \text{i.e.} \quad \nabla \cdot (\rho A A^* \mathbf{v}^g) = 0 \ . \tag{5.44}$$

The vector in parentheses is the energy flux, so that the above equation represents conservation of energy along rays.

In isotropic structures, the procedure for deriving the TE is analogous, but we have to substitute (2.31) for M_i. First, let us show this for P-waves. Writing α for the P-wave phase velocity we can express the polarization vector $\mathbf{g} = \mathbf{g}^{(3)} = \alpha \mathbf{p}$. Imposing the condition of orthogonality (5.41) we arrive at

$$
\begin{aligned}
M_i(A\mathbf{g})g_i &= (\lambda + 2\mu)(2A_{,i}p_i + 2\alpha^{-1}\alpha_{,i}p_i + 2A\alpha^2 p_{j,i}p_j p_i + Ap_{j,j}) \\
&\quad + (\lambda + 2\mu)_{,i}p_i A = 0 \ .
\end{aligned}
\tag{5.45}
$$

Recognizing that $p_{j,i}p_j p_i = \frac{1}{2}(p_j p_j)_{,i}\, p_i = \frac{1}{2}(\alpha^{-2})_{,i}\, p_i = -\frac{1}{\alpha^3}\alpha_{,i}p_i$ and substituting $\rho\alpha^2$ for $\lambda + 2\mu$ we obtain the transport equation for P-waves in isotropic media

$$\rho\alpha^2(2A_{,i}p_i + Ap_{j,j}) + (\rho\alpha^2)_{,i}\, p_i A = 0 \ . \tag{5.46}$$

Similarly to the anisotropic case it can also be written in the alternative, compact form

$$(\rho A A^* \alpha^2 p_i)_{,i} = 0 \quad \text{i.e.} \quad \nabla \cdot (\rho A A^* \alpha^2 \mathbf{p}) = 0 \ . \tag{5.47}$$

The physical meaning of this equation is the same as in the case of anisotropic media – conservation of energy. Indeed, in isotropic media the magnitude

of the P-wave group velocity vector is α and it is pointing in the direction normal to wavefront, i.e. $\mathbf{v}^g = \alpha^2 \mathbf{p}$, so that the equations (5.47) and (5.44) are in fact identical.

For S-waves the situation is a bit more complicated due to the fact that we have to deal with two polarization vectors, $\mathbf{g}^{(1)}, \mathbf{g}^{(2)}$. We multiply M_i in (5.41) by these two vectors in turn. When multiplying by $\mathbf{g}^{(1)}$ we get the condition

$$
\begin{aligned}
M_i(\mathbf{U})g_i^{(1)} &= (\lambda + \mu)(U_{j,i}p_j g_i^{(1)} + U_j p_{i,j} g_i^{(1)}) \\
&\quad + \mu(2U_{i,j}p_j g_i^{(1)} + U_i g_i^{(1)} p_{j,j}) + \lambda_{,i} g_i^{(1)} U_j p_j \\
&\quad \mu_{,j} U_i g_i^{(1)} p_j = 0 \ ,
\end{aligned}
\tag{5.48}
$$

in which $\mathbf{U}^{(S)} = B\mathbf{g}^{(1)} + C\mathbf{g}^{(2)}$ is to be substituted for $\mathbf{U}$. After simple derivation we obtain

$$
M_i(B\mathbf{g}^{(1)} + C\mathbf{g}^{(2)})g_i^{(1)} = \mu(2p_j g_i^{(1)} g_{i,j}^{(2)} C + Bp_{j,j}) + \mu_{,j} Bp_j + 2\mu B_{,j} p_j = 0 \ .
\tag{5.49}
$$

When deriving this equation we have utilized that $\mathbf{g}^{(1)}$ is the unit vector (i.e., $g_i^{(1)} g_i^{(1)} = 1$) orthogonal to $\mathbf{p}$ (i.e., $p_i g_i^{(1)} = 0$) which yields also identities $g_{i,j}^{(1)} g_i^{(1)} = 0$ and $p_{i,j} g_i^{(1)} = -p_i g_{i,j}^{(1)}$. In the same way, when multiplying M_i with $\mathbf{g}^{(2)}$, we obtain the analogous equation to the above one with interchanged roles of $\mathbf{g}^{(1)}$ and $\mathbf{g}^{(2)}$ and of B and C. Thus we are left with the system of two (mutually coupled) S-wave transport equations

$$
\begin{aligned}
\mu(2p_j g_i^{(1)} g_{i,j}^{(2)} C + Bp_{j,j}) + \mu_{,j} Bp_j + 2\mu B_{,j} p_j &= 0 \\
\mu(2p_j g_i^{(2)} g_{i,j}^{(1)} B + Cp_{j,j}) + \mu_{,j} Cp_j + 2\mu C_{,j} p_j &= 0 \ .
\end{aligned}
\tag{5.50}
$$

Up to now we have not specified the position of the two eigenvectors $\mathbf{g}^{(I)}$ in the plane perpendicular to ray. We can choose their position arbitrarily, keeping their mutual orthogonality. Let us make them coinciding with the vectors $\mathbf{e}_I$, the RCC basis vectors introduced in Sec. 4.1. Then the vectors are transported parallel along rays. For the change of $\mathbf{g}^{(I)}$ along the ray we have:

$$\frac{\mathrm{d}g_i^{(I)}}{\mathrm{d}s} = g_{i,j}^{(I)}\frac{\mathrm{d}x_j}{\mathrm{d}s} = g_{i,j}^{(I)}\beta p_j \ . \tag{5.51}$$

Note that the last equality is a consequence of the RTS. From the condition of the parallel transport (4.1) we know that $\mathrm{d}g_i^{(I)}/\mathrm{d}s = a_I p_i$. Thus, we can write

$$\beta^{-1}a_I p_i = \pm\beta^{-2}g_i^{(3)} = g_{i,j}^{(I)}p_j \ . \tag{5.52}$$

Multiplying in turn this equation for $I = 1$ with $g_i^{(2)}$ and for $I = 2$ with $g_i^{(1)}$, and taking into account the orthogonality of the eigenvectors of the Christoffel matrix, yields:

$$g_{i,j}^{(1)}p_j g_i^{(2)} = 0, \quad g_{i,j}^{(2)}p_j g_i^{(1)} = 0 \ . \tag{5.53}$$

Under this condition, however, the transport equations (5.50) simplify and decouple into

$$\mu B p_{j,j} + \mu_{,j} B p_j + 2\mu B_{,j} p_j = 0$$
$$\mu C p_{j,j} + \mu_{,j} C p_j + 2\mu C_{,j} p_j = 0 \ . \tag{5.54}$$

Substituting $\beta^2\rho$ for μ and applying the same procedure with complex conjugate scalar amplitude factors as in the case of the P-wave (and also the waves in anisotropic media) we finally arrive at the system of two compact decoupled transport equations for B and C

$$(\rho BB^*\beta^2 p_i)_{,i} = 0 \ , \quad (\rho CC^*\beta^2 p_i)_{,i} = 0 \ . \tag{5.55}$$

We see that, provided the polarization vectors coincide with the RCC basis vecors, we have obtained exactly the same equations both for B and for C, i.e., B and C change along the ray in exactly the same way. This means that the direction of the S-wave amplitude vector remains fixed with respect to the RCC basis along the whole ray. All the TE's (5.44), (5.47) and (5.55) are of the same form, so that the procedure to solve all these equations is the same.

5.6 Solution of the transport equation. Continuation formula

In the previous section, we have derived transport equations both for anisotropic as well as isotropic media for all types of waves propagating in these structures. We have found that the equation governing the transport of the scalar ray amplitude along rays has in all cases the form

$$(\rho AA^* v_i^g)_{,i} = 0 \ , \tag{5.56}$$

where A is the scalar ray amplitude factor to be found, ρ is density and v_i^g denotes the i-th component of the relevant group velocity vector. In general anisotropic structures it is given by the expression (3.82), in isotropic models it can be replaced by $v^2 p_i$, with v being either α for the P-wave, or β for the S-wave.

Regardless of the complexity of the model we can always find the analytic solution to the above TE along rays. Let us apply a volume integral over a volume V to the TE and convert it to the surface integral over the volume boundary S by the use of the well known Gauss theorem

$$\iiint\limits_V (\rho AA^* v_i^g)_{,i} dV = \iint\limits_S \rho AA^* v_i^g n_i^S dS = 0 \ . \tag{5.57}$$

In the above formula, n_i^S is the i-th component of the outer unit normal to the surface S.

The volume V in (5.57) is an arbitrary volume illuminated by the ray field of a given wave type. Especially, let it be the segment of the elementary ray tube, formed by rays described by the flow parameter τ, bounded by two wavefronts (at times τ_0 and τ, see Fig. 13). Then the surface integral in (5.57) simplifies because the contributions from the side walls of the tube vanish. Indeed, since the energy flows along rays, i.e. the group velocity is everywhere tangential to rays, and the outer normal is perpendicular to rays on the side walls, the inner product $v_i^g n_i^S$ vanishes there. We have the only non-vanishing contributions to the surface integral from the wavefront surface segments. On these segments we can determine $v_i^g n_i^S$ as

$$\begin{aligned} v_i^g(\tau_0) n_i^S(\tau_0) &= -v_i^g(\tau_0) n_i^\tau(\tau_0) = -c(\tau_0) \\ v_i^g(\tau) n_i^S(\tau) &= v_i^g(\tau) n_i^\tau(\tau) = c(\tau) \ , \end{aligned} \tag{5.58}$$

where c means the phase velocity and $\mathbf{n}^\tau$ denotes the normal to the wavefront. The minus sign in the first of the two equation is due to the opposite orientation of the outer normal to the ray tube and normal to the wavefront

at the point τ_0 on the ray along which we wish to solve the TE. The surface integral in (5.57) is then

$$\iint\limits_{\mathrm{d}S^{(\tau)}(\tau)} \rho(\tau)A(\tau)A^*(\tau)c(\tau)\mathrm{d}S - \iint\limits_{\mathrm{d}S^{(\tau)}(\tau_0)} \rho(\tau_0)A(\tau_0)A^*(\tau_0)c(\tau_0)\mathrm{d}S = 0 \ , \qquad (5.59)$$

where $\mathrm{d}S^{(\tau)}$ is the scalar surface element cut from wavefront by the elementary ray tube. It is defined as $\mathrm{d}S^{(\tau)} = \mathrm{d}\mathbf{S}^{(\tau)} \cdot \mathbf{n}^\tau$, where $\mathrm{d}\mathbf{S}^{(\tau)}$ is the vectorial surface element given by (5.1). Combining (5.8) and (5.4) we see that

$$\mathrm{d}S^{(\tau)} = c^{-1}J^{(\tau)}\mathrm{d}\gamma_1\mathrm{d}\gamma_2 \ . \qquad (5.60)$$

This makes it possible to put the two integrals in (5.59) into one and write

$$\iint\limits_{\gamma_1 \ \gamma_2} [\rho(\tau)A(\tau)A^*(\tau)J^{(\tau)}(\tau) - \rho(\tau_0)A(\tau_0)A^*(\tau_0)J^{(\tau)}(\tau_0)]\mathrm{d}\gamma_1\mathrm{d}\gamma_2 = 0 \ . \quad (5.61)$$

The above equation holds universally, it must not depend on any specific choice of the ray parameters γ_I. Thus the conclusion is that the expression in square brackets itself must vanish, i.e.

$$\rho(\tau)A(\tau)A^*(\tau)J^{(\tau)}(\tau) = \rho(\tau_0)A(\tau_0)A^*(\tau_0)J^{(\tau)}(\tau_0) \ . \qquad (5.62)$$

Since, in the standard ray theory, the quantities ρ and $J^{(\tau)}$ in the above equation are always real, we can write

$$A(\tau) = A(\tau_0)\sqrt{\frac{\rho(\tau_0)J^{(\tau)}(\tau_0)}{\rho(\tau)J^{(\tau)}(\tau)}} \ . \qquad (5.63)$$

The equation relates the scalar amplitude factor at a given point on the ray, say the point R (e.g., receiver), determined by τ, to the scalar amplitude factor at a reference (initial) point on the same ray, say S, determined by τ_0. Applying (5.9), this equation can be rewritten as

$$A(R) = A(S)\sqrt{\frac{\rho(S)v^g(S)J(S)}{\rho(R)v^g(R)J(R)}} \ , \qquad (5.64)$$

the most common form of the **continuation formula** in anisotropic models. The amplitude at R is inversely proportional to the quantity $\sqrt{J(R)}$, introduced in Sec. 4.2 as the geometrical spreading. To evaluate the amplitude at R we must moreover know the geometrical spreading at the reference

point S and the group velocity magnitude at the two points, calculated using (3.82), which requires to know also the slowness and the relevant eigenvector. These quantities are known from the RTS. Density is assumed to be known everywhere as it is the parameter of the model.

In isotropic media, we can rewrite the continuation formula by the use of $v^g = \alpha$ (for P-waves) or $v^g = \beta$ (for S-waves). For a P-wave the formula reads

$$A(R) = A(S)\sqrt{\frac{\rho(S)\alpha(S)J(S)}{\rho(R)\alpha(R)J(R)}} \ . \tag{5.65}$$

The only quantity to be calculated in order to evaluate the amplitude factor from the continuation formula in isotropic media is the geometrical spreading. In the case of an S-wave we must replace β for α and use the continuation formula for B (and C) amplitude factors (standing in the formula instead of A). In this way we obtain the amplitude vectors (4.6), expressed in the RCC. For practical use it is convenient to transform the RCC amplitude to the general Cartesian coordinates by multiplying with the transformation matrix $\mathbf{H}$, introduced in Sec. 4.1 (see Sec. 5.10).

5.7 Notes on the continuation formula

Let us have a ray connecting points S and R. According to the continuation formula we are able to calculate the scalar ray amplitude from S to R along this ray. Despite the fact that in the formula there are quantities specified only at the two points S and R, knowledge of the ray connecting them is essential to evaluate the geometrical spreading and, in anisotropic models, also the group velocity. If there would be no ray from S to R, for example when a shadow zone is present there, we have no chance to compute the ray amplitude at R by the use of the standard zero order ray method. This is, however, not an additional restriction of the method since the standard RM travel time is also known only along rays.

The continuation formula represents a very simple tool to compute the amplitudes, applicable in generally inhomogeneous complex models. There are, however, several specific situations in which a special operation has to be involved to evaluate the amplitude correctly. In certain situations the solution even breaks down and the formula cannot be used notwithstanding that the ray connecting the points R and S exists. All the above-mentioned situations relate to the cases of shrinking the elementary ray tube to zero cross-sectional area and, consequently, intersecting rays and vanishing the geometrical spreading.
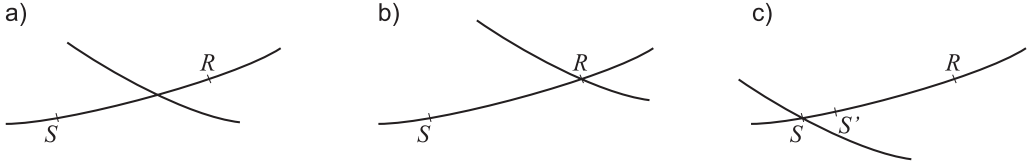
Figure 18: The sketch of three situations in which the continuation formula possibly meets problems. In all these cases the intersecting rays belong to the same elementary ray tube.

Let us first consider that there is a caustic point on the raypath between the points S and R, Fig. 18 (a). At the caustic point, the ray Jacobian J vanishes. After passing through the caustics, J becomes finite again, but usually changes sign (in the case of the first-order caustic). In order to continue with the solution after passing through the caustic, the proper phase shift has to be taken into account to choose the right root of $\sqrt{J}$. The phase shift is controlled by the index of the ray trajectory K (the KMAH index), see Sec. 5.4. In isotropic media, the index K increases by $\Delta K{=}1$ upon the first-order caustic, and by $\Delta K{=}2$ in the case of the second-order caustic. In anisotropic models the behavior of ΔK may be more complicated, as it is explained, e.g., by Bakker (1998) or Červený (2001). As many times as the ray passes through a caustic between S and R, that many times the proper ΔK must be added to the index K. In the presence of caustics between the points S and R it is necessary to rewrite $J(R)$ as $J(R) = |J(R)| \exp(i\pi K(S, R))$ and its square root in the continuation formula as

$$\sqrt{J(R)} = \sqrt{|J(R)|} \exp(\frac{1}{2}\pi K(S, R)) . \tag{5.66}$$

It is therefore useful to generalize the continuation formula writing the expression valid both in the presence as well as the absence of caustic points on the raypath connecting the points S and R. In anisotropic media we have

$$A(R) = A(S)\sqrt{\frac{\rho(S)v^g(S)|J(S)|}{\rho(R)v^g(R)|J(R)|}} \exp(i\frac{1}{2}\pi K(S, R)) , \tag{5.67}$$

where we have again used, for simplicity, the notation v^g for $|\mathbf{v}^g|$. The P-wave amplitude satisfies

$$A(R) = A(S)\sqrt{\frac{\rho(S)\alpha(S)|J(S)|}{\rho(R)\alpha(R)|J(R)|}} \exp(i\frac{1}{2}\pi K(S, R)) , \tag{5.68}$$

and the S-wave amplitude satisfies the analogous equations for B and C with β replacing α. When there are no caustic points in between S and R, the index of the ray trajectory K obviously equals zero, i.e., no additional phase shift is taken into account.

Second, let us imagine that the point R itself is a caustic point, see Fig. 18b. Then $|J(R)| = 0$ and the scalar amplitude at R is **infinite**. The caustic represents a **singularity of the ray theory**. At such a point and in its vicinity, the ray theory is locally invalid and the ray solution is in conflict with its ansatz (assuming slowly varying finite amplitude). We speak about the caustic region in which the ray method cannot be used.

Third, let us consider that the rays are intersecting at the point S. The very common such situation is when the rays are emanated from the point S — the point source. Then $|J(S)| = 0$, and provided finite $A(S)$, the continuation formula would yield zero amplitude everywhere along the ray. To obtain a non-trivial solution we have to generalize the continuation formula considering a finite limit when a point S' approaches S on the given ray (see Fig. 18 (c))

$$\lim_{S' \to S}[A(S')\sqrt{|J(S')|}] = \tilde{\mathcal{G}}(S) \; , \qquad (5.69)$$

which we substitute for $A(S)\sqrt{|J(S)|}$ into the continuation formula. This limit depends on the raypath along which the point S' approaches S. To emphasize this fact we add the ray parameters γ_I, specifying the given ray, to the parameters of the function $\tilde{\mathcal{G}}$. The function $\tilde{\mathcal{G}}(S, \gamma_1, \gamma_2)$ is then, in general, directionally dependent and describes the directional radiation of the point source.

In the case of a point source at S it is convenient to modify the continuation formula by useful normalizing of the geometrical spreading. More specifically, let us introduce the so-called **relative geometrical spreading**, $\mathcal{S}(R, S) = \sqrt{|J(R)|/\det \bar{\mathbf{P}}(S)} = \sqrt{|\det \bar{\mathbf{Q}}(R)|/\det |\bar{\mathbf{P}}(S)|}$, where the matrices $\bar{\mathbf{Q}}$ and $\bar{\mathbf{P}}$ are the solutions of the DRT in the RCC (or WOC, in the case of anisotropic medium) for a point source initial conditions. Note that away from the point source S, there is no effect of the above modification, since the multiplicators $(|\det \bar{\mathbf{P}}(S)|)^{-1}$ in numerator and denominator cancel each other. An important property of the relative geometrical spreading is its reciprocity, i.e. equal value when reversing the propagation direction: $\mathcal{S}(R, S) = \mathcal{S}(S, R)$ which is not a general property of $\sqrt{J}$ itself. For details the reader is referred to the paper by Kendall et al., 1992. See also Chapman (2004), or Červený (2001). It can be also shown, using the concept of the propagator matrix (briefly mentioned in Sec. 5.3), that the relative geometrical spreading does not depend on the parameterization of the ray field, i.e. on a specific choice of the ray parameters γ_1, γ_2. Consequently, the

modification allows us to consider, instead of $\tilde{\mathcal{G}}$, the finite limit $\mathcal{G}$

$$\lim_{S' \to S}[A(S')\mathcal{S}(S', S)] = \mathcal{G}(S, \gamma_1, \gamma_2) \ , \tag{5.70}$$

invariant with respect to parameterization of the ray field. Thus, this limit, being still directionally dependent, characterizes better the directional radiation of the point source itself, without being contaminated by directionally dependent residual factors due to the ray field parameterization (compare, for example, dependence on ψ_0 in the expression (5.35) for a point-source initial $\bar{\mathbf{P}}(S)$). The function $\mathcal{G}(S, \gamma_1, \gamma_2)$ is called the **radiation function**. Note that the parameters γ_I in the argument of the function $\mathcal{G}$ indicate only its directional dependence, but not a dependence on a specific choice of γ_I and we skip them in the following equations.

The generalized continuation formula for anisotropic media then reads

$$A(R) = \sqrt{\frac{\rho(S)c(S)}{\rho(R)c(R)}}\mathcal{S}(R, S)^{-1}\exp(\mathrm{i}\frac{1}{2}\pi K(S, R))\mathcal{G}(S) \ . \tag{5.71}$$

In isotropic media, e.g., for P waves, we can write

$$A(R) = \sqrt{\frac{\rho(S)\alpha(S)}{\rho(R)\alpha(R)}}\mathcal{S}(R, S)^{-1}\exp(\mathrm{i}\frac{1}{2}\pi K(S, R))\mathcal{G}(S) \ . \tag{5.72}$$

The modification for S waves is straightforward.

From the generalized continuation formula it is clear that the radiation function can be interpreted as a spreading-free amplitude (i.e., the amplitude not divided by the relative spreading) at the source: if $R = S$, $A(S) = \mathcal{S}(S, S)^{-1}\mathcal{G}(S)$. Note that the $\mathcal{G}$'s in the equations (5.71) and (5.72), corresponding to the isotropic and anisotropic case, differ from each other even for the same type of the point source.

The physical meaning of the radiation function $\mathcal{G}$ can be seen in a more explicit way in a homogeneous isotropic model. From Sec. 3.3 we know that the rays are straight lines in such a case. The ray Jacobian J can be expressed analytically. For example, for take-off angles as the ray parameters it is given by the equation (5.14) as $J = l^2 \sin\psi_0$, with l being the length of the ray (the distance between the points R and S), and ψ_0 being the declination of the ray (see Sec. 3.3). From equation (5.35) it follows that the determinant of the matrix $\bar{\mathbf{P}}$ at the source point S is $\det \bar{\mathbf{P}}(S) = v(S)^{-2} \sin\psi_0$. Thus,

from equation (5.72) we can see that for a point source S in a homogeneous isotropic medium the amplitude is, as expected, proportional to $1/l$. The physical meaning of the radiation function is then clear: in a homogeneous isotropic medium it can be viewed as the directionally dependent scalar ray amplitude on the sphere with its center at S and with the radius $l = 1/v$.

5.8   Radiation function and radiation pattern

The source types of seismological interest are namely a single force (important for Green's function computation), a force couple and a linear combination of the force couples, known as the moment tensor point source. Especially, combining three couples without a torque moment, acting along three mutually perpendicular axes, we can simulate the omnidirectional explosive source in isotropic media. However, the radiation function corresponding to such an omnidirectional source need not be calculated in this way as it is very simple: it represents a multiplicative constant, the same in all directions. Another special case of the moment tensor point source, extremely important in earthquake seismology, is the well known double couple. From the theoretical point of view, the most important is the single force point source. Knowing the corresponding radiation function allows us to calculate the Green's function (defined as a displacement due to a single force). Realizing that displacement due to a force couple is only a spatial derivative of the Green's function, we see that radiation functions for other above-mentioned source types can be easily derived from the basic radiation function for the single force. This source type we also choose here as an example for further explanation.

The point source radiation functions, introduced in the previous section, can be found by matching the general expressions (5.71) or (5.72) with analytical solution available for a homogeneous medium. The idea behind this is that the expressions (5.71) and (5.72), valid for a general inhomogeneous media, must also be adequate for the special case of a homogeneous medium, for which the analytical solution is known. For example, for a single force in an isotropic medium, the well known Stoke's solution (see, e.g, Aki and Richards, 1980) can be used to determine the radiation function. For the sake of writing it in a compact form, let us denote by $\boldsymbol{\mathcal{G}}^{(q)}$ the radiation vector, composed of 3 RCC radiation functions corresponding to 3 RCC basis (polarization) vectors. Assume a single force acting at the point S

$$\mathbf{f}(\mathbf{x}) = \delta(\mathbf{x} - \mathbf{x}(S))\mathbf{f}_0 \ , \tag{5.73}$$

expressed in general Cartesian coordinates. Then, the RCC radiation vector due to this force is given by the formula

$$\boldsymbol{\mathcal{G}}^{(q)}(S) = \frac{1}{4\pi\rho(S)v(S)}\mathbf{H}^T(S)\mathbf{f}_0(S) \;, \qquad (5.74)$$

in which the Cartesian vector $\mathbf{f}_0$ must be multiplied by the inverse transformation matrix $\mathbf{H}$, $\mathbf{H}^{-1} = \mathbf{H}^T$ (see Sec. 4.1). The first two components of the above radiation vector yield the S-wave radiation function (for which we specify β for v), while the third one yields the P-wave radiation function (with α inserted for v).

For the vertical point force (pointing along the axis x_3), the radiation function (5.74) is shown in the figure 19. In the left part of the figure, the P-wave radiation function is displayed in a 3D view. The right part provides the same, but for an S-wave. If we choose the RCC basis vector $\mathbf{e}_2$ being horizontal, the S-wave radiation function in Fig. 19 (right) corresponds to the S_1 component (scalar factor B), since the vertical force does not generate any S-wave displacement polarized in horizontal plane. Fig. 20 (left), shows a 2D vertical section of the radiation functions from Fig. 19.
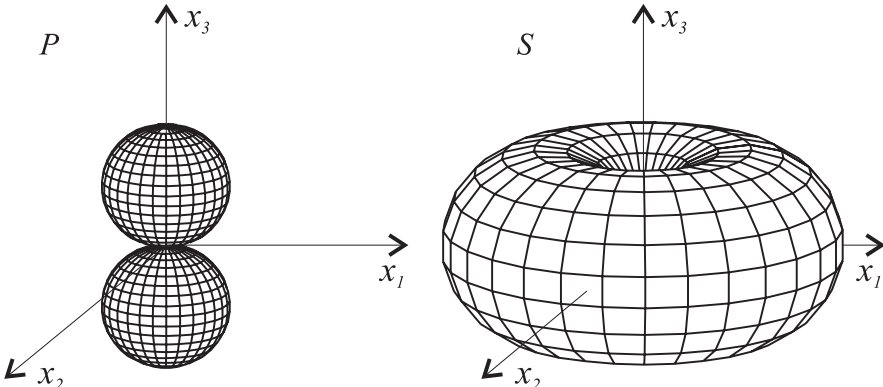
Figure 19: Radiation functions of P- (a) and S waves (b) due to a vertical point force in an isotropic medium.

To find the radiation function due to a single force in an anisotropic medium, we proceed in analogy to the isotropic case. For matching with the general solution we can use the solution for a homogeneous anisotropic medium presented by Pšenčík and Teles (1996) or Červený (2001). The analytic solution depends on the Gaussian curvature $\mathcal{K}$ of the slowness surface in the direction specified by the slowness vector of the considered wave. This quantity can be expressed as a product of the principal curvatures k_1, k_2 along the p_1- and p_2- axes: $\mathcal{K} = k_1 k_2$. The principle curvatures can be used to define the so-called index of the source, $\sigma_0 = 1 + \frac{1}{2}\mathrm{sgn}k_1 + \frac{1}{2}\mathrm{sgn}k_1$. Thus, $\sigma_0 = 0$ for $k_I < 0$ which indicates that the slowness surface is convex for a given direction of the slowness vector, $\sigma_0 = 2$ for $k_I > 0$ which
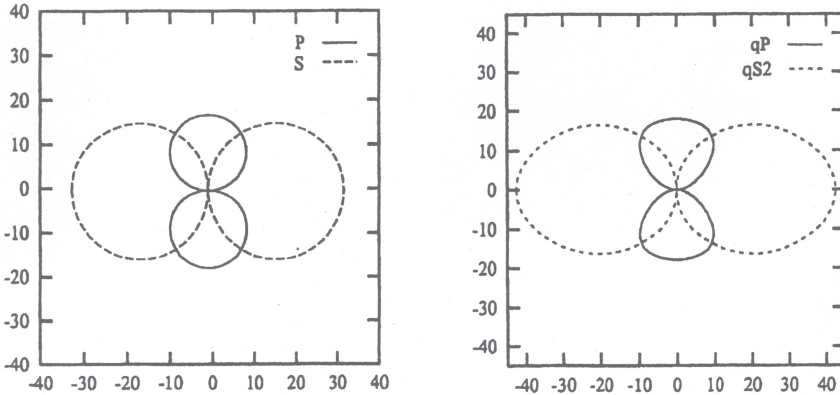
Figure 20: Left: 2D vertical section of the P- and S-wave radiation function due to the vertical point force in an isotropic medium. Right: the same, but for the qP- and qS-wave in a vertically transversally isotropic medium (from Pšenčík, 1994).

corresponds to a concave surface, and, finally, $\sigma_0 = 1$ for k_1 and k_2 having opposite signs, which corresponds to a saddle-shaped slowness surface. For example, in Fig. 8, the slowness surfaces of the qP- and qS_1-waves would be assigned by $\sigma_0 = 0$, while that one of the qS_2- would be assigned by $\sigma_0 = 1$ in certain slowness directions (note that the slowness surfaces in transversally isotropic media, corresponding to Fig. 8, left, are rotationally symmetrical with respect to the p_3-axis, the axis of the symmetry of the medium). For completeness let us add that in isotropic media, $\sigma_0 = 0$ in all directions both for P- as well as S-waves.

The radiation function due to a single force (5.73) for any of the three waves propagating in an anisotropic medium reads

$$\mathcal{G}(S) = \frac{g_k(S)f_{0k}(S)}{4\pi\rho(S)c(S)} \exp[\frac{1}{2}\pi\sigma_0(S)] , \tag{5.75}$$

where g_k is the polarization vector of the considered wave and c its phase velocity. The analogy with (5.74) is obvious, but the quantities $g_k(S)$ and $c(S)$ in the equation (5.75) are directionally dependent. An example of such radiation functions due to a vertical force in a transversally symmetric medium with vertical axis of symmetry is shown in Fig. 20, right. The figure provides the radiation functions of the qP- and qS_2-wave; the faster qS_1-wave, polarized horizontally in the given example, is not generated by the vertical force.

In connection with directional radiation from a point source, another important term, the so-called **radiation pattern**, frequently appears in seismological literature. Many authors (for example, Aki and Richards, 1980) define the radiation pattern as the amplitude on a unit sphere in a locally homogeneous medium, with its center at the source point.

$$\mathcal{R}(S) = (\mathcal{G}(S)/\mathcal{S}(R,S))_{l(R,S)=1} \ , \tag{5.76}$$

where $l(R,S)$ means the distance between R and S. This amplitude is, in general, directionally dependent. Let us explain the difference between the radiation function, we have defined in the previous section, and the radiation pattern.

In homogeneous isotropic media, the radiation function has the meaning of the ray amplitude on a sphere around the source, the radius of which is $1/v$. Thanks to the fact that the geometrical spreading in such a medium does not depend on direction, i.e. it is the same for all points situated on a given sphere with its center at S, the difference between $\mathcal{R}(S)$ and $\mathcal{G}(S)$ is only formal, given by proper scaling with v: $\mathcal{R}(S) = \mathcal{G}(S)/v(S)$. In the case of isotropy, $v(S)$ is a directionally independent constant. Thus, for example, Fig. 19 and Fig. 20 (left) could represent both $\mathcal{R}(S)$ as well as a normalized $\mathcal{G}(S)$ corresponding to the unit vertical force in a homogeneous isotropic medium. Note that the normalizing factor for P- and S-waves would be different.

In homogeneous anisotropic media, the radiation pattern $\mathcal{R}(S)$, given as (5.76), may differ considerably from $\mathcal{G}(S)$ due to possibly strong directional dependence of the relative geometrical spreading $\mathcal{S}(R,S)$. For an illustration see figure 21. In the left part, the figure provides an example of the so-called ray spreading diagram of qP-wave in a transversally isotropic medium. The diagram displays the relative geometrical spreading together with rays shot with equally spaced initial angles of the wavefront normals (slowness vectors). The rays terminate on the unit sphere around the source. The length of the rays in the diagram is a measure of the relative geometrical spreading in a given direction of initial slowness. Note that in the case of anisotropy, the ray direction does not coincide, in general, with the initial slowness direction. The angular spacing between rays is inversely proportional to the geometrical spreading. Fig. 21, right, shows the corresponding qP-wave radiation pattern. Let us notice a considerable difference in shape between $\mathcal{R}(S)$ and $\mathcal{G}(S)$ (compare Fig. 21, right, with the solid line in Fig. 20, right).

Let us end this section noting some practical aspects of the calculation of the ray synthetic wavefield due to a point source. In isotropic media, the traditional approach, commonly used by many authors, is to consider the standard radiation pattern as an "initial amplitude" at the source. This means that, in fact, we consider a homogeneous medium in the vicinity of
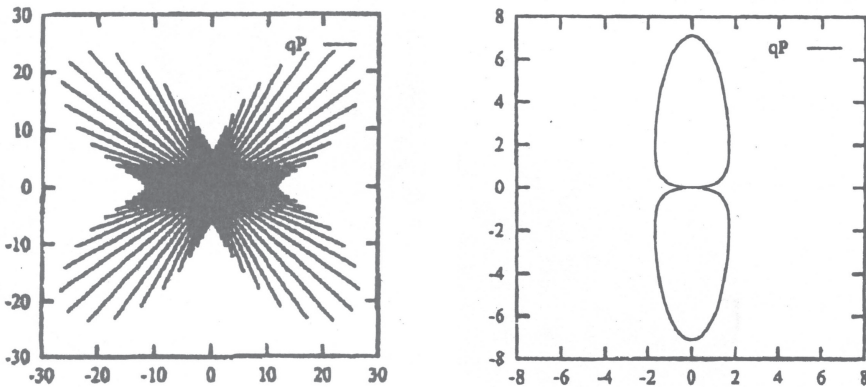
Figure 21: Left: 2D vertical section of the qP ray spreading diagram. Right: 2D vertical section of qP radiation pattern due to the vertical point force in a transversally isotropic medium with vertical axis of symmetry (from Pšenčík, 1994).

the source instead of the real inhomogeneous structure. It is assumed that replacing a small portion of the model in a small vicinity of the source-point by a homogeneous medium does not make a considerable difference for the final amplitude at a larger distance from the source. In ray theory, the minimum source-receiver distance is restricted by the validity conditions, see the chapter 7. This restriction also ensures the wavefield to be calculated away a near-source region in which the near-field terms, not computed in the RM, are negligible. Moreover, the RM validity conditions dictate that the structure must be varying only slowly with position. Under these circumstances, the substitution of the real medium in a small vicinity of the source by a homogeneous material may be acceptable. Nevertheless, there are models, treatable by the RM, in which the inhomogeneous character of the medium in the vicinity of the point source is more pronounced, and considering the standard radiation pattern would yield distorted results. For example, when the source occurs in the region of a velocity gradient, the amplitudes on a unit sphere around the source may depart significantly from those yielded by the standard radiation pattern. Another well known structural effect, resulting in amplitude directional behavior considerably different from the standard radiation pattern, is the presence of a structural interface (or the Earth's surface) in a close vicinity of the source (see Jílek and Červený, 1996). The effects due to local inhomogeneities in the source region would be frequency-dependent. For high frequencies the amplitude directional behavior could be similar to that in a locally uniform medium. With decreasing

frequency the amplitude may depart significantly from that computed by the use of the locally uniform medium approximation.

In anisotropic media, the standard radiation patterns, defined by (5.76), are not so widely used as in the case of isotropy. The reason is that, in the case of anisotropy, the radiation pattern itself does not describe well the directional radiation from the point source. Moreover, the approximation consisting in replacing the real medium by a homogeneous material inside the unit sphere around the source is neither well justified, nor computationally efficient. Many authors present the modified radiation patterns representing the amplitude over a unit sphere in real inhomogeneous media (see Pšenčík and Teles, 1996, Ben-Menahem et al., 1991, and others).

5.9   Ray amplitudes across a structural interface

Let us consider a slightly curved interface Σ. In Sec. 3.8, it has been shown how to transform the slowness vector across such an interface. In this section we explain how to transform the scalar amplitude factor and the ray Jacobian. Note that the amplitude polarization vectors of the waves generated at the interface, **g**, are assumed to be known. In anisotropic models or for P-waves in isotropic structures they are determined uniquely as the corresponding Christoffel matrix eigenvectors at a given point. For S-waves the polarization vectors can be, with advantage, identified as the RCC basis vectors tangent to wavefront. At the interface they can be, in principle, specified arbitrarily. However, they must be specified before the amplitude is transformed across the interface as the amplitude is expressed with respect to them.

For simplicity, let us assume that the interface separates two solid half-spaces in welded contact. According to the boundary conditions (BC), the displacement and traction must be equal on both sides of the interface. In Sec. 3.8 we have shown, that to satisfy these conditions universally (at any time and any point of the interface), not only the forms of the analytical signals describing the time dependence of our solution, but also their arguments must be the same for all the waves involved in the reflection/transmission (R/T) problem. Thus, dividing the BC equations by the analytical signals, we arrive at a system of algebraic equations for the scalar amplitude factors of the generated waves.

Let us start with the case of an anisotropic medium. As we know, three types of waves can, in general, propagate in such a model. Thus, on both sides of the interface an incident wave can generate three waves; altogether six generated waves can possibly propagate away from the interface. Let us distinguish them by the upper indices R and T, for reflections and transmissions, respectively, and by the lower-case index $k = 1, 2, 3$ for the given wave

type ($k = 1$ for the qS_1-wave, 2 for the qS_2-, and 3 for the qP-wave). Let us assume a wave with the i-the amplitude component $A_j g_i^{(j)}$, with j being again either 1, or 2, or 3, according to the type of the wave, incident from the first halfspace in Fig. 9. For displacement and traction the BC yield

$$
\begin{aligned}
A_1^{\mathrm{T}} g_i^{(1)\mathrm{T}} + A_2^{\mathrm{T}} g_i^{(2)\mathrm{T}} + A_3^{\mathrm{T}} g_i^{(3)\mathrm{T}} - A_1^{\mathrm{R}} g_i^{(1)\mathrm{R}} - A_2^{\mathrm{R}} g_i^{(2)\mathrm{R}} - A_3^{\mathrm{R}} g_i^{(3)\mathrm{R}} &= -A_j g_i^{(j)} \\
A_1^{\mathrm{T}} X_i^{(1)\mathrm{T}} + A_2^{\mathrm{T}} X_i^{(2)\mathrm{T}} + A_3^{\mathrm{T}} X_i^{(3)\mathrm{T}} - A_1^{\mathrm{R}} X_i^{(1)\mathrm{R}} - A_2^{\mathrm{R}} X_i^{(2)\mathrm{R}} - A_3^{\mathrm{R}} X_i^{(3)\mathrm{R}} &= -A_j X_i^{(j)} \ ,
\end{aligned}
$$

$$(5.77)$$

where the X_i's are given as

$$
\begin{aligned}
X_i^{(k)\mathrm{R}} &= c_{ijnl}^{(1)} \nu_j g_n^{(k)\mathrm{R}} p_l^{(k)\mathrm{R}} \ , \\
X_i^{(k)\mathrm{T}} &= c_{ijnl}^{(2)} \nu_j g_n^{(k)\mathrm{T}} p_l^{(k)\mathrm{T}} \ ,
\end{aligned}
\tag{5.78}
$$

with $\boldsymbol{\nu}$ denoting the unit normal to the interface (see Sec. 3.8) and $c_{ijkl}^{(m)}$ being used for the elastic parameters either in the first halfspace ($m = 1$, for reflected waves) or in the second halfspace ($m = 2$, for transmitted waves). In the above equations, $\mathbf{g}^{(k)\mathrm{R}}$ or $\mathbf{g}^{(k)\mathrm{T}}$, and $\mathbf{p}^{(k)\mathrm{R}}$ or $\mathbf{p}^{(k)\mathrm{T}}$, are used to denote the polarization and the slowness vectors, respectively, of the generated wave of the k-th type, involved in the R/T problem. The corresponding quantities without the upper index R or T relate to the incident wave.

The system (5.77) represents six algebraic equations for six unknown scalar amplitude factors which can be solved without difficulty. However, in general anisotropic media no explicit analytical expressions for the slowness and polarization vectors are available, so that the amplitude factors, as solutions of the system (5.77), must be sought fully numerically.

In practice it is convenient to modify the system (5.77) dividing it by the amplitude of the incident wave, and to consider the system for all three possible incident wave types. Instead of amplitude factors of the generated waves we then solve the system for the so-called R/T coefficients. Let us introduce displacement reflection coefficients R_{ij}^{R} as

$$
R_{ij}^{\mathrm{R}} = \frac{A_j^{\mathrm{R}}}{A_i} \ , \quad i, j = 1, 2, 3 \ .
\tag{5.79}
$$

In the above definition, A_j^{R} means the scalar amplitude factor of the reflected wave of the j-th type, and A_i denotes the scalar amplitude factor of the incident wave of the i-th type. For reflections let us consider the matrix of

above defined reflection coefficients

$$\mathbf{R}^{\mathrm{R}} = \begin{pmatrix} R^{\mathrm{R}}_{11} & R^{\mathrm{R}}_{12} & R^{\mathrm{R}}_{13} \\ R^{\mathrm{R}}_{21} & R^{\mathrm{R}}_{22} & R^{\mathrm{R}}_{23} \\ R^{\mathrm{R}}_{31} & R^{\mathrm{R}}_{32} & R^{\mathrm{R}}_{33} \, . \end{pmatrix} \tag{5.80}$$

Figure 22 illustrates schematically meaning of individual reflection coefficients, the elements of the matrix $\mathbf{R}^{\mathrm{R}}$. For transmissions we consider the matrix of transmission coefficients $\mathbf{R}^{\mathrm{T}}$, with elements R^{T}_{ij}, the meaning of which is in a straightforward analogy to R^{R}_{ij}.
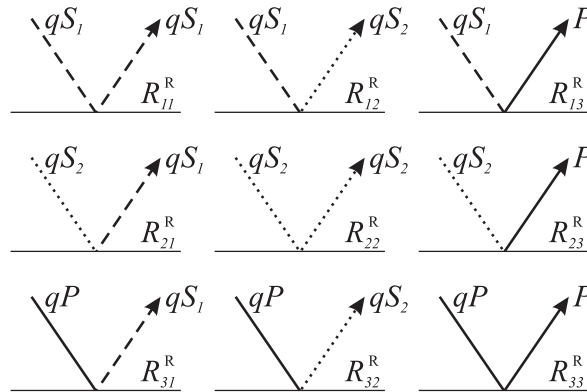
Figure 22: Scheme of the system of the reflection coefficients in general anisotropic medium.

The importance of the R/T coefficients in anisotropic media is mainly in the possibility of writing compact formulas for multiply reflected or transmitted rays containing the products of all the relevant R/T coefficients at all points of ray incidence to an interface along the raypath. In general anisotropy, there are no explicit analytic expressions for the coefficients (like in isotropic media, see below); they must be found by numerically solving the corresponding sets of algebraic equations.

In isotropic media we proceed analogously. Let us again assume a smoothly curved interface separating two solid halfspaces in welded contact, so that the BC controlling the R/T process are exactly the same as we have assumed above: continuity of displacement and traction across the interface. In isotropic models only two wave types can propagate: the P- and S-waves. An incident wave can, regardless of whether it is P- or S-, in principle, generate both of them on each side of the interface. Thus we have to deal with four R/T waves which together with the incident wave must satisfy the BC. The BC equations are analogous to (5.77). Despite having less generated

waves than in the case of anisotropy, the S-waves are represented by expressions $\mathbf{U}^{(S)} = B\mathbf{e}_1 + C\mathbf{e}_2$ (the equation (3.27) in Sec. 3.1 in which we have substituted the RCC basis vectors for the polarization vectors), so that two amplitude factors, B and C, we need to specify their amplitude vectors. For P-waves, linearly polarized, we have the simple expression (3.26): $\mathbf{U}^{(P)} = A\mathbf{e}_3$. Altogether, for a given incident wave we again have six unknown amplitude parameters for which we have the set of six BC equations:

$$
\begin{aligned}
A^{\mathrm{T}}e^{\mathrm{T}}_{3i} + B^{\mathrm{T}}e^{\mathrm{T}}_{1i} + C^{\mathrm{T}}e^{\mathrm{T}}_{2i} - A^{\mathrm{R}}e^{\mathrm{R}}_{3i} - B^{\mathrm{R}}e^{\mathrm{R}}_{1i} - C^{\mathrm{R}}e^{\mathrm{R}}_{2i} &= D_i \\
A^{\mathrm{T}}X^{\mathrm{T}}_{i} + B^{\mathrm{T}}Y^{\mathrm{T}}_{i} + C^{\mathrm{T}}Z^{\mathrm{T}}_{i} - A^{\mathrm{R}}X^{\mathrm{R}}_{i} - B^{\mathrm{R}}Y^{\mathrm{R}}_{i} - C^{\mathrm{R}}Z^{\mathrm{R}}_{i} &= E_i
\end{aligned}
\tag{5.81}
$$

(notation taken from the book by Červený, 2001). The right-hand side quantities in the above equations differ according to the wave-type of the incident wave. For the P-wave we substitute:

$$
D_i = Ae_{3i} \ , \quad E_i = AX_i \ ,
\tag{5.82}
$$

while for the S-wave we write:

$$
D_i = Be_{1i} + Ce_{2i} \ , \quad E_i = BY_i + CZ_i \ .
\tag{5.83}
$$

The quantities X_i, Y_i and Z_i are introduced only formally to shorten the written form of the equations (5.81)–(5.83). For example, for the incident wave, their meaning is the following:

$$
\begin{aligned}
X_i &= \lambda^{(1)}\nu_i e_{3k}p_k + 2\mu^{(1)}e_{3i}\nu_k p_k \ , \\
Y_i &= \mu^{(1)}\nu_j(e_{1i}p_j + e_{1j}p_i) \ , \\
Z_i &= \mu^{(1)}\nu_j(e_{2i}p_j + e_{2j}p_i) \ ,
\end{aligned}
\tag{5.84}
$$

where $\lambda^{(1)}, \mu^{(1)}$ are the model parameters of the first halfspace (from which the wave incidents the interface) and $\mathbf{p}$ denotes the corresponding incident slowness vector. For the R/T waves, distinguished by the upper indices R and T, the meaning of these quantities is the same, but the proper slowness vectors, RCC basis vectors and model parameters have to be substituted.

Let us add one important note to the equations (5.81) – (5.84). The RCC basis vectors standing in them do not generally form one mutually orthogonal vector triplet, since they correspond to different waves with different rays. For example, $\mathbf{e}_3^{\mathrm{R}}$ corresponds to the reflected P-wave, while $\mathbf{e}_I^{\mathrm{R}}$'s correspond to the reflected S-wave, leaving the interface in different direction (unless the α/β ratio is the same on both sides of the interface).

We can introduce R/T coefficients in a similar way as in the anisotropic case, using the following indexing convention, both for the incident as well as the R/T wave: 1 standing for the S_1 component of S-wave, corresponding to the unit vector $\mathbf{e}_1$ ($\mathbf{e}_1^{\mathrm{R}}$, $\mathbf{e}_1^{\mathrm{T}}$), 2 for the S_2 component of S-wave, corresponding to the unit vector $\mathbf{e}_2$ ($\mathbf{e}_2^{\mathrm{R}}$, $\mathbf{e}_2^{\mathrm{T}}$), and 3 for P-wave. The total number of the coefficients is 18. Similarly as in anisotropic media they form two 3×3 R/T coefficient matrices. However, the analytical solution of the system (5.81) is cumbersome.

An important simplification of the BC equation system (and its solution) in isotropic media can be achieved by choosing a special orientation of the vectors $\mathbf{e}_I$ respecting the so-called **plane of incidence** at the interface. The plane of incidence is the plane containing the slowness vector of the incident ray and the unit normal vector to the interface at the point of incidence. Let us choose the vectors $\mathbf{e}_2, \mathbf{e}_2^{\mathrm{R}}$ and $\mathbf{e}_2^{\mathrm{T}}$ perpendicular to this plane. Further, let us consider the local Cartesian system with the x_3-axis in the direction of the unit normal to the interface at the point of incidence and the $x_1 - x_3$ coordinate plane coinciding with the plane of incidence. Then, $\nu_1 = \nu_2 = 0$ and $\nu_3 = 1$. For the RCC basis vectors of the incident wave we can write $e_{32} = e_{23} = e_{12} = e_{21} = 0$ and $e_{22} = 1$. The same holds for the relevant vectors of the R/T waves. Under these circumstances the system (5.81) can be decomposed into two independent subsystems: the so-called $P - SV$ subsystem of four equations, containing only the $A^{\mathrm{T}}, B^{\mathrm{T}}, A^{\mathrm{R}}$ and B^{R} unknown amplitude coefficients:

$$
\begin{aligned}
A^{\mathrm{T}} e_{31}^{\mathrm{T}} + B^{\mathrm{T}} e_{11}^{\mathrm{T}} - A^{\mathrm{R}} e_{31}^{\mathrm{R}} - B^{\mathrm{R}} e_{11}^{\mathrm{R}} &= D_1 \\
A^{\mathrm{T}} e_{33}^{\mathrm{T}} + B^{\mathrm{T}} e_{13}^{\mathrm{T}} - A^{\mathrm{R}} e_{33}^{\mathrm{R}} - B^{\mathrm{R}} e_{13}^{\mathrm{R}} &= D_3 \\
A^{\mathrm{T}} X_1^{\mathrm{T}} + B^{\mathrm{T}} Y_1^{\mathrm{T}} - A^{\mathrm{R}} X_1^{\mathrm{R}} - B^{\mathrm{R}} Y_1^{\mathrm{R}} &= E_1 \\
A^{\mathrm{T}} X_3^{\mathrm{T}} + B^{\mathrm{T}} Y_3^{\mathrm{T}} - A^{\mathrm{R}} X_3^{\mathrm{R}} - B^{\mathrm{R}} Y_3^{\mathrm{R}} &= E_3 \ ,
\end{aligned}
\tag{5.85}
$$

and the so-called SH system of two equations for two unknowns C^{T} and C^{R}

$$
\begin{aligned}
C^{\mathrm{T}} - C^{\mathrm{R}} &= C \\
C^{\mathrm{T}}\rho^{(2)}\beta^{(2)}e_{22}^{\mathrm{T}} - C^{\mathrm{R}}\rho^{(1)}\beta^{(1)}e_{22}^{\mathrm{R}} &= C\rho^{(1)}\beta^{(1)}e_{22} \; .
\end{aligned}
\tag{5.86}
$$

The main advantage of the systems (5.85) and (5.86) is that they are fully decoupled. For example, when a wave with $C = 0$ (either P-wave or S-wave polarized in the plane of incidence) incidents at the interface, the system (5.86) yields zero amplitude coefficients C^{R} and C^{T}, i.e. no S-wave polarized perpendicularly to the plane of incidence is generated. We deliberately avoid the traditional terminology 'SH-wave' and 'SV-wave', since it may be misleading: they are not independent waves, but only the two S-wave components. Moreover, the S_1 component is not vertically polarized and, in the case of a generally inclined interface, even the S_2 component is not horizontally polarized, so that it is not useful to use the SV and SH attributes for them.

Decomposition of the BC equation system due to the specific choice of the local Cartesian coordinates and the $\mathbf{e}_2$ basis vector of all the waves involved in the R/T problem results in decrease of the number of the R/T coefficients. Instead of 18 we have only 5 nonvanishing reflection coefficients (see also the schematic figure 23)

$$
\mathbf{R}^{\mathrm{R}} = \begin{pmatrix} R_{11}^{\mathrm{R}} & 0 & R_{13}^{\mathrm{R}} \\ 0 & R_{22}^{\mathrm{R}} & 0 \\ R_{31}^{\mathrm{R}} & 0 & R_{33}^{\mathrm{R}} \end{pmatrix}, \tag{5.87}
$$

and 5 nonvanishing transmission coefficients (the corresponding matrix $\mathbf{R}^{\mathrm{T}}$ is fully analogous to $\mathbf{R}^{\mathrm{R}}$).

Figure 23: Scheme of the system of the reflection coefficients in isotropic media.

The advantage of the approach utilizing the two decomposed subsystems is obvious for incident P-waves, since solving (5.85) is always simpler than solving the system (5.81). For S-wave incidenting to the interface the procedure required is to rotate the RCC basis of the incident wave, computed

from (4.4), around the vector $\mathbf{e}_3$ to make $\mathbf{e}_2$ perpendicular to the plane of incidence. This rotation represents a recalculation of the original S-wave amplitude components, say B', C' to the new ones, B, C before transforming the amplitude across the interface.

Analytical expressions for R/T coefficients in isotropic media have been known in the seismological literature for a long time. The reader may know them under the name Zöptritz coefficients. The R/T coefficients used in the RM are exactly the same as those derived for plane waves at a plane interface. This is not surprising as the special form of the RM zero order solution, when substituted into the BC, yields exactly the same BC equations for amplitudes that would be obtained inserting a plane wave solution. When adopting the corresponding formulas from the literature one has to be careful about the definition of the R/T coefficients. Besides the displacement coefficient that we are dealing with in this text, there are also other types of the coefficients frequently published, for example the coefficients for seismic potentials or energies.
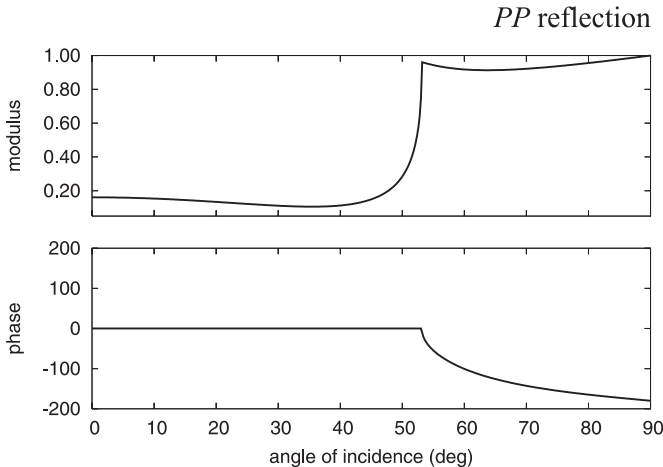
Figure 24: An example of a typical PP reflection coefficient R_{33}^{R} as a function of the angle of incidence, the acute angle between the incident slowness vector and the unit normal to the interface. Qualitatively, this example could correspond to the PP reflection from Moho discontinuity (refraction index $\alpha^{(1)}/\alpha^{(2)} = 0.8$).

Let us present and discuss here only one example of the analytic formulas for the R/T displacement coefficient: the coefficient for the PP reflection at an interface between two solid halfspaces in welded contact, see figure 24 (for other coefficients see Červený, 2001). The analytical expression for it reads:

$$R_{33}^{\mathrm{R}} = D^{-1}[q^2 p^2 P_1 P_2 P_3 P_4 + \rho^{(1)}\rho^{(2)}(\beta^{(1)}\alpha^{(2)}P_1 P_4 - \alpha^{(1)}\beta^{(2)}P_2 P_3)$$
$$-\alpha^{(1)}\beta^{(1)}P_3 P_4 Y^2 + \alpha^{(2)}\beta^{(2)}P_1 P_2 X^2 - \alpha^{(1)}\alpha^{(2)}\beta^{(1)}\beta^{(2)}p^2 Z^2] \,,$$

$$(5.88)$$

where the following notation has been used:

$$
\begin{aligned}
D &= q^2 p^2 P_1 P_2 P_3 P_4 + \rho^{(1)}\rho^{(2)}(\beta^{(1)}\alpha^{(2)}P_1 P_4 + \alpha^{(1)}\beta^{(2)}P_2 P_3) \\
&\quad + \alpha^{(1)}\beta^{(1)}P_3 P_4 Y^2 + \alpha^{(2)}\beta^{(2)}P_1 P_2 X^2 + \alpha^{(1)}\alpha^{(2)}\beta^{(1)}\beta^{(2)}p^2 Z^2 \,, \\
q &= 2[\rho^{(2)}(\beta^{(2)})^2 - \rho^{(1)}(\beta^{(1)})^2], \quad X = \rho^{(2)} - qp^2 \,, \\
Y &= \rho^{(1)} + qp^2, \qquad\qquad\qquad Z = \rho^{(2)} - \rho^{(1)} - qp^2 \,, \\
P_1 &= [1 - (\alpha^{(1)})^2 p^2]^{1/2}, \qquad\quad P_2 = [1 - (\beta^{(1)})^2 p^2]^{1/2} \,, \\
P_3 &= [1 - (\alpha^{(2)})^2 p^2]^{1/2}, \qquad\quad P_4 = [1 - (\beta^{(2)})^2 p^2]^{1/2} \,,
\end{aligned}
$$

$$(5.89)$$

and p denotes the ray parameter $p = \sin i/\alpha^{(1)}$ (the tangential slowness component) with i being the angle of incidence.

A remarkable feature of the formula (5.88) (together with (5.89)) is that the expression for the PP reflection coefficient contains all the square roots P_1, P_2, P_3, P_4 (representing normal slowness components of the R/T waves) and not only the root P_1, corresponding to the PP reflection. This is the consequence of the BC. Once any of these square roots becomes imaginary (which means that the corresponding generated wave becomes inhomogeneous), the reflection coefficient becomes complex-valued. In Fig. 24 this happens for the angle of incidence $53.13°$. Beyond this angle, the PP reflection coefficient becomes complex due to the fact that the PP transmitted wave becomes inhomogeneous. Such an angle is called the **critical angle**. For other types of the coefficients and other model parameters even more (maximum three) critical angles may exist. For the incidence angle larger than a critical angle (the so-called overcritical incidence), the shape of the R/T pulse is modified: the real part of the R/T coefficient scales the incident signal while the imaginary part introduces a scaling of the Hilbert transform of the signal which is superposed to obtain the resulting shape (see also Chap. 6).

Fig. 24 may serve to elucidate one weakness of the ray method which we have seen already in the Introduction. From the continuation formula we know that the ray amplitude decreases with increasing geometrical spreading. In simple models the amplitude usually decreases with raypath length and, consequently, with distance from the source. For R/T waves the ampli-

tude moreover follows roughly the shape of the corresponding R/T coefficient curve, including the steep amplitude increase toward the peak at the critical distance (the distance corresponding to the critical angle). Thus the amplitude of a reflected PP-wave, plotted versus distance from the source, may qualitatively look like the gray line in the figure 25a. The real amplitude, however, would be influenced by interference with the head wave which comes at close times in the vicinity of the critical distance. The amplitude curve of the real wavefield may look qualitatively like the black curve in Fig. 25a. The discrepancy between the amplitudes predicted by the RM and the real ones beyond the critical distance can be also observed in the detailed figure cut from Fig. 3, see the figure 25b.
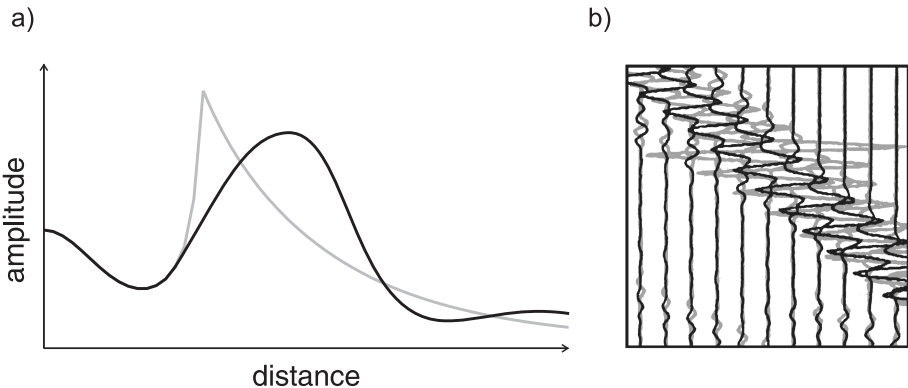
Figure 25: a) The RM predicted amplitude (gray) and the real amplitude (black) affected by interference with head wave beyond the critical angle (a sketch). b) An example of the amplitude discrepancy for synthetic seismograms calculated by the RM (gray) and FDM (black) for the model PICRO-COL, see also Fig. 3, Sec. 1.

In this section we have explained the R/T problem for ray amplitudes for a solid-solid interface only. The other interface type would be characterized by different BC, however, the corresponding BC equations for amplitudes could be obtained from the solid-solid interface equations by proper specification of the medium parameters. For example, in an isotropic medium we can insert μ (or β) equal zero for a liquid halfspace. Similarly, all medium parameters must be set equal to zero for a vacuum. In this way, we can obtain corresponding R/T coefficients for a solid-fluid interface or the free-surface coefficients. The coefficients can be calculated directly applying the Zöpptritz formulas substituting zeros for the relevant model parameters.

The free-surface reflection coefficients are sometimes understood in a generalized sense by taking into account the fact that the displacement of a receiver situated at the free surface is affected not only by the incident wave but also by all the waves reflected from the surface, since at the receiver

all these waves exist at the same time. Such coefficients are called the **co-efficients of conversion**. They can, with advantage, be calculated using transmission coefficients at the free surface which, as such, have only formal meaning (no wave is transmitted to vacuum). For details, see Červený (2001).

In layered/blocky media, not only the scalar amplitude factors but also the ray Jacobian J has to be properly transformed across a structural interface wherever rays incident at the interface and the reflected/transmitted rays are calculated. Realizing that J is a measure of the cross-sectional area of the ray tube (see Sec. 5.1), the reader can easily perceive, with the help of the schematic figure 26, that the ray Jacobian J of the incident wave is related to the Jacobian $\tilde{J}$ of a R/T wave as

$$\frac{J}{\tilde{J}} = \frac{t_i \nu_i}{\tilde{t}_k \nu_k} = \pm \frac{\cos(i)}{\cos(\tilde{i})} \ , \tag{5.90}$$

where i denotes the angle of incidence and $\tilde{i}$ the angle of reflection/transmission, $\boldsymbol{\nu}$ is the unit normal to the interface, and $\mathbf{t}$ and $\tilde{\mathbf{t}}$ are the unit tangents to the rays of the incident and R/T wave, respectively. All the quantities in (5.90) relate to the point of incidence. For the normal $\boldsymbol{\nu}$ oriented 'against' the incident wave (see Fig. 26), the '+' sign corresponds to the transmitted wave, while the '-' sign to the reflected wave. The formula (5.90) is valid both in isotropic as well as anisotropic structures.
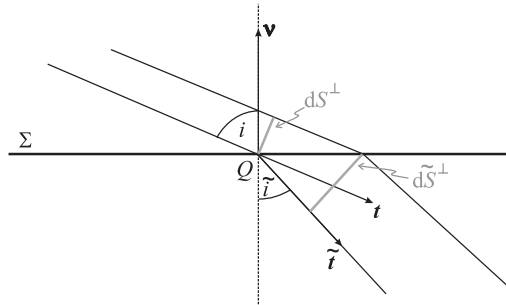
Figure 26: Outline of a ray tube and its cross-sectional area $\mathrm{d}S^\perp$ of the wave incident to and transmitted across a structural interface Σ at a point Q (2D case).

5.10 Point source ray amplitude in a layered structure. Ray theory Green's function

Let us have a ray Ω propagating from a point S to a point R through a layered model (Fig. 27). Let us assume we know the 'ray history', i.e. at

which interfaces the ray is reflected, at which it is transmitted, and at which it is possibly converted to the ray of other wave type. The task is to compute the ray solution at R along this ray.
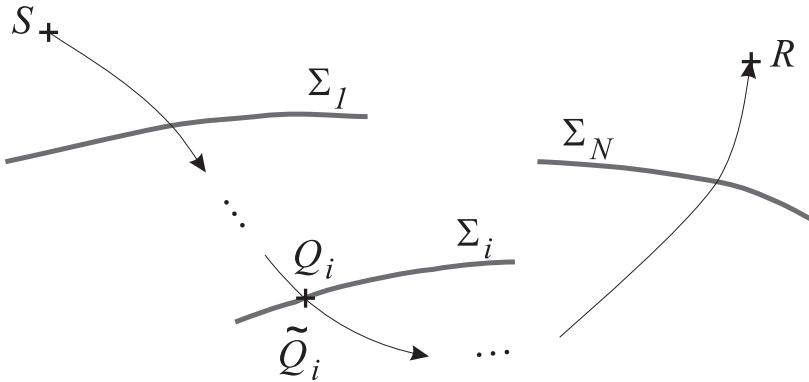
Figure 27: A ray propagating through a layered structure.

We will write the formula for the zero order ray solution along such a ray. Specifically, let us assume S to be a point source dynamically equivalent to a single impulse force, so that the corresponding displacement we seek represents the Green's function, the important solution in various seismological applications.

The i-th RM displacement component, along the given ray, at R due to the single impulse force at S pointing in direction of the n-th Cartesian axis reads

$$G_{in}^{(\Omega)}(R,S,t) = U_{in}^{(\Omega)}(R,S)\delta^{(A)}(t - \tau^{(\Omega)}(R,S)) \ , \qquad (5.91)$$

where $U_{in}^{(\Omega)}$ is the i-th component of the Green's function amplitude and $\tau^{(\Omega)}$ means the travel time along the given ray from S to R. Without loss of generality, we have assumed the source to act at the time $t = 0$, not written explicitly as an argument of the Green's function. The function $\delta^{(A)}$ is the analytical signal corresponding to the Dirac delta function: $\delta^{(A)}(t) = \delta(t) - i\pi/t$. In the above equation, the upper index (Ω) is used to emphasize that the equation does not yield a complete RM Green's function, but only the contribution related to the specific ray Ω. The RM Green's function would be obtained by summing contributions related also to other rays connecting the points S and R, the rays having different 'ray history', i.e. the rays corresponding to different so-called elementary waves (for explanation see Chap. 6). In the case of multipathing, even more rays with the same 'ray history', starting at S, can be captured by the receiver R, carrying different contributions to the final RM Green's function. In the following we treat

only the contribution due to the ray Ω, but, for the sake of simplicity, we skip the upper index (Ω) in the equations below.

In anisotropic media, the Cartesian amplitude component U_{in}^G is given as

$$U_{in} = g_i(R) \left[\frac{\rho(S)c(S)}{\rho(R)c(R)}\right]^{1/2} \frac{\exp(\mathrm{i}\frac{1}{2}\pi K(R,S))}{\mathcal{S}(R,S)} \mathcal{W}^C \mathcal{G}^n(S) \ , \qquad (5.92)$$

where g_i is the i-th component of the relevant polarization vector, corresponding to the wave type of the last ray segment (the segment in the layer containing the receiver R), ρ is density, v^g the group velocity magnitude, K the index of the ray trajectory controlling possible phase shift due to caustics between the points S and R, $\mathcal{S}(R,S)$ denotes the relative geometrical spreading and $\mathcal{G}^n(S)$ is the scalar radiation function corresponding to a unit single force in n-th direction

$$\mathcal{G}^n(S) = g_n(S)[4\pi\rho(S)c(S)]^{-1} \exp[\mathrm{i}\frac{1}{2}\pi\sigma_0(S)] \ , \qquad (5.93)$$

(see (5.75)). The quantity $\mathcal{W}^C$ represents the **product of all normalized R/T coefficients** corresponding to the ray interaction with interfaces in the model:

$$\mathcal{W}^C = \prod_{k=1}^{N} \mathcal{W}(Q_k) \left[\frac{\rho(\tilde{Q}_k)v^g(\tilde{Q}_k)\cos i(\tilde{Q}_k)}{\rho(Q_k)v^g(Q_k)\cos i(Q_k)}\right]^{1/2} \ . \qquad (5.94)$$

The 'normalization' factor in square brackets ensures that the moduli of the normalized R/T coefficients never exceeds unity, which does not hold for the displacement coefficients introduced in the previous section. For explanation see Červený (2001). In the above equation, Q_k is the k-th point of incidence on the way of the raypath and $\tilde{Q}_k$ is the adjoint starting point of the generated wave, i.e., in the case of a reflection it coincides with the point Q_k, while for a transmission it is the point situated on the opposite side of the interface. The group velocity magnitude at such a point corresponds to the type of the wave the ray of which we follow. The angle $i(Q_k)$ is the angle of incidence and $i(\tilde{Q}_k)$ is the relevant R/T angle. The above formula is clearly understandable. Let us consider the first interface and the point of incidence Q_1. From S to Q_1 the standard continuation formula for a point source is applied, containing the expression $[\rho(Q_1)v^g(Q_1)]^{1/2}$ in denominator. From Q_1

to $\tilde{Q}_1$ the scalar amplitude factor must be recalculated applying the relevant displacement R/T coefficient (for the ray in Fig. 27 it is the transmission coefficient, $\mathcal{W}(Q_1) = R_{lm}^{\mathrm{T}}(Q_1)$, with l defining the type of the incident and m the type of the transmitted wave). Transforming the geometrical spreading across the interface gives rise to the factor $[\cos i(\tilde{Q}_1)/\cos i(Q_1)]^{1/2}$ in the expression for the amplitude at $\tilde{Q}_1$, see (5.90). The point $\tilde{Q}_1$ is the new initial point for the continuation formula, applied for the ray segment from $\tilde{Q}_1$ to the next point of incidence, Q_2, so that the expression $\rho(\tilde{Q}_1)v^g(\tilde{Q}_1)$ appears in the nominator and $[\rho(Q_2)v^g(Q_2)]^{1/2}$ in the denominator of the formula. The amplitude must be transformed across the second interface and the same calculation is successively applied at each interface the ray interacts with. Thus, in the presence of interfaces between the points S and R, the final amplitude multiplier is $\mathcal{W}^C$ given by the equation (5.94). When the receiver R is situated on the earth's surface, relevant free-surface coefficients (the coefficients of conversion) at R should be also involved in the product $\mathcal{W}^C$.

The final expression for the RM Green's function contribution at R, due to the ray Ω propagating through an anisotropic layered structure is

$$
\begin{aligned}
G_{in}(R,S,t) = {} & \frac{g_n(S)g_i(R)}{4\pi[\rho(S)\rho(R)c(S)c(R)]^{1/2}\mathcal{S}(R,S)}\exp \mathrm{i}[-\tfrac{1}{2}\pi(K(R,S)+\sigma_0(S))] \\
& \times(\prod_{k=1}^{N}\mathcal{W}(Q_k)\left[\frac{\rho(\tilde{Q}_k)v^g(\tilde{Q}_k)\cos i(\tilde{Q}_k)}{\rho(Q_k)v^g(Q_k)\cos i(Q_k)}\right]^{1/2})\delta^{(A)}(t-\tau(R,S)) \, .
\end{aligned}
\tag{5.95}
$$

As it is discussed by Červený (2001), the relative geometrical spreading is reciprocal when interchanging the roles of the points S and R, i.e. reversing the propagation direction. The same holds also for the normalized R/T coefficients forming $\mathcal{W}^C$ as well as for the argument of the exponential function in (5.95). Thus the RM Green's function in anisotropic media is reciprocal:

$$
G_{in}(R,S,t) = G_{ni}(S,R,t) \, .
\tag{5.96}
$$

To find the ray solution along Ω in an isotropic structure, we proceed in a similar way and the final expression for the RM Green's contribution at R is analogous to (5.95) with proper v substituted for v^g; v equals either α or β according to the wave type corresponding to given ray segment. Of course, the proper radiation function, corresponding to the isotropic model, has to

be inserted. The most remarkable difference is that in isotropic media the continuation formulas (derived in Sec. 5.6) correspond to the RCC amplitude components. Thus, we deal with the RCC amplitude vector equal to $(B, C, 0)^T$ (T used to denote transposition) for an S-wave, or to $(0, 0, A)^T$ for a P-wave. Since along the ray Ω both wave types may occur in the ray history, we consider formally, with advantage, the joint RCC amplitude vector $(B, C, A)^T$ in the continuation formula, but it must be correctly interpreted from the physical point of view (independently for the P- and S-waves). The same holds for the RCC radiation vector composed from the RCC radiation functions. For the unit single force pointing along the n-th Cartesian axis the RCC components of the radiation function read (see (5.74))

$$\mathcal{G}_i^{n(q)}(S) = \frac{1}{4\pi\rho(S)v(S)} H_{ni}(S) \; , \tag{5.97}$$

where we put $i = 3$ for P-waves ($v = \alpha$) and $i = 1, 2$ for S-waves ($v = \beta$). Before the final amplitude expression is used in seismological applications it is useful to transform it into the general Cartesian system, i.e. we have to multiply the RCC amplitude vector by the transformation matrix $\mathbf{H}$, see Sec. 4.1. Thus the final Green's function along Ω in a layered isotropic medium reads

$$
\begin{aligned}
G_{in}(R, S, t) = &\frac{1}{4\pi[\rho(S)\rho(R)v(S)v(R)]^{1/2}\mathcal{S}(R, S)} \exp(\mathrm{i}\tfrac{1}{2}\pi K(R, S)) \\
&\times W_{in}(R, S)\delta^{(A)}(t - \tau(R, S)) \; ,
\end{aligned}
\tag{5.98}
$$

where $W_{in}(R, S) = H_{ik}(R)\mathcal{W}_{kl}^C H_{nl}(S)$ with $\mathcal{W}^C$ being the 3×3 matrix resulting from the product of the relevant matrices of the normalized R/T coefficients along the raypath (possibly containing the coefficient of conversion in the case of the receiver situated on the earth's surface):

$$\mathcal{W}^C = \prod_{k=1}^N \mathcal{W}^T(Q_k) \left[\frac{\rho(\tilde{Q}_k)v(\tilde{Q}_k)\cos i(\tilde{Q}_k)}{\rho(Q_k)v(Q_k)\cos i(Q_k)} \right]^{1/2} \; , \tag{5.99}$$

where $\mathcal{W}^T(Q_k)$ is the transposed matrix of the relevant Zöptritz coefficients at the point Q_k (either reflection or transmission) and v stands for the P- or S- wave velocity. The exact meaning of the product $W_{in}(R, S)$ depends on

the wave type of the first and last ray segments. There are four alternatives how to interpret this quantity:

1)P-wave at S and P-wave at R results in $W_{in}(R,S) = H_{i3}(R)\mathcal{W}^C_{33}H_{n3}(S)$,

2)P-wave at S and S-wave at R results in $W_{in}(R,S) = H_{iK}(R)\mathcal{W}^C_{K3}H_{n3}(S)$,

3)S-wave at S and P-wave at R results in $W_{in}(R,S) = H_{i3}(R)\mathcal{W}^C_{3L}H_{nL}(S)$, and finally

4)S-wave at S and S-wave at R results in $W_{in}(R,S) = H_{iK}(R)\mathcal{W}^C_{KL}H_{nL}(S)$.

Similarly as in anisotropic media, in isotropic models it is also possible to show that $G_{in}(R,S,t)$ in the equation (5.98) is reciprocal when interchanging the source and receiver points (for details see Červený, 2001)

$$G_{in}(R,S,t) = G_{ni}(S,R,t) \; . \qquad (5.100)$$

The reader probably knows well the reciprocity of a general elastodynamic Green's function in homogeneous, isotropic, unbounded medium. Let us emphasize that here we speak on the Green's function reciprocity in inhomogeneous, layered, possibly bounded models, both isotropic as well as anisotropic. Nevertheless, the reciprocity has not been proved in general, but only under the assumption of our high-frequency asymptotic zero-order solution.

For the reader's convenience let us end this section with the expressions for the RM Green's functions in the frequency domain which are also very useful and may allow us to simplify the calculus in many seismological applications. In anisotropic media, the frequency domain Green's function is given as

$$
\begin{aligned}
G_{in}(R,S,\omega) = {}& \frac{g_n(S)g_i(R)}{4\pi[\rho(S)\rho(R)c(S)c(R)]^{1/2}\mathcal{S}(R,S)} \\
& \times \left(\prod_{k=1}^{N}\mathcal{W}(Q_k)\left[\frac{\rho(\tilde{Q}_k)v^g(\tilde{Q}_k)\cos i(\tilde{Q}_k)}{\rho(Q_k)v^g(Q_k)\cos i(Q_k)}\right]^{1/2}\right) \\
& \times \exp i[-\tfrac{1}{2}\pi(K(R,S)+\sigma_0(S))+\omega\tau(R,S)] \; ,
\end{aligned}
\qquad (5.101)
$$

while, in the case of isotropy the expression reads

$$
\begin{aligned}
G_{in}(R,S,\omega) = {}& \frac{1}{4\pi[\rho(S)\rho(R)v(S)v(R)]^{1/2}\mathcal{S}(R,S)}H_{ik}(R)\mathcal{W}^C_{kl}H_{nl}(S) \\
& \times \exp(i\tfrac{1}{2}\pi K(R,S)+i\omega\tau(R,S)) \; .
\end{aligned}
$$

$$(5.102)$$

6 Ray synthetic seismograms

In this chapter we explain the brief basic steps of a procedure commonly used to calculate ray synthetic wavefields. For the sake of simplicity we consider isotropic models only; in anisotropic media the procedure would be analogous in many respects, but a more complicated model description would be necessary (more parameters have to be specified), more wave types can possibly propagate, and a special treatment should be adopted regarding possible quasi-shear wave singularities. The procedure described is applied, for example, in the program packages SEIS (Červený and Pšenčík, 1984, 2002) and CRT (Červený et al., 1988), designed for computing the ray synthetic seismograms in laterally varying 2D and/or 3D isotropic structures. Other ray tracing codes may use a procedure modified in details, but the basic steps should be analogous to those explained below. For details see also Červený et al. (1988). Some ray tracers compute the wavefields completely in the time domain. We, however, prefer to evaluate the Fourier spectrum first and then use the inverse Fourier transform to obtain synthetic seismograms which allows us to take into account certain frequency-dependent effects also.

Applying the RM, we can directly calculate the relevant solution (for example, displacement) due to a point source. Optionally we can calculate the ray theory Green's function by specifying the proper source type (point force) and time dependence of the input signal (Dirac delta function). In the case of a finite extent source the solution is obtained by discretizing the representation integral which results finally in a superposition of point sources regularly spaced along the fault surface.

This section is meant to not only provide the reader with basic ideas about ray synthetic wavefield calculation, but also with knowledge useful to better understanding the computer code ZRAYAMP, as well as the structure of its input/output data (see the chapter 8). The program is designed for fast ray calculations in spherically symmetric (1D) models and it is useful for numerical exercises in this course. The code and several solved numerical examples can be found on the attached CD.

6.1 The basic procedure step-by-step

Step 1
Before any ray calculations start, the structure have to be properly specified. The model suitable for the RM can contain several first-order discontinuities (interfaces), but the structure in between them should be **smooth**. A fine layering (with layer thicknesses smaller than the maximum seismic wave-

length) should be avoided as it violates the RM applicability conditions (see Chap. 7). Stacks of thin layers are inappropriate even in the case of linear velocity increase inside the layers, separated by second-order interfaces with jumps of model parameter derivatives, not of the parameters themselves. Such structural features would lead to undesirable amplitude effects (see, for example, Červený, 1985). Figure 28 shows schematically an example of a structure containing thin homogeneous layers separated by first-order interfaces (left) being replaced by a smooth approximation of the structure seen in Fig. 28 (right), keeping the most pronounced velocity jump.

a)   b)
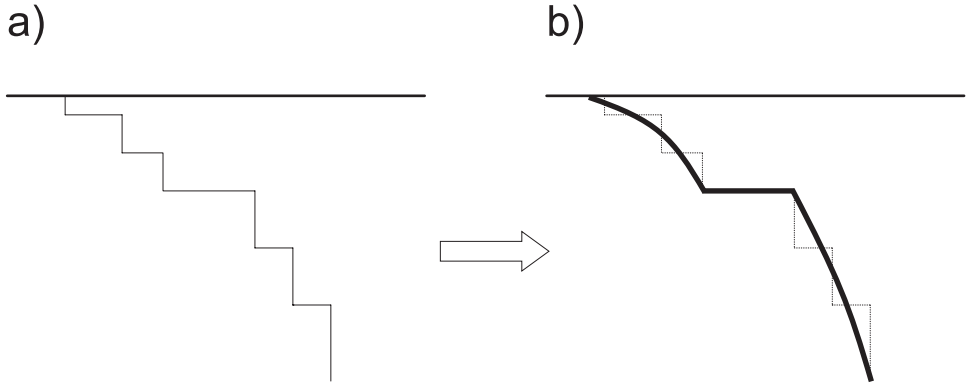
Figure 28: An example of the approximation of the model for the RM: a step-wise structure (left) should be replaced by its smoothed approximation (right) to avoid fine layering in the model. The largest discontinuity in the model is retained.

Apart from interfaces, the model should be specified in such a way to allow the model parameters (e.g., propagation velocities α and β in the case of an isotropic structure) to be smoothly interpolated in any point $\mathbf{x}$. In order to solve the RTS, the parameters must be known at any point of the model. In many ray tracing programs the model is specified in a grid and the cubic spline interpolation is used as a relatively robust technique, providing the interpolant smooth together with its derivatives. The user should however specify the model in such a way to avoid undesirable oscillations of the interpolant. At least a visual inspection of the interpolated structure before the ray computation starts is very worthwhile.

If the structure is known one has to specify the position of the source as well as the receiver(s) in the model.

Step 2
The RM is able to return synthetic seismograms being a superposition of a finite number of the so-called elementary waves, treated individually. These are the waves of a given type (i.e., *P*- or *S*-) propagating throughout the

model in a way uniquely specified. At interfaces they can be transmitted or reflected (possibly multiply) and also be converted (from P- to S- and vice versa). For example, let us consider the case of one layer above a halfspace with a source situated in the layer and a receiver at the surface. Restricting ourselves to direct and primarily reflected (and possibly converted) waves, we can consider six elementary waves: two direct waves, P and S, and four reflections, PP, SS, PS, SP. Allowing for multiples, the number of possible elementary waves is infinite. As the complexity of the medium (in terms of number of layers) gradually grows, the elementary wave description becomes more complex as the ray trajectory of such a wave can contain many segments propagating through individual layers. The list of the elementary waves taken into account in ray synthetics depends on expected amplitudes (the waves weak in amplitude, like those reflected/converted many times in the structure, can be neglected) and the expected arrival times (only the waves coming in the time window of interest should be included). The final decision about the list may differ for different specific applications and it is up to the user of the ray-tracing program. The number of the considered waves should be limited to, let us say several tens, otherwise we could lose the advantage of the computing speed of the RM, especially when the so-called two-point ray tracing is needed (see below).

Each elementary wave under consideration has to be uniquely specified by a proper coding. The simplest way to do this is to utilize the numbers assigned to individual layers/blocks in the model. The P- and S-wave segments can be further distinguished by the '+' and '-' signs, respectively. In figure 29a we see an example of rays of individual elementary waves in a three-layered structure, provided the source radiates P-wave only, no multiples are allowed and conversions are allowed only in connection with the reflection. Fig. 29b provides the codes of the considered elementary waves, the rays of which are plotted in part a. This type of coding of elementary waves is adopted in the program ZRAYAMP (see Chap. 8).

Step 3

For each elementary wave under consideration the rays connecting the source and the specified receivers must be traced. This is because, in the standard zero-order RM, we can evaluate the wavefield along rays only. The rays are traced by solving a proper RTS. However, this requires us to perform the so-called **two-point ray tracing** (see Sec. 6.2) in order to find a ray starting at the source point and terminating at the given receiver. We are faced with a situation where we do not know in advance initial direction of such a ray. Two possibilities of how to solve this problem are described in section 6.2. However, in complex models, this part of the calculation represents usually the most time consuming part of the whole synthetic seismogram
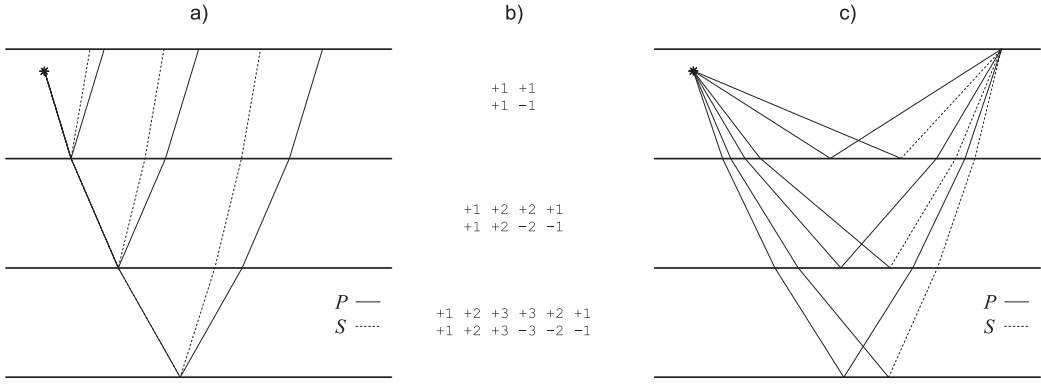
Figure 29: An example of elementary waves taken into account in a three-layered model: (a) the rays of the individual waves, generated as P-waves at the source, propagating through the model, (b) the numerical codes specifying these waves, (c) the same as in the part (a), but for the case of the 'two-point' rays.

computation.

After a successful ray tracing, for every ray captured in the given receiver we have to store the travel time corresponding to the ray endpoint (receiver). The slowness at the ray endpoint should also be stored for purposes of succeeding calculations (for example, it enables us to calculate the $\mathbf{e}_3$ RCC basis vector). Besides these quantities related to the ray endpoint, it is also useful to store the initial direction of the ray. This allows us to specify, with advantage, the type of the source in a later stage of the calculation by means of multiplication of the amplitude by a proper radiation function factor.

Step 4

Along 'successful' rays captured at the specified receivers, the RCC basis vectors should be evaluated (this is dropped in the case of in-plane rays in which the knowledge of the slowness is sufficient to determine the complete RCC basis system, see Sec. 4.1). Further, we have to calculate the geometrical spreading, preferably by solving the DRT system, or by the 'finite-difference' approach, see Sec. 5.2. For the evaluation of ray amplitudes, the geometrical spreading should be known at the ray endpoint. In the presence of structural interfaces, the RCC basis vectors should be known, in addition to the ray endpoint, at all the points of incidence of the ray to these interfaces. This allows us to apply the decomposed BC systems (5.85) and (5.86) in step 5.

Note that we have described the solution of the DRT system and the evaluation of the RCC basis as an independent step in the procedure. Op-

tionally, all the corresponding equations can be solved together with the RTS as the ray is traced from one point to the next point. Nevertheless, solving the equations separately brings two advantages: 1) we can consider different flow parameters in both these calculation phases, and, 2) we evaluate the RCC basis and the geometrical spreading only along the 'successful' rays connecting the source and a given receiver. For example, in the shooting method described in Sec. 6.2, certain trial rays, after completition of their computation, are rejected. Thus it would be useless to perform parallelly any other calculations along them.

Step 5
In the presence of structural interfaces in the model, the proper R/T coefficients have to be evaluated at each interface that the ray under consideration incidents. For this, the RCC basis system at a point of incidence should be rotated properly to coincide with the local coordinate system used in evaluating the coefficients. The coefficients are successively multiplied, according to the equation (5.99). At the free surface, the corresponding coefficients of conversion have to be involved.

After the completion of this phase of the calculation, at each ray endpoint we know, besides the travel time, also the geometrical spreading and the product of all the relevant normalized R/T coefficients along the ray paths — the quantities necessary to calculate the ray amplitude components in the RCC system. The multiplication by the proper amplitude factor due to the radiation pattern can be involved in this stage (which would require us to specify the type of the point source). Such an approach has the advantage that once the rays are computed we can easily alternate the type of the source (changing the multiplication factors only) without recomputing the rays.

In the procedure proposed here, the amplitudes are computed in the RCC system, so that finally we have to transform the RCC amplitude components to the general Cartesian coordinates, more suitable for practical applications. For this we use the relevant transformation matrix $\mathbf{H}$.

At this point we split the procedure description into two branches according to whether we compute the seismograms in the time or in the frequency domain. Let us explain first the approach in the time domain.

Step 6a
We have to sum contributions (indexed by $l = 1, \ldots, L$) for all the rays connecting the source and the given receiver. The summation is basically over all the elementary waves under consideration, but, in the case of multipathing, for certain elementary waves we can have more than one contribution. We

compute the so-called **impulse seismogram**. Its n-th Cartesian component is given by a complex-valued sum

$$u_n^{imp}(t, R) = \sum_{l=1}^{L} \{U_n(R)\delta(t - \tau(R))\}^{(l)} , \qquad (6.1)$$

where U_n is the n-th component of the ray amplitude of the individual contribution, computed in the previous steps (it involves the radiation pattern, R/T coefficients, geometrical spreading, etc.). Note that the complex-valuedness of the impulse seismogram (6.1) is due to possible complex-valuedness of the amplitude coefficients U_n, for example as a consequence of complex-valued R/T coefficients for overcritical ray incidence.

Step 7a
The final synthetic seismogram is then obtained from the impulse seismogram by convolving it with the proper analytical signal (corresponding to the source-time function, see Sec. 6.3) and taking the real part of the convolution

$$u_n(t, R) = \Re\{F(t)*u_n^{imp}(t, R)\} = \Re\{F(t)*\sum_{l=1}^{L}\{U_n(R)\delta(t-\tau(R))\}^{(l)}\} . \quad (6.2)$$

Let us mention that the seismogram (6.2) is not generally the same as if we would convolve the impulse seismogram with the real-part of the analytic signal, the actual source-time function (see Sec. 6.3). The shape of the waveform may be influenced not only by the source-time function, but also by its Hilbert transform, the imaginary part of the corresponding analytical signal.

Step 6b
In the frequency domain we first evaluate the so-called **frequency response**. It also consists of a sum of L contributions for all the rays connecting the source and the given receiver (R). The sum corresponds to the Fourier spectrum of the impulse seismogram (6.1) and is given as

$$u_n^{fr}(\omega, R) = \sum_{l=1}^{L} \{U_n(R) \exp(i\omega\tau(R))\}^{(l)} . \qquad (6.3)$$

In practice, the frequency response must be evaluated for discrete frequencies ω_k running over the frequency range of interest with sufficiently small frequency step $\Delta\omega$. This can be done in a very efficient way, applying the

so-called **fast frequency response algorithm**:

$$
\begin{aligned}
u_n^{fr}(\omega_k, R) &= \sum_{l=1}^{L} \{U_n(R)\exp(\mathrm{i}\omega_k\tau(R))\}^{(l)} \\
&= \sum_{l=1}^{L} \{U_n(R)\exp[\mathrm{i}(\omega_1 + (k-1)\Delta\omega)\tau(R)]\}^{(l)} \\
&= \sum_{l=1}^{L} \{U_n(R)\exp[\mathrm{i}\omega_1\tau(R)]\exp[\mathrm{i}\Delta\omega\tau(R)]^{k-1}\}^{(l)} \\
&= u_n^{fr}(\omega_1, R)\chi^{k-1} ,
\end{aligned}
\tag{6.4}
$$

where χ is the complex-valued constant $\chi = \exp[\mathrm{i}\Delta\omega\tau(R)]$ and $u_n^{fr}(\omega_1, R)$ is the frequency response evaluated for the first frequency of the range, ω_1. Knowing the frequency response for the first frequency ω_1 we obtain the response for every other frequency by one complex-valued multiplication by the constant χ. This approach avoids the necessity of a time-consuming evaluation of trigonometric functions for each frequency step, which increases the efficiency of calculations considerably, so that computing the synthetic seismograms in the frequency domain does not represent any numerical problem. The frequency domain approach provides the possibility to easily adapt the method to allow for a frequency-dependent amplitude, for example, when involving higher-order terms of the ray series, or considering certain dissipative filters, instrumental filters, etc. The approach may be also useful in considering a frequency-dependent radiation pattern and also when combining the RM with other methods in a hybrid computation, since the other methods usually provide the frequency-dependent amplitudes. Certain other interesting applications of the frequency domain approach are briefly discussed by Červený (2001).

Step 7b
The frequency response has to be multiplied by the spectrum of the analytical signal corresponding to the source-time function. Examples of such functions can be found in Sec. 6.3. In this way we come to the spectrum of the synthetic seismogram. By performing the inverse Fourier transform, taking the real part of it, we obtain the final synthetic seismogram.

6.2 Boundary ray tracing. Two-point ray tracing

Boundary ray tracing is a procedure necessary to be performed when the ray wavefield is to be calculated, for example, at specified receivers. In such a procedure, the ray is not specified by its initial conditions, but by other conditions related to different points on the ray. A special case of the boundary ray tracing is the so-called **two-point ray tracing** in which we seek the ray that connects two fixed points, say S and R. Note that this corresponds to the definition of the ray by the Fermat variational principle.

The most important approaches to perform the two-point ray tracing are:

1. **Shooting method**. This is a procedure using initial-value ray tracing (rays are specified by initial direction, e.g. take-off angles) from the point S in an iterative loop, changing the initial direction, until a successful ray (captured at R with a prescribed tolerance) is found. The method is illustrated in the figure 30a. In principle, the shooting method is able to find even more than one ray of the given elementary wave connecting the two points (the case of multipathing). The method is applied in the program ZRAYAMP (Chap. 8).

2. **Bending method** — a procedure in which an initial ray path is guessed and perturbed iteratively to find the relevant two-point ray, see Fig. 30b. The guessed trajectory may be an auxiliary reference curve connecting points S and R, e.g. the straight line; for its perturbation a method based on minimizing the travel time or fitting the ray tracing equations can be used.
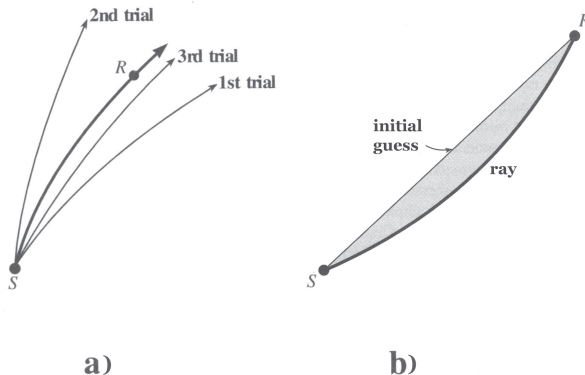
Figure 30: Shooting (a) and bending (b) methods (from Červený, 2001).

For more details concerning the boundary ray tracing the reader is referred to the book by Červený (2001).

6.3 Useful time functions broadly used in the ray method

Here we present several examples of the time signals having been broadly used in the computation of the ray synthetic seismograms. Note that when interpreted as the real time function at the source, for example when comparing the seismograms with the ones obtained by other methods, these signals would correspond to the particle velocity at source (i.e. the first

time derivative of displacement, for example the slip velocity in the case of a fault-type source). The source-time functions, $f(t)$, presented below are real-valued; the corresponding analytical signals are obtained by adding imaginary parts equal to their Hilbert transforms $\mathcal{H}[f(t)]$. In the zero-order RM, the form of the analytical signal, specified at one point of ray (e.g., the source point), remains preserved along the entire ray. Note that this no longer holds for the actual shape of the solution in time (real part of the solution) when caustics are present on the raypath and also when the ray incidents overcritically a structural interface.

The most popular source-time functions used in the ray method are:

1. **Ricker signal**, defined using two free parameters b and t_i (initial time) as

$$f(t) = [1 - 2b^2(t - t_i)^2]\exp[-b(t - t_i)^2] . \qquad (6.5)$$

An example of such a signal (with $b = 8$ and $t_i = 1$s), together with its Hilbert transform, is shown in the figure 31.
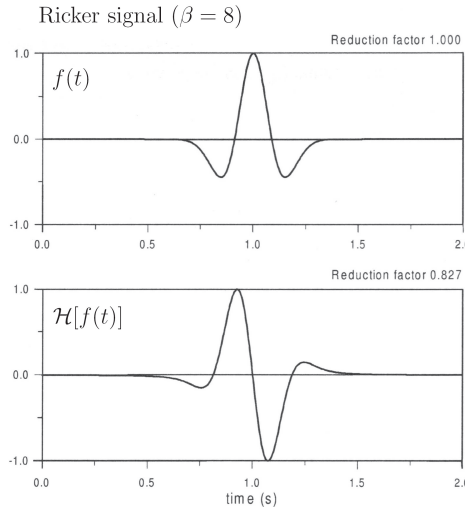
Figure 31: An example of the Ricker signal $f(t)$ and its Hilbert transform $\mathcal{H}[f(t)]$ (from Červený, 2001).

2. **Gabor signal**, defined by the use of four free parameters, the prevailing frequency ω_M, υ controlling the width of the signal, phase shift ϖ and initial time t_i, as

$$f(t) = \exp[-(\omega_M(t - t_i/\upsilon)^2]\cos[\omega_M(t - t_i) + \varpi] . \qquad (6.6)$$

For the choice $\omega_M = 15.7$Hz, $\upsilon = 4$, $\varpi = 0$, and $t_i = 1$s the signal is plotted, together with its Hilbert transform, in Fig. 32.
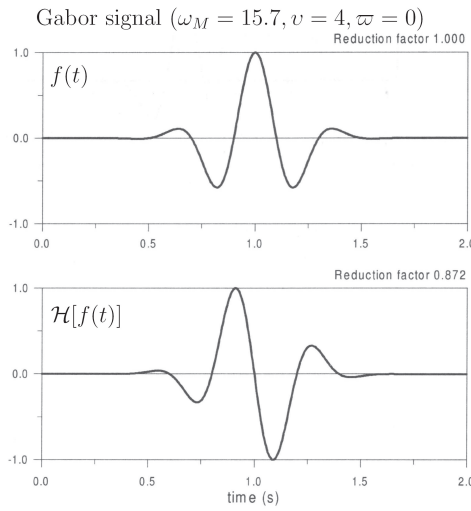
Figure 32: An example of the Gabor signal $f(t)$ and its Hilbert transform $\mathcal{H}[f(t)]$ (from Červený, 2001).

3. **Berlage signal**. It equals zero up to time t_i. In later times it is given as

$$f(t) = (t - t_i)^N \exp[-b(t - t_i)] \sin[\omega_M(t - t_i)], \quad t > t_i , \qquad (6.7)$$

where ω_M, b and N are free parameters. For $t_i = 0.5$s and $\omega_M = 15.7$Hz, $b = 3$, $N = 0$, the signal and the corresponding Hilbert transform are shown in figure 33.
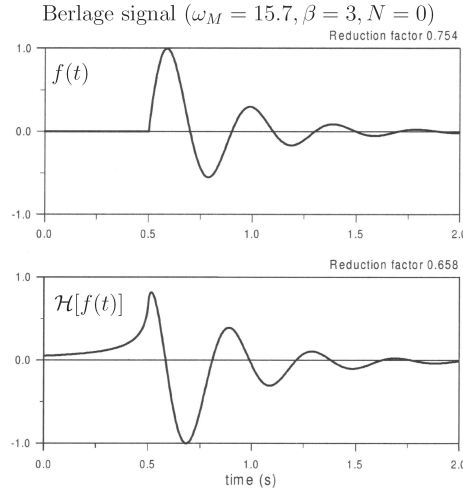
Figure 33: An example of the Berlage signal $f(t)$ and its Hilbert transform $\mathcal{H}[f(t)]$ (from Červený, 2001).

115

Why are such signals more useful for the RM than others? First, they are high-frequency signals, which means a low amplitude at zero frequency and in its vicinity. Since the RM deals with, in principle, a high-frequency approximation of the wavefield, the zero frequency and low frequencies close to zero must be removed anyway by a proper filtering. In the case of the above signals, such a filtering would not change their shape considerably. The second advantage concerns the question of causality. Except for the causal Berlage signal, the above signals are not strictly causal, but they can be qualified as 'effectively' causal. The same holds for their Hilbert transforms. The Hilbert transform contributes to the actual time behavior of the solution provided the ray under consideration incidents overcritically a structural interface, which results in a complex-valued R/T coefficient, as explained in Sec. 5.9.

Considering both of the above-mentioned aspects it is now clear why certain time signals, commonly used in other methods (the box-car, for example), are not suitable for the RM unless they are properly modified (e.g., by a suitable high-pass filtering).

7   Ray theory validity range

The asymptotic ray theory is based on the asymptotic ray series for frequency ω tending to infinity. In practical seismic applications, however, the maximum frequency is of a finite value. The applicability of the asymptotic ray theory is limited by several qualitative conditions, usually formulated as certain inequalities for the frequency of the wavefield or alternatively, for the wavelength. The inequalities relate the frequency (wavelength) to certain quantities, derived from the model parameters or from the wavefield parameters, by the use of operator $\gg$, i.e., 'much larger' ($\ll$, 'much smaller'). If any of these inequalities is not satisfied, the RM results are not generally reliable and may even be completely wrong. The problem is that it is difficult to estimate to what extent the results are wrong in such a case. In practice, it is not clear what the $\gg$ or $\ll$ really means, i.e., by how much the above quantities should be larger (shorter) than the frequency (wavelength). Numerical experiments confirm that the results may be reasonably accurate and acceptable even in certain situations in which some of the conditions are not strictly satisfied. Beydoun and Ben-Menahem (1985) have studied the breakdown of the asymptotic ray theory on certain canonical examples comparing the ray results with the exact solution obtained by the FDM or discrete wave number method (Bouchon, 1981). Some authors (e.g., Beydoun and Keho, 1987) even propose certain recommendations, based on numerical tests, as to how to translate the inequalities into the numbers determining how many times the frequency (or wavelength) should be larger (or smaller) than certain quantities. They propose the values of order of units (i.e., up to ten-times) that guarantee the inequalities to be well satisfied. However, due to the numerical costs of the 'exact' methods, especially for high frequencies which are of interest to us, such numerical tests can be done for relatively simple models which are, moreover, relatively small in that the wavefield is not computed too far from the source. In no case can the above-mentioned recommendations be considered as universally applicable rules.

The following **general validity conditions**, formulated using the wavelength λ in a qualitative way, are presented by Červený (2001). They are, in principle, consistent with the conditions given by Ben-Menahem and Beydoun (1985) and Beydoun and Keho (1987). The conditions are as follows:

1. Let us consider the so-called characteristic lengths of the model, $l_i, i = 1, 2, \ldots$. Among these quantities there are, for example, dimensions of the model, source-receiver distance, layer thicknesses h_k ($k = 1, \ldots, K$ with K being the number of layers in the model), radii of curvature of structural interfaces K_j, ($j = 1, \ldots, K - 1$), but also the scale length of inhomogeneities like $v/|\nabla v|$ (with v being α or β, the P- or S-wave speed, respectively), $\rho/|\nabla \rho|$, where ρ denotes density, etc.

The first condition requires that the wavelength considered in the RM calculations is much smaller than the minimum characteristic length

$$\lambda \ll \min(l_1, l_2, \dots) . \qquad (7.1)$$

This condition expresses the high-frequency character of the wavefield. Comparisons of the RM solutions with exact solutions, if they are available, show, however, that the RM can be applied even in certain situations when some of the characteristic lengths do not satisfy the condition (7.1). It has been shown, for example, that for the RM it is much more critical if the radii of interface curvature or scale lengths of inhomogeneities violate the condition than if layer thicknesses are not much larger than λ, or they are even comparable to λ (see Moczo et al., 1987).

Alternatively, some authors express this condition in frequencies using the so-called medium threshold frequency $\omega_0 = \frac{1}{2} \max(|\nabla\alpha|, |\nabla\beta|, \alpha|\nabla\rho|/\rho, \alpha/h_i, \alpha K_j, \dots)$ in which case the condition reads $\omega \gg \omega_0$. Beydoun and Ben-Menahem (1985) call this condition the mode decoupling condition. It has been proved for certain simple isotropic models that this condition restricts the frequency to be high enough for decoupling elastic waves into P- and S- waves. Ben-Menahem and Beydoun (1985) have shown that the mode decoupling condition implicitly contains the assumption of slow variations (with respect to wavelength) of the slowness vector. The authors also explicitly specify the so-called high-frequency condition, requiring $\omega \gg \omega_c = v(\nabla^2 A/A)^{\frac{1}{2}}$, where ω_c is called the cut-off frequency and A denotes the scalar ray amplitude factor (e.g., the RCC amplitude component). The condition requires A to be a sufficiently slowly varying function of position within a wavelength. It can be included into the above condition (7.1) by involving $l_c = \sqrt{A/\nabla^2 A}$ in the list of l_i's.

Let us point out that this condition elucidates what is meant by a high-frequency which qualifies the RM to be applied as a high-frequency approximation. It is clear that an answer to the question whether a given frequency is high enough for the RM or not depends only on the structure model considered. In slowly varying smooth models, far from the source as well as the model boundaries and interfaces, it may happen that the threshold frequency is nominally low (for example, lower than 1Hz).

2. The second condition given by Červený (2001) relates the wavelength to the distance d from a surface where the wavefield is not regular, like a caustic surface, shadow zone boundary, etc. It requires the wavefield

to be computed not closer to these surfaces than at distances much larger than the wavelength under consideration. The condition reads

$$\lambda \ll d .\tag{7.2}$$

One may consider this condition to be involved in the above condition (7.1) requiring $\lambda \ll l_c = \sqrt{A/\nabla^2 A}$. Indeed, this requirement, in principle, restricts the RM to be used in a close vicinity of surfaces along which the ray field is not regular because the ray amplitude obviously violates the condition there.

In many textbooks on the ray theory, there can be found the third qualitative condition restricting maximum length of rays. This condition, however, becomes important only when higher-order terms of the ray series are involved. For the zero-order solution it is of no concern. Since in these course notes we concentrate mainly on the zero-order solution, we will skip this condition for its irrelevance to our context.

The above presented conditions are written with an implicit assumption of isotropic models. Possibly slightly modified, they can be considered for anisotropic models as well (this is why the equations are not framed). However, in anisotropic structures an additional condition must be taken into account – the condition ensuring that the quasi-shear waves are not coupled (see Kravtsov and Orlov, 1990, Pšenčík, 1994). The condition reads

$$\frac{\bar{c}|c_{,i}|}{\omega} \ll \Delta c ,\tag{7.3}$$

where ω is the frequency prevailing in the wavefield, $\bar{c}$ means the average of the phase velocities of both quasi-shear waves propagating in the same direction, $|c_{,i}|$ is the magnitude of the larger of the gradients of the phase velocities, and Δc is the difference between the phase velocities of the two qS-waves.

Another possibility to judge the applicability of the RM has been proposed by Popov and Camerlynk (1996). They suggest a criterion based on the theory of asymptotic series (see, Sec. 2.3). The criterion relates the amplitudes of the zero- and first-order terms in the ray series. The basic idea is to detect, for a given frequency, whether there is a descending branch in behavior of individual terms in the ray series with respect to the index of the series. If not, the ray series as such cannot be used to approximate the solution. Indeed, if the terms in the series successively increase, it makes no sense to sum up to any N (including $N = 0$) since the error, estimated by (2.18), is higher in order than the approximated value. Note that, in contrast to the previously mentioned condition, this one concerns the validity

of the zero-order term, although a higher-order term is taken into account in the formulation of the condition. Although the condition itself is very simple, it is not very suitable for practical use. In order to check whether it is satisfied we would have to compute the first-order term of the ray series.

Kravtsov and Orlov (1980) propose more quantitative RM validity conditions, based on the concept of the so-called **Fresnel volumes**. The Fresnel volumes are sometimes called also the physical rays in contrast to the 'mathematical' rays of infinitely small thickness. Let us assume a ray Ω from a point S to a point R. The RM wavefield at R is directly influenced by the structure parameters (and their variations) along the ray itself, i.e. only at points through which the ray passes. However, from various numerical experiments using other numerical techniques yielding an 'exact' solution, as well as from physical measurements it follows that in reality, the wavefield at R is also affected by the parameters in a certain vicinity of the ray Ω. This vicinity represents the Fresnel volume. Kravtsov and Orlov (1980) propose a very simple definition of the Fresnel volume in terms of travel times, assuming a point F in the vicinity of Ω (see figure 34). For example, for a monochromatic wave of frequency ω, propagating from S to R, the point F belongs to the Fresnel volume corresponding to the ray Ω from the point S to the point R only if

$$|\tau(F, S) + \tau(R, F) - \tau(R, S)| < \pi\omega^{-1} , \qquad (7.4)$$

where $\tau(B, A)$ means the travel time the wave needs to reach the point B from the point A. The physical meaning of this condition is obvious: the points for which the time difference on the left-hand side of the inequality (7.4) is larger than one half of the period (π/ω) do not contribute significantly to the wavefield at R because of a destructive interference. Clearly, the width of the volume depends on frequency: the higher the frequency, the narrower the volume is.

To determine the Fresnel volumes in the model we need to know travel times not only along rays but also those corresponding to virtual points in their vicinity. An effective way to approximate these times is to calculate the so-called paraxial times, for which a solution of the DRT system is essential. However, such a paraxial approximation is beyond the scope of these course notes. For details see Červený, 2001. The Fresnel volumes have found many applications in seismology as well as in seismic exploration, see, e.g., Lindsley (1989), Knapp (1991) or Kvasnička and Janský (1991).

The Fresnel volume RM validity conditions are as follows:

1. Ray amplitude, the slowness vector as well as the medium parameters should vary only slightly over a cross-sectional area of the Fresnel volume. This condition can be easily understood from the point of view
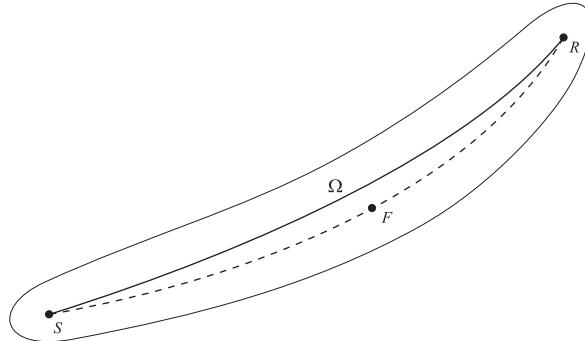
Figure 34: A Fresnel volume (2-D section) corresponding to the ray Ω connecting the points S and R.

of the underlying physics: since the ray synthetic wavefield, in principle, carries 'information' from points along the ray only, it would not be affected by other points inside the Fresnel volume while the real wavefield would be influenced by them. So, the RM would return erroneous results in the case of significant changes of the solution and model parameters inside the volume. Kravtsov and Orlov quantify the conditions using r_F, the maximum cross-sectional dimension of the given Fresnel volume, as

$$r_F \left| \frac{\nabla_\perp v}{v} \right| \ll 1, \dots , \tag{7.5}$$

where instead of v (propagation velocity) other medium parameters or quantities as slowness components and amplitude factors may stand. The symbol $\nabla_\perp$ denotes the gradient perpendicular to the ray.

2. In the case of more rays arriving at the same receiver point, the corresponding Fresnel volumes must not penetrate into each other significantly. This can be expressed as

$$V_{\cup V_{F_i}} \gg V_{\cap V_{F_i}} , \tag{7.6}$$

where $V_{\cup V_{F_i}}$ denotes the sum of all the volumes V_{F_i}, while $V_{\cap V_{F_i}}$ their common part.

Kravtsov and Orlov have proved in many special cases that the Fresnel volume conditions can replace other validity conditions proposed by other authors, usually hard to be translated in quantitative criteria suitable for a practical use. However, neither of the Fresnel conditions are easy to use in practice in deciding the applicability of the RM or even in estimating its accuracy.

All the above-mentioned conditions have been studied, on canonical examples, mostly in isotropic media. Although some of the conditions could, in principle, be generalized for the case of anisotropy (for example the Fresnel volume conditions), it is not clear how relevant the conditions would be in such a case. As it has been already mentioned, in anisotropic media, compared to isotropic models, the situation is much more complicated due to the fact of possible coupling between the quasi-S waves (see, for example, Coates and Chapman, 1990). Numerical studies comparing the ray solutions with the exact solutions in anisotropic structures are very rare up to now. In this context, the paper by Bulant et al. (2004) has to be mentioned.

For the reader's convenience, let us close this chapter by summarizing briefly the most common situations in which the ray theory may fail. A more detailed discussion can be found in the Červený's book (2001).

- *Fine layers* are present in the model (Fig. 35a), which are too thin with respect to the wavelength. The RM validity conditions are not fulfilled. If a stack of thin layers appears in the structure, the situation is even more complicated due to the increase of relevant multiply reflected/transmitted waves, mutually interfering. The RM is completely inadequate to handle such a case. Matrix or other related methods should be used instead.

- *Regions of high-velocity gradients* in the model (Fig. 35b). Rays can be formally passed through without difficulties, but the ray solution could be inaccurate.

- *Objects (blocks) with dimensions smaller or comparable to the wavelength* are situated inside the model (Fig. 35c). If the objects are even much smaller in dimensions than the wavelength under consideration they act as scatterers. The scattered wavefield, however, cannot be calculated by the standard RM.

- *Edges and vertices in interfaces* (Fig. 35d and also Figs. 1 – 3) complicate the situation for several reasons. First, the normal to such an interface cannot be uniquely defined on the edge or vertex, so that the ray calculation cannot continue after incidence at such a point of the interface. Further, such interface features form shadow zones beyond them. The ray wavefield does not penetrate into the shadows. Moreover, the shadow boundary represents a singularity in the model. Finally, the edges (vertices) are usually the source of diffracted waves which are not treatable by the standard RM.

- *Layer unconformities* in the structure, especially the angular unconformities (Fig. 35e), where the beds beneath such an unconformity

are not parallel with those above, and the nonconformities that are usually between overlying stratified sediments and underlaying unbedded rocks. These features introduce edges (vertices) into the layer boundaries and form shadow zones. Moreover, close to the tip of an unconformity the layer thickness approaches zero. An example of such unconformities and their effects on the ray wavefield can be seen in Figs. 1 – 3.
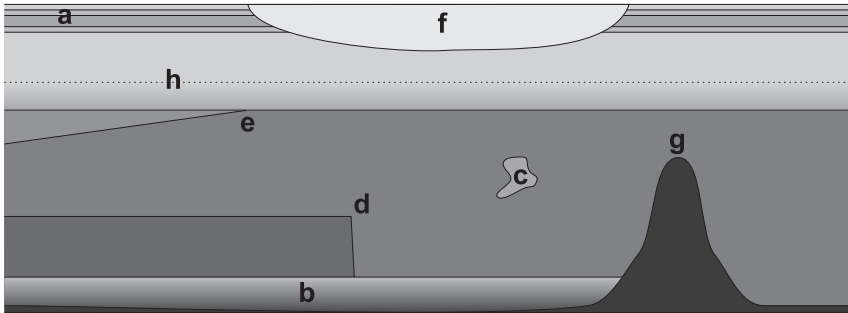
Figure 35: A sketch of structural features possibly making the RM inapplicable.

- *Basins and reservoirs* (Fig. 35f) as well as *lens-shaped rock bodies* inside the model are the structures producing mutually interfering multiply reflected waves. In such situations, where strong interference effects are a consequence of superposition of a large number of elementary waves, the RM may fail or, at least, its application becomes cumbersome. Similarly to the layer unconformities mentioned above, the thickness of the filling approaches zero at the ends of such structures.

- Presence of *interfaces with small radii of curvature* (with respect to the wavelength) clearly does not meet the RM validity conditions. Typically, caps of dome-like structures represent examples of such interfaces (Fig. 35g). Rays interacting with such an interface can be formally traced without problems, but the calculated ray synthetic wavefield could be very inaccurate.

- The model contains *higher-order interfaces*, i.e. the interfaces with step discontinuity of derivatives of medium parameters while the pa-

123

rameters themselves remain continuous across the interface (Fig. 35h). Such interfaces are often introduced formally by inappropriate (e.g., piecemeal) approximation of the model. This is why a spline interpolation is preferred over a linear interpolation to approximate the model (see Sec. 6.1). The rays and travel times of the waves reflected or transmitted at such interfaces of higher order can be computed in a standard way. However, since the corresponding waves are higher-order waves (similar to head waves) their amplitudes provided by the standard zero-order RM may be completely wrong.

- *Rays incidenting overcritically at an interface* in the model. In the case of an overcritical incidence, the slowness of some of the generated waves is complex-valued (which corresponds to inhomogeneous waves). Tracing of the corresponding rays has to be stopped since the RM is not able to handle inhomogeneous waves. The rays of the generated waves with real-valued slownesses can be calculated, but the carried wavefield is singular in the vicinity of the critical region. The amplitude may depart considerably from the exact solution (see Figs. 3 and 25) beyond the critical point. The waveform shape of the relevant reflection or transmission, predicted by the RM as a linear combination of the input signal and its Hilbert transform, does not include a head wave contribution which may be significant and coming at nearly the same time as the reflection/transmission in a close vicinity of the critical point.

- *Rays tangent to an interface locally or globally (the grazing rays).* A ray locally tangent to a smooth interface can be easily traced. However, the wavefield in the vicinity of such a ray is singular beyond the point at which the ray touches the interface. Beyond this point a shadow zone is usually formed between the ray and the interface and the ray itself becomes a boundary ray separating the shadow and the illuminated region. The standard RM is not capable of handling any waves penetrating to the shadow (for example, smooth interface diffractions). It may happen also that a ray is globally tangent to an interface (e.g., in the case of a plane interface and straight line rays) like, for example, the transmitted ray for a critical incidence. Such a wave would generate head waves the rays of which (containing a segment tangent to the interface) could be formally traced but their amplitudes cannot be computed by the standard zero-order RM as the waves belong to the class of higher-order waves.

- Rays form *Caustics.* The standard ray theory predicts infinite amplitude at a caustic point. In a vicinity of the caustic the wavefield

is anomalous and its ray amplitude is not reliable. In space, caustic points are not isolated, they form what is called the caustic surface (ray field envelope). See, for example, CC_1 and CC_2 in Fig. 16. On one side of a caustic surface a caustic shadow zone is created into which the ray theory wavefield cannot penetrate (in contrast to the real wavefield). To summarize, the ray wavefield is singular while the real wavefield is finite and smooth in the vicinity of a caustic.

- *Chaotic behavior of rays.* Multiple scattering by irregularities of the model gives rise to ray chaos. Where the chaos exists, the calculation of ray paths is extremely sensitive to the initial conditions, and the number of ray paths connecting two points grows rapidly with the distance separating the points. The chaotic rays diverge exponentially despite having originally been close to each other. Such a behavior of rays can be described by the so-called chaos theory (Ott, 1993). The chaotic-like-behavior is reasonable to expect in complex models, characterized by multiply reflecting features of interfaces and refractive ray-trapping medium properties. However, it can be observed as well in much simpler structures (compare the well known 'billiard-table' problem).

- *Quasi-shear wave coupling in anisotropic media.* The standard RM cannot be used when the qS_1- and qS_2-waves are coupled (their phase velocities are close to each other). This can happen either globally, in a weakly anisotropic medium (close to isotropic), or locally, in the vicinity of quasi-shear wave singular directions.

8   Computer program ZRAYAMP

The program ZRAYAMP is designed for fast computation of body-wave ray travel times and amplitudes in spherically symmetric, radially inhomogeneous, isotropic media. Arose from the program ZESY82 (Červený and Janský, 1985) it has been modified by J. Janský. It is written in FORTRAN77 programming language. It utilizes several routines and algorithms adopted from the SEIS81 program package, designed for the computation of ray synthetic seismograms in 2D laterally varying structures (Červený and Pšenčík, 1984, 2002). The program intrinsically utilizes the Earth flattening transformation, see Sec. 3.3.

The program is suitable to demonstrate certain features of the RM, explained in these course notes. Despite it only performs calculations in 1D models, running the program and creating input data for it may help the reader to understand better some practical aspects of the method. It also allows the reader to easily compare the results with the results yielded by other methods, applicable possibly in less-dimensional media only. However, the program is not presented here only as a suitable training tool for computer exercises. It can be used for calculations in certain global seismological problems on the spherically symmetric Earth. For example, it has been applied to obtain P-wave amplitudes and dynamic strains inside the Earth (Duda et al., 2000). Nevertheless, for more complex models, another ray tracing programs must be employed. For example, for 2D isotropic laterally varying structures, the above-mentioned program package SEIS81 is widely used. For 3D models, the CRT program has been developed (Červený et al., 1988). I. Pšenčík has developed the well-known program ANRAY for ray calculations in 2D anisotropic media (http://sw3d.mff.cuni.cz).

8.1   Brief description of the program

The program reads in data describing the 1D structure in which the ray calculations are to be performed. The structure is specified using the Cartesian coordinate x_3 (depth, in km), increasing downwards. It is bounded from above by the Earth's surface ($x_3 = 0$) and from below by the bottom of the model. The velocity distribution is specified at n gridpoints x_3^i, starting from the gridpoint $x_3^1 = 0$, corresponding to the surface of the Earth. At these gridpoints, the velocity is either continuous, or continuous with discontinuous first derivative (interface of the second order), or discontinuous (first-order interface). In the last mentioned case, two velocity values must be specified at such a gridpoint x_3^i: one just above the interface and the second immediately below it. The velocity between individual interfaces is approximated by the smoothed splines. More specifically, instead

of the velocity-depth distribution $v = v(x_3)$, the function $x_3 = x_3(v)$ is approximated as $x_3 = a_j + b_j v^{-2} + c_j v^{-4} + d_j v^{-6}$ for the depths between two successive grid points $x_3^j \leq x_3 \leq x_3^{j+1}$. The coefficients a_j, b_j, c_j and d_j are calculated using the cubic spline algorithm. This spline interpolation procedure guarantees continuity of the first and second derivatives of velocity and does not generate false low-velocity layers (oscillations in the velocity-depth function). The spline smoothing algorithm may slightly change the gridpoint depths (x_3^i), except the depths of the structural interfaces which are fixed.

The model is further determined by several parameters specifying the ratios of the S- and P-wave velocities within individual layers and densities above and below each interface (densities inside layers are of no relevance for calculating rays as well as ray amplitudes). Optionally, the program allows to specify quality factor in order to describe attenuation. Note that in dissipative media, rays as well as eikonals should be complex-valued. The program does not compute complex rays and attenuation is introduced by applying the so-called t^*-approximation (see, e.g., Duda and Yanovskaya, 1993). Note that attenuation results in the form of the ray solution which is in conflict with its original ansatz. The problems of attenuation and the corresponding dissipation filters are beyond the scope of this book.

The program is designed to calculate rays radiated from a point source. The source position is specified by the Cartesian coordinates x_1^S (horizontal coordinate, increasing from the left to the right) and x_3^S (depth, increasing downwards). The point source may be situated at any depth, except the depths corresponding to the first-order structural interfaces. It can be situated also at the Earth's surface. The x_1^S coordinate may be arbitrary, but the receiver positions must be specified properly with respect to the given epicenter. There are two options for the radiation function: either omnidirectional or a double-couple. The omnidirectional radiation for S-waves is three times larger in magnitude than that for P-waves. The double couple source is characterized by the seismic moment, strike, dip and rake (for definitions see Aki and Richards, 1980). At the source point, density must be specified.

The receivers may be distributed regularly or irregularly along the Earth's surface. Their positions are specified by horizontal distances x_1^{Rj} (in km) or simply by the distance of the first receiver (the closest to the epicentre) and step in their spacing. The receivers must be situated to the right from the epicenter, i.e. $x_1^{Rj} \geq x_1^S$. The epicentral distance of j-th receiver is then $x_1^{Rj} - x_1^S$. The epicentral distances of the successive receiver must grow or decrease monotonically (they form a monotonic sequence).

Each elementary wave under consideration is defined by the numerical code of the wave. The codes can be specified manually (in input data) or they

can be generated automatically by the program. The ZRAYAMP program is able to generate automatically only the codes of direct (refracted), primarily reflected monotypic *P*- and *S*- waves, and primarily converted waves at the reflection point. The code is defined in the same way as it is explained in Sec. 6.1 (Step 2). The whole ray is divided into elements, each of which lies between two successive points at which the ray strikes the interfaces. If the end points of such an element lie on different interfaces, it is called a simple element. When the end points lie on the same interface (in the case of refracted waves), it is called a compound element. Any compound element is formally regarded as two simple elements. Thus, the refracted waves corresponding to rays with a turning point in certain layer are not distinguished by the code itself from the wave of the same type reflected from the bottom of the given layer.

The program reads in the range of ray declinations (measured in radians clockwise from the Earth's surface to the tangent to the ray at the source) covering the region of interest. This means that the angles have to be specified in such a way that the corresponding rays can reach the specified region (for example, set of receivers). The angle range may also be used to separate the refracted wave from the reflected one, having the same numerical code. Further, the step in ray declinations has to be given.

For the elementary waves specified, rays are calculated either by the so called initial-value ray tracing (with regular step in the ray declination) or by the two-point ray tracing (rays terminating at specified receivers) in which case the shooting method is employed. The shooting method determines the ray parameter p, see Sec. 3.3, of a successful ray (the ray captured at a given receiver). The step in declinations is used only for initial trials in such a case; the actual declination ψ of the successful ray is related to the ray parameter p of the ray as $p = |\cos\psi|/v$, with v being either the *P*-wave velocity α, or the *S*-wave velocity β. Note that in 1D media the ray parameter is preserved along the whole ray as it is shown in Sec. 3.3.

In the shooting algorithm, special care must be devoted to certain singular regions. Difficulties may arise in the vicinity of shadow zones or in those parts of the ray field which are characterized by multiple arrivals of the given elementary wave (multipathing). Problems can appear also in critical region (for angles of incidence close to the critical angle). For example, the rays of slightly refracted (transmitted) wave are very sensitive to the initial declination there. The shooting procedure itself is algorithmically very robust to handle many peculiar features of the ray field (reverse branches, shadows, etc.).

In the program ZRAYAMP, the rays are not traced in the standard way, i.e. solving numerically the RTS. Thanks to the 1D character of the model and the special approximation of the velocity distribution inside layers (be-

tween structural interfaces), it is possible to find analytically an increment in the horizontal coordinate x_1^i, corresponding to each depth level x_3^i, for any ray with the given ray parameter p. The same holds for travel time increments as the ray passes through individual depth levels. The geometrical spreading at the ray endpoint, necessary to determine amplitude from the continuation formula, is also given analytically in our case. This makes the computations very fast. The calculations are performed in Cartesian geometry, in which also the input data must be given, and the results are transformed to those corresponding to the spherical geometry using the EFT.

For each ray and each depth level x_3^i, the program returns the angular distance, measured from the vertical passing through the epicentre, travel time and vertical amplitude (modulus) at the corresponding ray point. In addition to this, all the three amplitude components (moduli and phases) are stored at the ray endpoints. These data are written in a simple ASCII form and can be processed further by user supplied auxiliary programs for plotting, convolution with the relevant source-time function, etc.

Detailed description of the structure of the input and output data is given in Sec. 8.2. Sec. 8.3 provides several solved numerical examples. The program, its description, input data and results for the numerical examples can be found on the attached CD.

8.2   Input and output data

The program reads one input and generate two output files. The structure of the input data **ZRAYAMP.DAT** is as follows:

1: TEXT — one line, format (A80)
Arbitrary alphanumeric comment on the model.

2: K2, MPRINT, KX — one line, free format

K2   Controls the extent of calculation.

> K2 = 1   travel times only.
>
> K2 = 2   calculation of arrival times, amplitudes and phase shifts (i.e., the quantities needed to compute the elementary impulse seismograms).

MPRINT Controls the printout of the description of the model in the output file ZRAYAMP.OUT.

> MPRINT = 0 only input data are printed.

MPRINT = 1 input data and list of subintervals of depths together with the relevant parameters are printed.

MPRINT = 2 printout as for MPRINT = 1, plus velocity-depth distribution.

KX   Controls the type of ray calculations.

KX = 1   Two-point ray tracing (necessary for the calculation of synthetic seismograms).

KX = 2   Initial-value ray tracing. In this case data in 6 have no influence, but must be formally given in harmony with parameter MEP - see 5).

3: H(I), A1, VU(I), D1, E, SREL, REL(I), QF(I) — set of lines, free format
System of data for individual grid points of the model - one line for one grid point.

H(I)   Depth of the grid point [km]. This value can be slightly changed in the process of smoothing the velocity-depth distribution, with the exception of the interfaces. H(1) = 0.

A1   A1 = 0   No velocity jump occurs at the grid point. The first and second derivatives of the velocity are smooth at this grid point. Put A1 = 0 for the Earth's surface.

A1 = 100   Interface of the second order (the velocity is smooth but not its derivative).

0.1 < A1 < 99   Interface of the first order. A1 then gives the P velocity immediately above the interface. The quantity VU(I) then represents the velocity immediately below the interface.

VU(I) P-wave velocity at the grid point (from bellow) [km/s].

D1, E   Densities immediately above and bellow the interface [g/cm^3]. Put D1 = E = 0 if A1 = 0 or A1 = 100 with the exception of the Earth's surface where D1 = 0 and E is given.

SREL   The ratio of the S and P velocities from above at the grid point. Put SREL = 0 if A1 = 0 or A1 = 100.

REL(I)   The ratio of the S and P velocity at the grid point (from below).

QF(I)   Quality factor for the *P*-waves between two grid points. Quality factor for *S*-waves = 2.25QF(I). For QF = 0 no attenuation is considered. The frequency dependence of the attenuation is applied in the program in the way that the TSTAR (integral along the ray from the source to the receiver from $1/(\text{velocity} \times \text{quality factor})$) is multiplied by 0.6366atan(1.5923/FHZ). (FHZ see bellow.)

The last grid point of the model is considered as the first-order interface. Termination of the input of model: 8 numbers in free format, the first should be equal to -1.

4: OD, TDD. — one line, free format
Controls the application of the smoothed spline algorithm to the depth-velocity distribution.

OD   Degree of smoothing of the depth-velocity distribution by splines [km]. Higher accuracy (lower smoothing) is obtained for smaller OD.

TDT   Absolute value of the step in variable $1/v^2$ [(km/s)$^{-2}$] for computation and print of the tables of the depth-velocity distribution (actually the depth - $1/v^2$ distribution). This distribution is calculated for each layer independently. If TDT < 0.0001, the depth-velocity distribution is not calculated even for MPRINT = 2. The depth-velocity distribution is not printed for a layer with the constant velocity. TDT has no meaning for MPRINT < 2.

5: ICONT, MEP, MOUT, IBP, IBS, IDP, IDS, IREAD, MPSOUR, ITMAX, NLAY — one line, free format

ICONT   Controls the continuation of the computation.

          ICONT = 0   termination of the computation. Last line in input data.

          ICONT = 1   computation continues, line 6 follows.

MEP   ABS(MEP) — the number of receiver positions, 1 < |MEP| < 100. The sign of MEP controls the way in which the system of receiver positions is specified.

          MEP > 0   The receivers are distributed regularly along the profile. Only the position of the first receiver and the step in the x_1^R-coordinate are read - see 6).

	MEP < 0	The receivers are distributed irregularly along the profile. The x_1^{Ri}-coordinates of all receiver positions are read in 6.

MOUT   Controls the print of results on the screen. The input data are always reproduced. The printout then continues as follows:

	MOUT $= 0$	Only the codes of generated waves are printed.
	MOUT $= 1$	Elementary impulse seismograms (with the x_1^{Ri}-coordinate of the receiver) and external wave codes are printed.
	MOUT $= 2$	More detailed print that allows to monitor the calculation.

IBP-IBS   Switches which control the automatic generation of numerical codes of elementary waves. Only direct, refracted and primarily reflected waves (possibly converted at the point of reflection) can be generated automatically.
IBP controls the automatic generation of refracted and primarily reflected waves for a P-wave source.

	IBP $= 0$	No refracted and primarily reflected waves are generated.
	IBP $= 1$	PP refracted and PP primarily reflected waves are generated.
	IBP $= 2$	PS primarily reflected waves are also generated.

IBS controls the automatic generation of refracted and primarily reflected waves for a S-wave source.

	IBS $= 0$	No refracted and primarily reflected waves are generated.
	IBS $= 1$	SS refracted and SS primarily reflected waves are generated.
	IBS $= 2$	SP primarily reflected waves are also generated.

IDP   controls the automatic generation of the direct P-wave (upwards from the source).

	IDP $= 0$	Direct P wave is not generated.
	IDP $= 1$	Direct P wave is generated.

IDS   controls the automatic generation of the direct S-wave.

> IDS = 0   Direct S wave is not generated.
>
> IDS = 1   Direct S wave is generated.

IREAD   Controls the manual generation of numerical codes of elementary waves.

> IREAD = 0   No numerical codes are generated manually.
>
> IREAD = 1   Numerical codes of certain elementary wave are manually generated, see line set 10.

MPSOUR   Controls the source radiation pattern.

> MPSOUR = 0 The radiation pattern does not depend on the ray parameter (isotropic radiation).
>
> MPSOUR = 7 Double-couple radiation pattern applies for both P- and S- waves.

ITMAX   Number of iteration permitted in the determination of the ray parameter in two-point ray tracing (maximum 99). If ITMAX = 0, then ITMAX = 20.

NLAY   Controls the generation of the numerical code of the waves that propagate in the last layer (if IBP > 0 and/or IBS > 0).

> NLAY = 1   The waves are not generated.
>
> NLAY = 0   The refracted P- and S- waves in the last layer are generated. The waves reflected and possibly converted at the bottom of the model are not computed. Thus, in the computation the last layer represents a vertically inhomogeneous halfspace.

6: Specification of receiver positions along the surface of the Earth.

MEP > 0   RMIN, RSTEP [km] — one line, free format
     The receivers are distributed regularly along the profile. The x_1^{Ri} coordinate of the i-th receiver is given by the formula DST(I) = RMIN + RSTEP*(I-1). Take RSTEP > 0!

MEP < 0   DST(1), ..., DST(ABS(MEP)) —- one line, free format
     DST(I) gives the x_1^{Ri}-coordinate of the i-th receiver. The receivers may be distributed irregularly along the profile. Take the receiver positions from left to right so that DST(I) > DST(I-1) for any I.

7: XSOUR, ZSOUR, TSOUR, REPS, ROZD, FHZ — one line, free format

XSOUR The x_1^S-coordinates of the source [km].

ZSOUR The x_3^S-coordinate of the source [km], ZSOUR $\geq$ 0. ZSOUR must not be equal to depth H(I) of any of the first-order interfaces (with exception of the Earth's surface).

TSOUR Initial hypocentre time [s].

REPS The required accuracy [km] in the two-point ray tracing. If REPS = 0, then REPS = 0.05km.

ROZD Density [g/cm^3] at the source.

FHZ Frequency of waves [Hz] used in calculation of the attenuation. Put FHZ = 0 if attenuation is not considered (QF=0, see line 3).

8: PPAR(1), PPAR(2), PPAR(3), PPAR(4) — one line, free format
Double couple source parameters (see Aki and Richards). Given only if MPSOUR = 7. If MPSOUR$\neq$7, isotropic source is supposed. In this case the amplitude radiated as the S-wave is three times larger than the P-wave amplitude.

PPAR(1) Dip [rad]

PPAR(2) Seismic moment Mo [10^9 Nm], then displacement in μm.

PPAR(3) Strike [rad]

PPAR(4) Rake [rad]

9: AMIN1, ASTEP1, AMAX1, AMIN2, ASTEP2, AMAX2 — one line, free format
Control the basic system of initial angles in the determination of the parameter of rays in the shooting method.

AMIN1,ASTEP1,AMAX1 Minimum ray declination, declination step, and maximum ray declination. The values determine the system of initial angles [rad] for refracted, primarily reflected and converted waves generated automatically and for other manually generated elementary waves, the first element of which propagates from the source downwards.

AMIN2,ASTEP2,AMAX2 Minimum ray declination, declination step, and maximum ray declination. The values determine the system of initial angles for refracted, primarily reflected and converted waves generated automatically and for other manually generated elementary waves, the first element of which propagates from the source upwards. In both cases the parameters represent the initial value, the step and the end value of the angle [rad]. The ray with initial angle equal to zero emerges from the source parallelly with the x_1-axis in the direction of increasing x_1. The following conditions must be generally fulfilled: $0 \leq$ AMN1 $<$ AMX1 $\leq \pi$, ASTEP1 > 0 and $0 \geq$ AMIN2 $>$ AMAX2 $\geq -\pi$, ASTEP2 < 0. For MPSOUR $= 7$ (see 5)) value π is replaced by $\pi/2$.

10: KC, KCA, JC(1), ..., JC(KCA) — set of lines, free format
Manual generation of numerical codes of elementary waves. Given if IREAD $= 1$. For each code the following data must be given.

KC   KC $= 1$ The ray propagates from the source downwards.

        KC $=-1$ The ray propagates from the source upwards.

KCA   The number of segments of the ray. KCA < 100.

JC(I)   ABS(JC(I)) gives the ordinal number of the layer where the i-th physical element of the ray is situated. JC(I) > 0 : P-wave element, JC(I) < 0 : S-wave element. I $= 1, 2, ...,$ KCA.

The last line for the whole set must contain 3 zeros (the indication of the end of the elementary code list).

The program generates two outputs. The output file **ZRAYAMP.OUT** is partly of an informative character. It allows the user to check whether the input data have been read in correctly and provides information about the calculation. Possibly, the reasons why the calculations had to be stopped are given. Optionally, for MOUT=1 (see 5 in ZRAYAMP.DAT), it provides the resulting travel times and amplitudes at the ray endpoints. The structure is as follows:

1. Input data are always printed under appropriate heading.

2. Approximation of the model. The extent of the printed data depends on the value of MPRINT, see the input data, line 1

```
Sample model     ... 1: Description of the model
 2  0 (2)         ... 2: Control switches

  Depth          α              ρ              β/α        Q
   0.   0.      5.8000  0.      2.72    0.      .5793  0.
  10.   0.      6.0000  0.      0.      0.      .5769  0.
  20.   0.      6.2000  0.      0.      0.      .5769  0.
                             .
                             .                                    3: Structure model
                             .                                    (each line corresponds to
 2871.  0.     13.6866  0.      0.      0.      .5331  0.          one depth)
 2889. 13.6908  8.0087  5.550   9.915   .5333   0.01   0.
 2890.  0.      8.0087  0.      0.      0.      0.01   0.
   -1.  0.      0.      0.      0.      0.      0.     0.
  1.  .0002                          ... 4: Controls model smoothing (splines)
  1 60 1 (1)(0)(1) 0 (1)(7) 99 1       ... 5: Control switches
  200.    200.                       ... 6: Receivers
  0. (710.) 0.  .3   3.32   .03125   ... 7: Source
  1.57 1.e4 0.8 0.8                   ... 8: Double couple source parameters (optional)
  .01 .05 1.5707 -.01 -.05 -1.5707  ... 9: Angle ranges for rays
  1 5 4 4 3 2 1
  -1 4 4 3 2 1                        10: Numerical codes of elementary waves
  0 0                                 (optional)
```

Figure 36: An example of the input data file. Circles denote the most frequently changed switches controlling the computation.

if MPRINT = 1   The division of the medium into layers and parameters of the depth-velocity distribution in individual layers are printed under the heading: V (P velocity), 1/V**2, HZ (input grid depth), H (smoothed grid depth used in further computations), A, B, C, D (coefficients of the depth- velocity distribution), I (ordinal number of the grid point).

if MPRINT = 2   The same output as for MPRINT = 1 plus data on the depth-velocity distribution under the heading: V, 1/V**2 (with step TDT and independently for each layer), H, HV/DH (derivative of the *P*-wave velocity with respect to depth). The position of each first-order interface is marked by a row of asterisks.

3. Output for individual waves for a given set of input data 5-10.

if MOUT = 0   Internal wave codes (consecutive numbers of the wave in generation of the numerical codes) and external wave codes (parameters KC, KCA and JC(I), I = 1, 2, ..., KCA).

if MOUT = 1   Also coordinates of the receivers, corresponding arrival times, horizontal and vertical amplitudes and phase shifts of the displacement vector. For KX = 2 the first number in the line corresponds to the value of the initial angle of the ray (the one from the basic system of initial angles - see 8)). For KX = 1, the ray angle (ob-

tained by iterations in two-point ray tracing) is given as the last number in the line.

if MOUT = 2   The output is completed by certain results of iterations in the process of determining the ray parameter in the shooting method. These are:

- IND, XO, AA - for each endpoint of the ray in the basic system of rays.

- IND, ITER, DD, XO, PNEW - for each endpoint of the ray in the iterations to the receiver position.

- IND, ITER, XO, PNEW - for each endpoint of the ray in iterations for some special rays. Examples are the boundary rays between the shadow and illuminated regions (labeled SH), the critical rays (labeled CR)

The meaning of individual symbols:

XO   - x_1-coordinate of the endpoint of the ray.

DD   - x_1-coordinate of the receiver. It should not differ from XO by more than the shooting tolerance REPS (see 7 in ZRAYAMP.DAT)

ITER   - The successive number of the iterations.

AA   - Initial angle in the basic system of the initial angles.

PNEW - Initial angle of the ray, in iteration to the receiver positions.

IND   - Reason of the termination of the ray calculation:

IND = 3   The termination point is situated at the surface of the medium (successful ray).

IND = 9   Overcritical incidence at an interface where the numerical code of the wave requires a transmission.

IND = 14   The ray specified by the manual generation of the code does not exist in a given model.

IND = 18   The ray turned downwards by refraction in the first layer whereas it should reach the surface of the medium.

IND = 19   The deepest point of penetration of the ray in the ray in the refraction occurs exactly at the boundary of the layer.

IND = 20   Required conversion of the wave is not possible because a refraction occurs at the deepest point of penetration of the ray instead of a reflection.

The output file **ZRAYAMP.RES** contains the results of ray calculations for all rays point-by-point. The system of data for individual ray points is:

DELTA(I), Z(I), T(I), STRAIN(I), AMPZ(I)

DELTA(I)   - angle distance of the i-th point in degrees

Z(I)   - depth of the point in km

T(I)   - time at the point in sec

PHASEZ(I)   - phase of the amplitude at the point

AMPZ(I)   - modul of the amplitude of the vertical displacement component at the point (the amplitude includes radiation pattern, geometrical spreading, R/T coefficients and coefficients of conversion if the point is situated at the free surface)

The end of ray is indicated by the line:
9000.000000   9000.000000   9000.000000   9000.000000
9000.000000
After this, data for a new ray follow.

8.3 Numerical examples

All the following examples including complete input/output data and figures can be found on the attached CD in separate directories.

Example 1 – Model 1

The first example illustrates ray propagation in relatively complex structural model consisting of four inhomogeneous layers, separated by interfaces with jumps in velocities. The model is based on the PREM model, however it is much simplified. Fig. 37 shows the model in terms of velocity-depth distribution (part a) and the corresponding part of the input file (part b). The source is located in the forth layer. It represents an explosive source, i.e., it radiates only *P*-waves and the radiation is isotropic (the same in all directions). The considered elementary waves are direct *P*-wave (going up from the source) and refracted/reflected *P*-waves in the forth layer. The

numerical codes of elementary waves under consideration are generated automatically. Initial-value ray tracing is used, so that the ray endpoints are spaced irregularly. In this case the receiver positions are of no relevance, although at least one receiver has to be formally specified in the input data. The ray diagram is shown in Fig. 38. Fig. 39 shows the travel times and vertical amplitudes at the ray endpoints. In this example all the ray amplitudes are real-valued. Note the later arrivals and lower amplitudes of the reflected wave.

a)

b)

```
  0.   0.        5.8000   0.     2.72   0.      .5793  0.
 10.   0.        6.0000   0.     0.     0.      .5769  0.
 20.   0.        6.2000   0.     0.     0.      .5769  0.
 35.   6.5000    8.0400   2.92   3.32   .5769   .5559  0.
 45.   0.        8.0412   0.     0.     0.      .5563  0.
 50.   0.        8.0418   0.     0.     0.      .5565  0.
 60.   0.        8.0430   0.     0.     0.      .5569  0.
 71.   0.        8.0442   0.     0.     0.      .5573  0.
120.   0.        8.0500   0.     0.     0.      .5591  0.
171.   0.        8.1917   0.     0.     0.      .5506  0.
210.   0.        8.3000   0.     0.     0.      .5448  0.
271.   0.        8.5227   0.     0.     0.      .5430  0.
371.   0.        8.8877   0.     0.     0.      .5403  0.
410.   9.0300    9.3600   3.55   3.75   .5393   .5417  0.
471.   0.        9.5650   0.     0.     0.      .5436  0.
571.   0.        9.9010   0.     0.     0.      .5464  0.
660.  10.2000   10.7900   4.07   5.00   .549    .5514  0.
760.   0.       11.0558   0.     0.     0.      .5617  0.
771.   0.       11.0756   0.     0.     0.      .5614  0.
871.   0.       11.2506   0.     0.     0.      .5593  0.
971.   0.       11.4172   0.     0.     0.      .5574  0.
1071.  0.       11.5761   0.     0.     0.      .5555  0.
1171.  0.       11.7279   0.     0.     0.      .5537  0.
1271.  0.       11.8732   0.     0.     0.      .5519  0.
1371.  0.       12.0127   0.     0.     0.      .5503  0.
1471.  0.       12.1469   0.     0.     0.      .5486  0.
1571.  0.       12.2764   0.     0.     0.      .5471  0.
1671.  0.       12.4020   0.     0.     0.      .5456  0.
1771.  0.       12.5241   0.     0.     0.      .5441  0.
1871.  0.       12.6435   0.     0.     0.      .5427  0.
1971.  0.       12.7607   0.     0.     0.      .5413  0.
2071.  0.       12.8764   0.     0.     0.      .5400  0.
2171.  0.       12.9911   0.     0.     0.      .5387  0.
2271.  0.       13.1055   0.     0.     0.      .5374  0.
2371.  0.       13.2203   0.     0.     0.      .5362  0.
2471.  0.       13.3359   0.     0.     0.      .5350  0.
2571.  0.       13.4531   0.     0.     0.      .5338  0.
2671.  0.       13.5725   0.     0.     0.      .5327  0.
2740.  0.       13.6564   0.     0.     0.      .5319  0.
2771.  0.       13.6636   0.     0.     0.      .5322  0.
2871.  0.       13.6866   0.     0.     0.      .5331  0.
2889. 13.6908    8.0087   5.550  9.915  .5333   0.01   0.
2890.  0.        8.0087   0.     0.     0.      0.01   0.
  -1.  0.        0.       0.     0.     0.      0.     0.
```

Figure 37: Model 1: Velocity-depth distribution (a) and the corresponding input data (line set 3) (b).

Example 2 – Model 1

Here we adopt the same structure model as in the previous example. The source is situated at the surface and it represents a double couple with strike of 0.8rad, dip of 1.57rad and rake of 0.8rad. Only the following elementary waves are taken into account: S-waves refracted in the third and fourth layer, and S-waves reflected from the bottoms of the second, third, and fourth layer. The elementary wave codes are generated manually. The wave refracted in the second layer, not differing in the code from the corresponding reflection, is excluded by restricting the range of allowed ray declinations. Two-point ray tracing is applied assuming regular distribution
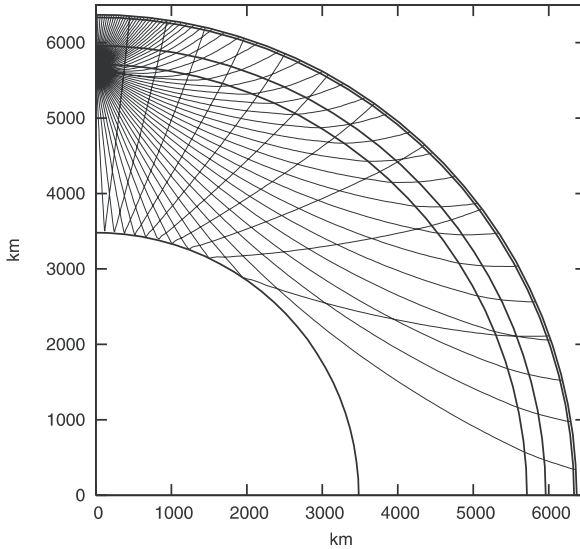
Figure 38: Rays from the Example 1.

a) b)
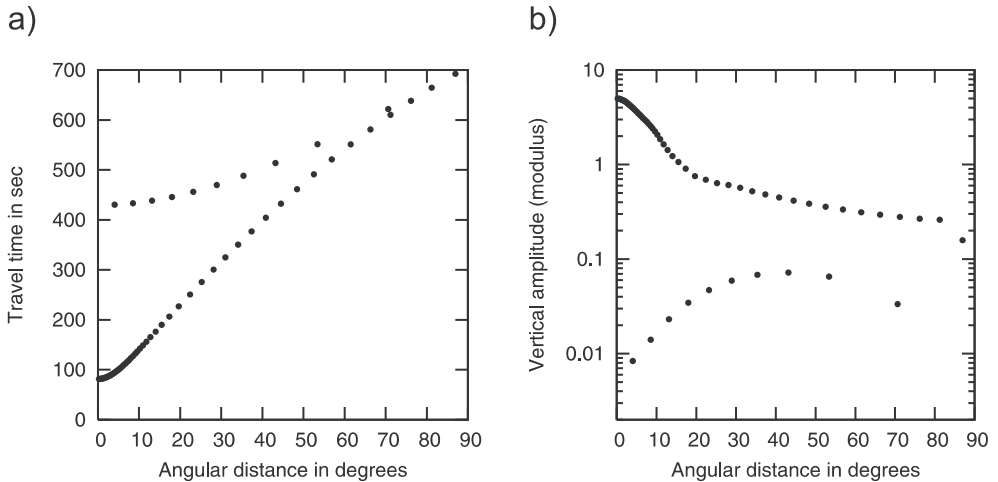
Figure 39: Travel times (a) and vertical displacement amplitudes (b) corresponding to the ray endpoints from Fig. 38 (Example 1).

of receivers with the receiver spacing 600km. The rays (calculated by the shooting procedure) are shown in Fig. 40. Fig. 41 shows travel times and amplitudes at the receivers. Circles corresponds to the waves refracted in the forth layer and reflected from its bottom (the waves analogous to those considered in the previous example), while triangles correspond to the waves refracted and reflected in the third layer and the waves reflected from the bottom of the second layer (not considered in the previous example). When comparing Figs. 41a and 39a (circles) we see similar hodochrons but longer
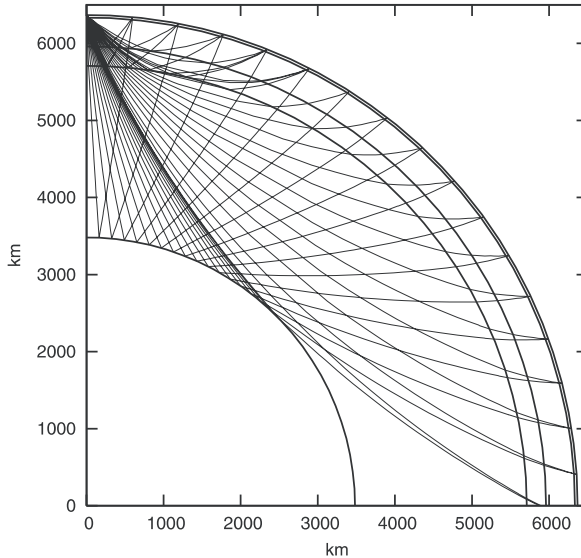
Figure 40: Rays from the Example 2.

a)
b)
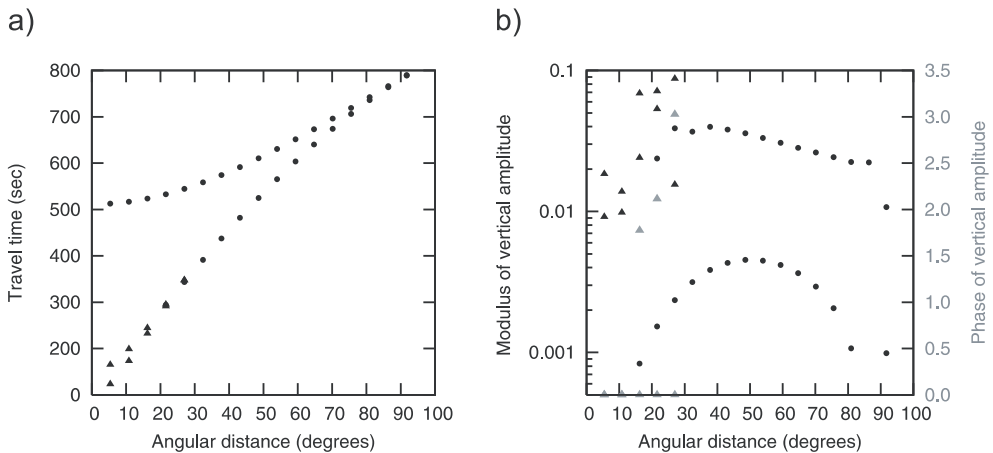
Figure 41: Travel times (a) and vertical displacement amplitudes (b) corresponding to the ray endpoints from Fig. 40 (Example 2). Grey triangles indicate phases of the rays reflected from the bottoms of the second and third layer.

travel times in Example 2. This is because of slower *S*-waves considered in Example 2 (and longer raypaths due to the surface source location). A relatively complicated amplitude behavior is mostly due to the strong directional dependence of the radiation pattern. A remarkable feature are the complex-valued amplitudes due to overcritical incidence of the rays reflected from the bottom of the second layer at the third receiver, and from the bottom of the third layer at the forth and fifth receiver.

Example 3 – Model 1
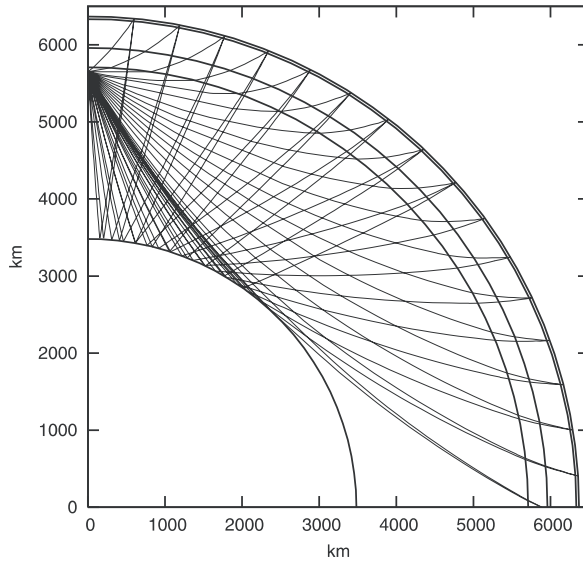
Figure 42: Rays from the Example 3.
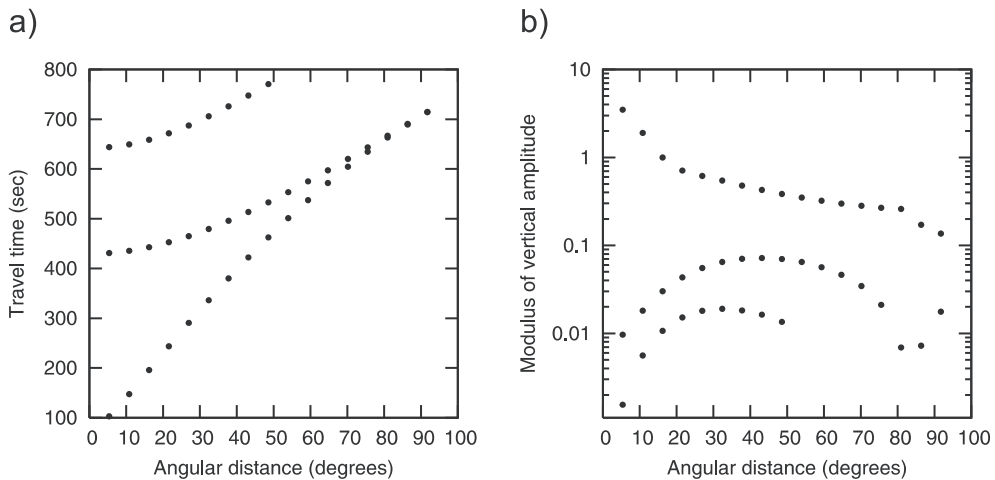
Figure 43: Travel times (a) and vertical displacement amplitudes (b) corresponding to the ray endpoints from Fig. 42 (Example 3).

In this example, the structure, source position, and the source type are the same as in Example 1. The receivers are distributed regularly in the same way as in Example 2. The codes of direct P-waves, their primarily refraction/reflections and conversion from P to S at the fifth interface are generated automatically. Figs. 42 and 43 shows the corresponding ray diagram, and time- and amplitude-diagrams, respectively. As expected, the

converted waves have latest arrival times and smallest amplitudes. All the amplitudes are real-valued.

Example 4 – Model 1

The fourth example is the same as the third one in terms of structure, source and receivers. The only difference is in elementary wave specification: instead of automatic generation of numerical codes the manual specification is used to involve the P-wave primarily refracted/reflected in the fourth layer and multiply reflected in the third layer (the codes are 4 3 3 3 2 1 and 4 4 3 3 3 2 1). These multiple reflections are considered here only for illustration how to construct the corresponding elementary wave code, not for their seismological importance. The resulting rays are in Fig. 44, travel times and amplitudes in Fig. 45. All the amplitudes are real-valued. Note that the amplitudes of the multiples are much lower than those obtained in Example 3 for the waves primarily refracted/reflected in the fourth layer (without the multiple reflections in the third layer) – compare Figs. 43b and 45b.
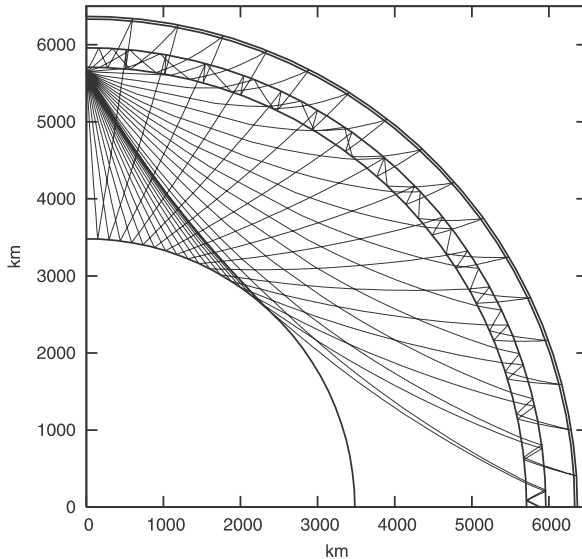
Figure 44: Rays from the Example 4.

Example 5 – Model 2

The last example illustrates the effect of a low-velocity zone in a smooth gradient model. The zone is at depths from 600km to 1200km and it is not separated by structural interfaces. The velocity structure is shown in Fig.

a)

b)
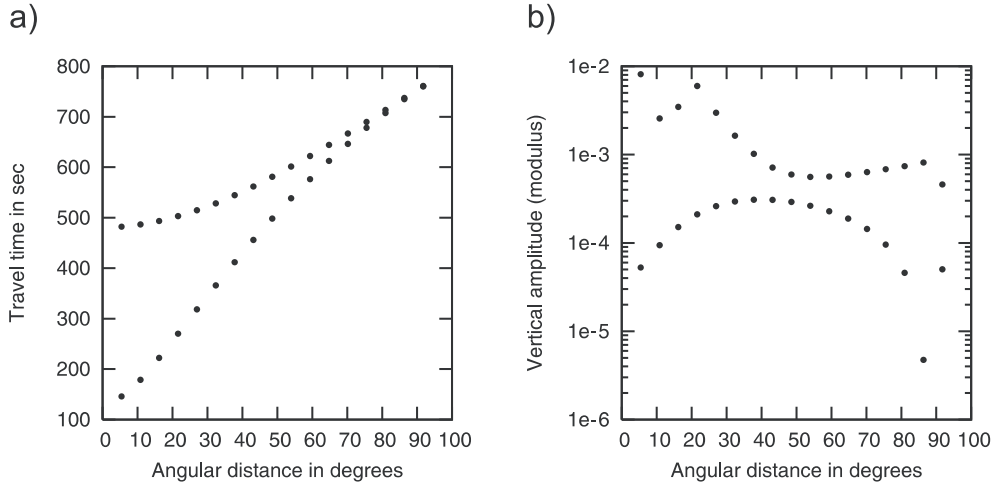
Figure 45: Travel times (a) and vertical displacement amplitudes (b) corresponding to the ray endpoints from Fig. 44 (Example 4).

a)

b)


```
   0.0000   0.00   3.4641   0.00   3.00   0.00   0.5774   0.00
  40.8163   0.00   3.6055   0.00   0.00   0.00   0.5774   0.00
  81.6327   0.00   3.7469   0.00   0.00   0.00   0.5774   0.00
 122.4490   0.00   3.8883   0.00   0.00   0.00   0.5774   0.00
 163.2653   0.00   4.0297   0.00   0.00   0.00   0.5774   0.00
 204.0816   0.00   4.1711   0.00   0.00   0.00   0.5774   0.00
 244.8979   0.00   4.3125   0.00   0.00   0.00   0.5774   0.00
 285.7143   0.00   4.4538   0.00   0.00   0.00   0.5774   0.00
 326.5306   0.00   4.5952   0.00   0.00   0.00   0.5774   0.00
 367.3469   0.00   4.7366   0.00   0.00   0.00   0.5774   0.00
 408.1633   0.00   4.8780   0.00   0.00   0.00   0.5774   0.00
 448.9796   0.00   5.0194   0.00   0.00   0.00   0.5774   0.00
 489.7959   0.00   5.1608   0.00   0.00   0.00   0.5774   0.00
 530.6122   0.00   5.3022   0.00   0.00   0.00   0.5774   0.00
 571.4286   0.00   5.4436   0.00   0.00   0.00   0.5774   0.00
 612.2449   0.00   5.4603   0.00   0.00   0.00   0.5774   0.00
 653.0612   0.00   5.2237   0.00   0.00   0.00   0.5774   0.00
 693.8776   0.00   5.0448   0.00   0.00   0.00   0.5774   0.00
 734.6938   0.00   4.9236   0.00   0.00   0.00   0.5774   0.00
 775.5102   0.00   4.8601   0.00   0.00   0.00   0.5774   0.00
 816.3265   0.00   4.8544   0.00   0.00   0.00   0.5774   0.00
 857.1428   0.00   4.9063   0.00   0.00   0.00   0.5774   0.00
 897.9592   0.00   5.0160   0.00   0.00   0.00   0.5774   0.00
 938.7755   0.00   5.1833   0.00   0.00   0.00   0.5774   0.00
 979.5918   0.00   5.4084   0.00   0.00   0.00   0.5774   0.00
1020.4081   0.00   5.6912   0.00   0.00   0.00   0.5774   0.00
1061.2245   0.00   6.0317   0.00   0.00   0.00   0.5774   0.00
1102.0408   0.00   6.4299   0.00   0.00   0.00   0.5774   0.00
1142.8572   0.00   6.8858   0.00   0.00   0.00   0.5774   0.00
1183.6735   0.00   7.3994   0.00   0.00   0.00   0.5774   0.00
1224.4897   0.00   7.7059   0.00   0.00   0.00   0.5774   0.00
1265.3062   0.00   7.8473   0.00   0.00   0.00   0.5774   0.00
                                  .
                                  .
                                  .
3673.4692   0.00  16.1894   0.00   0.00   0.00   0.5774   0.00
3714.2856   0.00  16.3308   0.00   0.00   0.00   0.5774   0.00
3755.1021   0.00  16.4722   0.00   0.00   0.00   0.5774   0.00
3795.9182   0.00  16.6136   0.00   0.00   0.00   0.5774   0.00
3836.7346   0.00  16.7549   0.00   0.00   0.00   0.5774   0.00
3877.5510   0.00  16.8963   0.00   0.00   0.00   0.5774   0.00
3918.3672   0.00  17.0377   0.00   0.00   0.00   0.5774   0.00
3959.1836   0.00  17.1791   0.00   0.00   0.00   0.5774   0.00
    -1.     0.       0.     0.       0.     0.       0.     0.
```

Figure 46: Model 2: Velocity-depth distribution (a) and the corresponding input data (line set 3) (b).

46. An explosive source is located at the Earth's surface. Since the model is smooth, no reflections can be calculated. The only possible wave is the direct P-wave — its numerical code is generated automatically. The receivers are

regularly distributed along the Earth's surface with the spacing 200km. The two-point ray tracing is performed. Rays are shown in Fig. 47. In the figure, the low-velocity zone is demarcated by two dashed lines (not representing structural interfaces). The corresponding travel times and amplitudes at the Earth's surface are in Fig. 48. Grey points correspond to the arrivals with phase shifts due to passage through caustics.
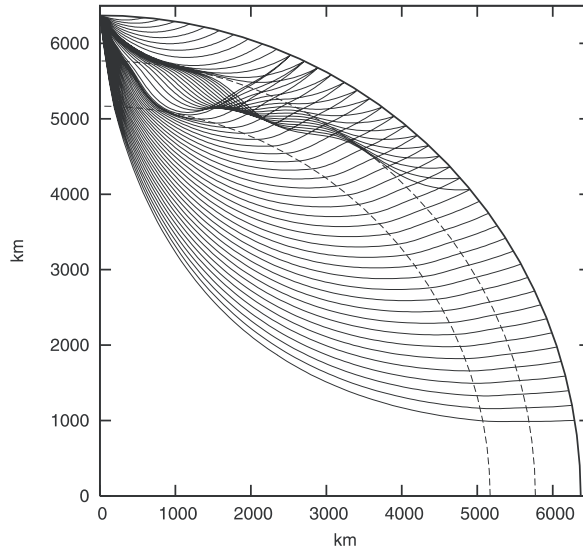

Figure 47: Rays from the Example 5.
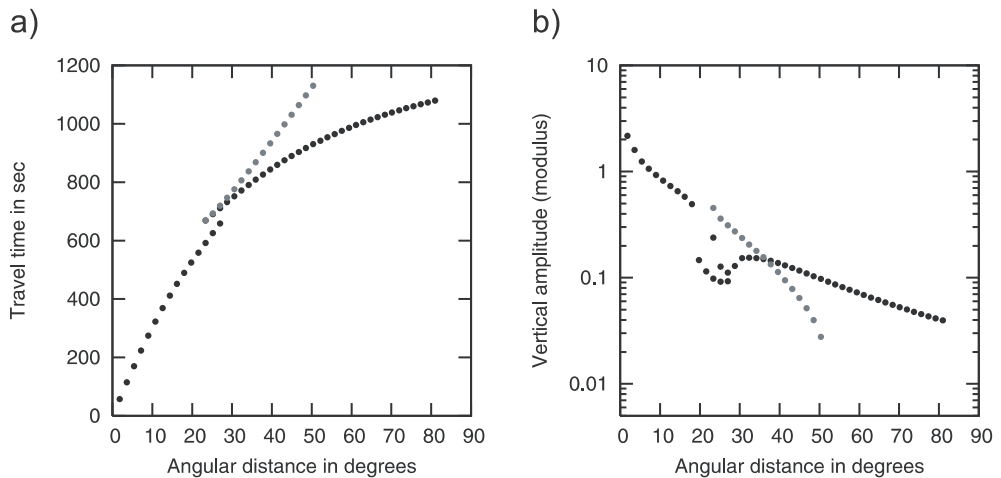
Figure 48: Travel times (a) and vertical displacement amplitudes (b) corresponding to the ray endpoints from Fig. 47 (Example 5). The ray endpoints with phase shifts due to caustics are shown in grey.

8.4   Troubleshooting tips

The following table presents several hints which can help the reader to solve situations when the program does not function well, returns no results or results which are obviously wrong. Neither the list of the problems, nor the list of possible solutions is complete. The table provides only some of the most frequently appearing situations.

PROBLEM	POSSIBLE REASON	SUGGESTED SOLUTION
At certain receivers, no rays are captured.	The receiver is in a shadow zone	None. The result is correct.
	Accuracy required in the shooting method is too high.	Increase REPS.
	Insufficient angular range or angle step too high.	Check AMIN, AMAX, ASTEP.
	The receiver is situated to the left from the source.	None. Rays can be traced only to the right from the source.
	The sequence number of the receiver is larger than 99.	Decrease the number of receivers. Maximum number is 99.
More than one ray of the given elementary wave terminates at a certain receiver.	This may be correct in certain situations (multi-pathing).	None.
	Angle step too small.	Increase ASTEP.
	The tolerance of capturing the ray in the shooting method is too high.	Decrease REPS.
The program does not return any ray of the given elementary wave.	Insufficient angular range.	Adjust AMIN and AMAX.
	The first ray segment is assigned by different number than that corresponding to the layer in which the source is situated.	Adjust the elementary wave code.

Continued on the next page

PROBLEM	POSSIBLE REASON	SUGGESTED SOLUTION
	The elementary wave code for rays radiated downwards from the source does not contain the compound element (related to the turning point of the ray)	Adjust the elementary wave code. The code must contain doubled number of the layer in which rays turn upwards (similarly to the case of reflected rays).
	The number of ray segments in the elementary wave code does not agree with KCA.	Adjust KCA.
	KC does not correspond to the initial direction of the ray.	Set KC=1 for rays going downward from the source and KC=-1 for rays going upward from the source. This should also be in correspondence to the angular range (AMIN,AMAX).
	The elementary wave code does not describe rays terminating at the Earth's surface.	Adjust the code. The last ray segment must be coded by 1.
The program returns exactly same ray trajectories both for *P*- and *S*-waves.	This may be correct for monotypic waves (without conversions) provided α/β ratio is constant throughout the whole structure.	None. The result is correct.
Reflections from the last interface in the model are not computed.	The program does not calculate rays reflected from the bottom of the model.	Add a line corresponding to a formal layer below this interface (like in Fig. 37b)
Sparse discretization of rays.	Sparse discretization in the velocity model (the rays are computed only at the depths of the model grid points).	Refine the velocity model. Note that the results are correct even for the sparse discretization, but problems may appear when plotting such rays (for example, the rays do not look smooth in the vicinity of their turning points).

Continued on the next page

PROBLEM	POSSIBLE REASON	SUGGESTED SOLUTION
After the source location has been changed, the program stops computing any rays.	Elementary wave codes do not correspond to the new source location (the source is no longer situated in the same layer as before).	Adjust the elementary wave code. Also do not forget to properly change ROZD.
After the structure has been changed, the program stops computing any rays.	Elementary wave codes do not correspond to the new structure (missing layers or new layers are present).	Adjust elementary wave codes.

When problems with calculations (possibly not mentioned in the above table) appear, it is always recommended to set MOUT=2 in ZRAYAMP.DAT and check the file ZRAYAMP.OUT, especially the IND values indicating the reasons why the calculation was not successful. However, if the output file ZRAYAMP.OUT is to be used by the plotting routines included in the attached CD, MOUT must be set equal to 1.

References

Aki, K., and Richards, P. (1980), *Quantitative seismology. Theory and methods*, Freeman, San Francisco

Babich, V.M. (1956), Ray method of the computation of the intensity of wave fronts (in Russian), *Dokl. Akad. Nauk SSSR*, **110**, 355 – 357

Bakker, P.M. (1998), Phase shift at caustics along rays in anisotropic media, *Geophys. J. Int.* , **134**, 515 – 518

Ben-Menahem, A., and Beydoun, W.B. (1987), Range of validity of seismic ray and beam methods in general inhomogeneous media - I. general theory, *Geophys. J. R. astr. Soc.* , **82**, 207 – 234

Ben-Menahem, A., Gibson, R.L., Sena, G. (1991), Green's tensor radiation patterns of point sources in general anisotropic inhomogeneous elastic media, *Geophys. J. Int.* **107**, 297 – 308

Beydoun, W.B. and Ben-Menahem, A. (1987), Range of validity of seismic ray and beam methods in general inhomogeneous media - II. a canonical problem, *Geophys. J. R. astr. Soc.* , **82**, 235 – 262

Beydoun, W.B., and Keho, T.H. (1987), The paraxial ray method, *Geophysics*, **52**, 1639 – 1653.

Bleistein, N. (1984), *Mathematical Methods for Wave Phenomena*, Academic Press, New York

Bouchon, M. (1980), A simple method to calculate Green's functions for elastic layered media, *Bull. seismol. Soc. Am.* , **71**, 959 – 971

Brokešová, J., Dekker, S., and Duijndam, A. (1994) Applicability of high-frequency asymptotic methods for the model PICROCOL, In: Extended Abstracts of the 64th Annual SEG Meeting and Exposition, Los Angeles, 1994

Bulant, P., Klimeš, L., Pšenčík, I., and Vavryčuk, V. (2004), Comparison of ray methods with the exact solution in the 1-D anisotropic 'simplified twisted crystal' model, *Stud. Geophys. Geod.* , **48**, 675 – 688

Červený, V. (1985), Ray synthetic seismograms for complex two-dimensional and three-dimensional structures, *J.Geophys.*, **58**, 2 – 26

Červený, V. (2001), *Seismic Ray Theory*, Cambridge University Press, Cambridge

Červený, V. (2002), Fermat's variational principle for anisotropic inhomogeneous media, *Stud. Geophys. Geod.* , **46**, 567 – 588

Červený, V., and Janský, J. (1985), Fast computation of ray synthetic seismograms in vertically inhomogeneous media, *Stud. Geophys. Geod.* , **29**, 49 – 67

Červený, V., Klimeš, L., and Pšenčík, I. (1988), Complete seismic-ray tracing in three-dimensional structures. In *Seismological algorithms*, ed. D. J. Doornbos, pp. 89 – 168, Academic Press, New York.

Červený, V., and Pšenčík, I. (1984), SEIS-83 – Numerical modelling of seismic wave field in 2-D laterally varying layered structures by the ray method. In *Documentation of Earthquake Algorithm World Data Center (A) for Solid Earth Geophysics*, ed. E.R Engdahl, pp. 36 – 40, Boulder CO., Paper SE-35.

Červený, V., and Pšenčík, I. (2002), Ray-theory amplitudes and synthetic seismograms in 2-D inhomogeneous isotropic layered structures. Program packages SEIS Seismic Waves in Complex 3-D Structures, Report 12, pp. 53 – 65, Department of Geophysics, Charles University, Prague (see also http://sw3d.mff.cuni.cz/papers/r12vc1.htm)

Chapman, C.H (2004), *Fundamentals of seismic wave propagation*, Cambridge University Press, Cambridge

Coates, R.T., and Chapman, C.H. (1990), Quasi-shear wave coupling in weakly anisotropic 3-D media, *Geophys. J. Int.* , **103**, 301 – 320

Duda, S.J., and Yanovskaya, T.B. (1993), Spectral amplitude-distance curves for *P*-waves: effects of velocity and *Q* distribution, *Tectonophysics*, **217**, 255 – 265

Duda, S.J., Janský, J., and Kvasnička, M. (2000), P-wave amplitudes and dynamic strains inside the Earth, *Acta geophysica Polonica*, Vol. XLVIII, No.2, 179 – 193

Jílek, P., and Červený, V. (1996), Radiation patterns of point sources situated close to structural interfaces and to the Earth's surface, *PA-GEOPH*, **148**, 175 – 225

Jobert, N., and Jobert, G. (1987), Ray tracing for surface waves, In *Seismic tomography with applications in global seismology and exploration geophysics*, ed. G. Nolet, pp. 275 – 300, Reider, Dordrecht

Karal, F.C., and Keller, J.B. (1959), Elastic wave propagation in homogeneous and inhomogeneous media, *J. Acoust. Soc. Am.*, **31**, 694 – 705

Kendall, J.M, Guest, W.S., and Thomson, C.J. (1992), Ray-theory Green's function reciprocity and ray-centered coordinates in anisotropic media, *Geophys. J. Int.* , **108**, 364 – 371

Knapp, R.W. (1991), Fresnel zones in the light of broadband data, *Geophysics*, **65**, 354 – 359

Kravtsov, Yu.A., and Orlov, Yu.I. (1980), *Geometrical optics of inhomogeneous media* (in Russian), Nauka, Moscow. (Translation to English by Springer, Berlin, 1990)

Kvasnička, M., and Janský, J. (1999), Fresnel volumes corresponding to PKP waves in the IASP91 model, *J. Seismology*, **3**, 375 – 391

Lindsey, J.P. (1989), The Fresnel zone and its interpretative significance, *The Leading Edge*, **8**, 33 – 39

Miller, G. (1977), Earth-flattening approximation for body waves derived from geometric ray theory - improvements, corrections and range of applicability, *J. geophys.*, **42**, 429 – 436

Moczo, P., Bard,P.Y., and Pšenčík, I. (1987), Seismic response of 2-D absorbing structures by the ray method. *J.Geophys.*, **62**, 38 – 49.

Moczo, P., Kristek, J., and Halada, L. (2004), *The finite-difference method for seismologists. An introduction*, Comenius University, Bratislava (see also http://www.spice-rtn.org)

Opršal, I., Brokešová, J., Faeh, D., Giardini (2002), 3D Hybrid Ray-FD and DWN-FD Seismic Modeling For Simple Models Containing Complex Local Structures, *Stud. Geophys. Geod.* , **46**, 711-730

Ott, E. (1993), *Chaos in dynamical systems*, Cambridge University Press, Cambridge

Podvin, P., and I. Lecomte (1991), Finite difference computation of travel times in very contrasted velocity models: a massively parallel approach, *Geophys. J. Int.* , **105**, 271–284.

Popov, M.M., and Camerlynck, C. (1996), Second term of the ray series and validity of the ray theory, *J. Geophys. Res.* , **101**, 817 – 826

Press, W.H., Teukolsky, S.A., Vetterling, W.T., and Flannery, B.P. (1996) *Numerical Recipes in Fortran 90* (2nd ed.), Cambridge University Press, Cambridge

Pujol, J. (2003), *Elastic Wave Propagation and Generation in Seismology*, Cambridge University Press, Cambridge

Pšenčík, I. (1994), *Seismic Ray Method for Inhomogeneous Isotropic and Anisotropic Media*, ICTP Lecture Notes, Trieste

Pšenčík, I., and Teles, N.T. (1996), Point source radiation in inhomogeneous anisotropic structures, *PAGEOPH*, **148**,591 – 623

Vavryčuk, V., and Yomogida, K. (1995), Multipolar elastic fields in homogeneous isotropic media by higher-order ray approximations, *Geophys. J. Int.* , **121**, 925 – 932

Vidale, J.E. (1990), Finite-difference calculation of traveltimes in three dimensions, *Geophysics*, **55**, 521–526. **Sethian, J.** (1999), *Level set methods and fast marching methods*, Cambridge University Press, Cambridge

Abbreviations

ART   Asymptotic ray theory

BC   Boundary conditions

DRT   Dynamic ray tracing

EDE   Elastodynamic equation

EE   Eikonal equation

EFT   Earth's flattening transformation

FDM   Finite difference method

P.V.   Cauchy principal value

RC   Ray coordinates

RCC   Ray centered coordinates

RM   Ray method

R/T   Reflection/transmission

RTS   Ray tracing system

TE   Transport equation

WOC   Wavefront orthogonal coordinates

Selected notations

a_{ijkl}	Density normalized elastic parameter
A	Scalar ray amplitude of a linearly polarized wave (P, qP, qS_1, or qS_2)
$\mathbf{b}$	Unit binormal to a ray
B	Scalar ray amplitude factor of the S-wave
c	Phase velocity
C	Scalar ray amplitude factor of the S-wave
c_{ijkl}	Elastic parameter (elastic tensor component)
E	Elastic energy
E_W	Strain energy
E_K	Kinetic energy
$\mathbf{e}_i$	RCC basis vector
f	Source-time function (real part of the analytic signal F)
$\mathbf{f}$	Body force per unit volume
F	Analytical signal
$\mathcal{F}$	Fourier transform
G	Eigenvalue of the Christoffel matrix
$\mathbf{g}$	Eigenvector of the Christoffel matrix (amplitude polarization vector)
$\mathcal{G}$	Radiation function
G_{ij}	Green's tensor
h	Heaviside step function
H	Hamiltonian
$\mathbf{H}$	Transformation matrix from the RCC to the Cartesian coordinates
$\mathcal{H}$	Hilbert transform
i	Imaginary unit
i	Angle of incidence
$\mathbf{i}_i$	Cartesian coordinate basis vector
I	Fermat's functional
J	Ray Jacobian
K	KMAH index (index of the ray trajectory)
k_I	Principal curvature of the slowness surface along the p_I-axis
$\mathcal{K}$	Gaussian curvature of the slowness surface
l	Length of the ray in homogeneous media (source-receiver distance)
L	Lagrangian
$\mathbf{L}$	Differential operator in the ART EDE approximation (zero-order)
$\mathbf{M}$	Differential operator in the ART EDE approximation (first-order)

N	Differential operator in the ART EDE approximation (second-order)
n	Unit normal to a ray
$\mathbf{n}^S$	Unit outer normal to a closed surface S
$\mathbf{n}^\tau$	Unit normal to a wavefront
p	Slowness vector (normal to the wavefront)
$\mathbf{p}^\nu$	Slowness component normal to the interface
$\mathbf{p}^\Sigma$	Slowness component tangent to the interface
p	Ray parameter
P	Transformation matrix from the RC to the slowness components
Q	Point of incidence
Q	Transformation matrix from the RC to the Cartesian coordinates
q_i	RCC coordinates
r	Radius in the spherical or polar coordinates
R	Receiver point
R_{ij}^{R}	Displacement reflection coefficient
R_{ij}^{T}	Displacement transmission coefficient
$\mathcal{R}$	Radiation pattern
$\Re$	Real part
s	Ray flow parameter (arclength)
S	Source point
S	Energy flux
$\mathrm{d}S^\perp$	Cross-sectional area of the ray tube
$\mathrm{d}\mathbf{S}^{(\tau)}$	Vectorial surface element cut from the wavefront by the ray tube
$\mathrm{d}S^{(\tau)}$	Scalar surface element cut from the wavefront by the ray tube
$\mathcal{S}$	Relative geometrical spreading
t	Time
t	Vector tangent to the ray
T	Torsion of the ray
T	Traction
u	General flow parameter along the ray
u	Particle displacement
U	Leading term amplitude (zero-order)
$\mathbf{U_1}$	Amplitude of the first-order term in the ray series
v	Wave propagation velocity in isotropic media
$\mathbf{v}^g$	Group velocity
v^g	Group velocity magnitude
x	Position vector
x_i	Cartesian coordinate

α	P-wave velocity
β	S-wave velocity
γ_i	Ray coordinate (for $i = I$ also ray parameter)
Γ_{ij}	Christoffel matrix
δ	Dirac delta-function. Variance
δ_{ij}	Kronecker's symbol
ε_{ij}	Strain tensor element
θ	Colatitude in the spherical coordinates
ϑ	Azimuth of the ray
λ	Wavelength; Lamé elastic parameter
μ	Lamé elastic parameter (rigidity, shear modulus)
$\boldsymbol{\nu}$	Unit normal to a structural interface
ρ	Density
σ_0	Index of the source in anisotropic media
Σ	Structural interface
τ	Eikonal (travel time)
ϕ	Longitude in the spherical coordinates
φ	Rytov angle
Φ	Angle between normal to the wavefront and tangent to the ray
ψ	Declination of the ray
ω	Circular frequency
Ω	Reference ray